

Engineering and implementation of synthetic (opto-) genetic tools for *Ustilago maydis* and reconstruction of (signaling) pathways in orthogonal Systems

Inaugural-Dissertation

zur Erlangung des Doktorgrades
der Mathematisch-Naturwissenschaftlichen Fakultät
der Heinrich-Heine-Universität Düsseldorf

vorgelegt von

Nicole Heucken
aus Hagen

Düsseldorf, Mai 2020

Aus dem Institut für Synthetische Biologie
der Heinrich-Heine-Universität Düsseldorf

Gedruckt mit der Genehmigung der
Mathematisch-Naturwissenschaftlichen Fakultät der
Heinrich-Heine-Universität

Berichtersteller:

1. Prof. Dr. Matias D. Zurbriggen
2. Prof. Dr. Michael Feldbrügge

Tag der mündlichen Prüfung: 15.12.2020

Eidesstattliche Erklärung

Ich versichere an Eides Statt, dass die Dissertation von mir selbständig und ohne unzulässige fremde Hilfe unter Beachtung der „Grundsätze zur Sicherung guter wissenschaftlicher Praxis an der Heinrich-Heine-Universität Düsseldorf“ erstellt worden ist.

Düsseldorf, den 27.05.2020

Nicole Heucken

Table of contents

Eidesstattliche Erklärung	I
Table of contents	II
Danksagung	IV
Figures	V
Abbreviations	VI
Summary	VII
1. Introduction	1
1.1 Engineering and implementation of synthetic (opto-) genetic tools for <i>Ustilago maydis</i>	1
1.1.1 Emerging role for <i>Ustilago maydis</i> as a production host for high value compounds.....	1
1.1.2 Quantitative reporter genes.....	2
1.1.3 Bioluminescent reporter genes.....	2
1.1.4 SEAP.....	4
1.1.5 Tools for bicistronic vectors.....	5
1.1.5.1 2A-peptides.....	5
1.1.5.2 IRES sequences.....	7
1.1.5.3 Bidirectional promoters.....	7
1.1.6 Regulation of gene expression.....	7
1.1.6.1 DNA-binding proteins and their operating sequences – constitutive and chemically regulatable gene expression.....	8
1.1.6.2 Light regulated gene expression.....	9
1.2 Reconstruction of Phytohormone signaling pathways in plant and orthogonal cell systems	12
1.2.1 Gibberellins.....	13
1.2.2 Abscisic Acid.....	14
1.2.3 Ratiometric biosensors and the development of a cloning method for integration of short sequences.....	15
2. Aims	17
3. Results and Discussion	18
3.1 Engineering and Implementation of a synthetic (opto-) genetic toolbox for <i>Ustilago maydis</i>	18
3.1.1 Establishment of enzymatic, quantitative reporter genes in <i>Ustilago maydis</i>	19
3.1.1.1 A fast screening platform for the generation and characterization of <i>U. maydis</i> strains.....	23
3.1.1.2 Gene expression normalization with quantitative reporter genes.....	25
3.1.2 Implementation of tools for bicistronic expression in <i>U. maydis</i>	27
3.1.2.1 IRES sequences.....	27
3.1.2.2 Bidirectional promoters.....	30
3.1.3 DNA binding protein – operating sequence interaction studies.....	32
3.1.3.1 Pristinamycin-based chemical regulation of gene expression.....	34
3.1.4 Orthogonal promoters for <i>U. maydis</i>	36
3.1.5 Light regulated gene expression in <i>U. maydis</i>	37
3.2 Reconstruction of phytohormone signaling pathways	39
3.2.1 Interaction studies of the COP1/SPA1 complex with proteins of the Gibberellin signaling pathway.....	39
3.2.1.1 Microscopy studies.....	40
3.2.2 Mammalian 2- and 3-hybrid.....	42

3.2.3	Quantitative analysis of increased PYL8 after ABA sensing in <i>Arabidopsis thaliana</i> mesophyll protoplasts.....	45
3.2.4	Development of pifold and an upgrade to AQUA	47
4.	Conclusion.....	51
5.	Material and Methods.....	53
5.1	Establishment of a synthetic toolbox in <i>Ustilago maydis</i>.....	53
5.1.1	Plasmid generation	53
5.1.2	Strains and growth conditions of <i>Ustilago maydis</i>	53
5.1.3	Preparation of chemically competent <i>Ustilago maydis</i> protoplasts	53
5.1.4	Transformation of <i>Ustilago maydis</i>	54
5.1.5	Extraction of genomic DNA from <i>Ustilago maydis</i>	54
5.1.6	Genotyping by PCR	55
5.1.7	DIG-Southern Blot.....	55
5.1.8	Protein isolation from <i>Ustilago maydis</i>	57
5.1.9	Light experiments.....	57
5.2	Phytohormone signaling	58
5.2.1	COP1/SPA1/DELLA interactions	58
5.2.1.1	Plasmid generation	58
5.2.1.2	Mammalian cell culture	58
5.2.1.3	PEI transfection	58
5.2.1.4	Fixing cells for microscopy.....	58
5.2.2	Application of an ABA biosensor and construction of the potential-induction-fold-determination sensor pifold in plant protoplasts	58
5.2.2.1	Plasmid generation	58
5.2.2.2	Plant material	59
5.2.2.3	Protoplast isolation and transformation.....	59
5.2.2.4	Hormone treatment	60
5.2.3	Reporter Assays	60
5.2.3.1	Luciferase Assays	60
5.2.3.2	SEAP reporter Assay	60
5.2.3.3	Fluorescence measurements via Plate Reader	61
5.2.3.4	Fluorescence microscopy	61
5.3	Software.....	61
5.4	Plasmids	62
5.5	Oligonucleotides.....	75
5.6	<i>Ustilago maydis</i> strains	82
6.	References.....	84
7.	Appendix: original publications and manuscripts	96
7.1	AQUA 2.0: an upgrade to AQUA cloning.....	97
7.2	COP1 destabilizes DELLA proteins in <i>Arabidopsis</i>	113

Danksagung

Zunächst möchte ich mich bei Herrn Prof. Dr. Matias Zurbriggen für die Möglichkeit bedanken, meine Promotion in seinem Institut durchzuführen. Hier hatte ich die Möglichkeit meine Laborfähigkeiten um diverse Methoden zu bereichern und selbstständig verschiedenste Forschungsbereiche zu erkunden.

Ein weiterer Dank geht an Prof. Dr. Michael Feldbrügge für seine Arbeit als Mentor und die Kooperation mit dem Institut der Mikrobiologie, ohne welches diese Arbeit kaum realisierbar gewesen wäre.

Weiterhin danke ich Anita Loeschke als meine Co-Betreuerin, aber auch für ihre ausgezeichnete Arbeit als Leiterin des CombiCom Focus Labs. Sie hat allen beteiligten Doktoranden und Post Docs zu jeder Zeit mit einem offenen Ohr zur Seite gestanden.

Außerdem möchte ich allen Mitgliedern des Instituts für synthetische Biologie für die gemeinsame Zeit danken. Vor allem Dr. Sofia Romero, Dr. Kun Tang und Estefania Pavesi, sowie die Gast-Doktorandinnen Pamela und Paula haben für eine sehr angenehme Arbeitsatmosphäre gesorgt. Ganz besonders hervorheben möchte ich Lisa Hüsemann, die gleichzeitig mit mir, im Rahmen des CombiCom, ihre Doktorarbeit begonnen hat. Gemeinsam sind wir diverse Male umgezogen, haben ein ganzes Labor eingerichtet und uns mit dem kleinen Uschi herumgeschlagen. Ich danke dir auch für unsere zahlreichen ‚fruitfull discussions‘!

Vielen Dank auch an alle Mitarbeiter der Mikrobiologie, die uns in ihren Laboren herzlich willkommen geheißen haben.

Danken möchte ich auch Jessica Müller, Michaela Gerads und Reinhild Wurm für ihre Unterstützung und Expertise im Laboralltag.

Mein Dank gilt außerdem meiner Familie und besonders meiner Schwester, die mir im Beruflichen und Privaten jederzeit beigestanden haben.

Ein ganz besonderer Dank gilt meinem Freund, der mich im letzten halben Jahr davor bewahrt hat, den Stress gewinnen zu lassen.

Zu guter Letzt bedanke ich mich bei den lieben Lurchen und Ottern, der zwei besten deutschen Twitch Communities die es gibt, für ihre aufmunternden Worte, die ich virtuell empfangen durfte. Ihr habt mich während der drei Jahre meiner Doktorarbeit, sowie auch davor, immer wieder abgelenkt und zum Lachen gebracht.

Figures

Figure 1: Enzymatic reactions catalyzed by quantitative reporters.	4
Figure 2: Mechanism of tools for the construction of bicistronic expression vectors.	6
Figure 3: Mechanism of synthetic constitutive and chemically regulatable gene expression systems.	8
Figure 4: Spectral sensitivity of photoreceptors and mechanisms of light regulated gene expression.	11
Figure 5: Gibberellin signaling components and perception in <i>Arabidopsis thaliana</i> .	13
Figure 6: Abscisic acid signaling components and perception in <i>Arabidopsis thaliana</i> .	15
Figure 7: General genetically encoded, ratiometric, degradation-based phytohormone biosensor design.	16
Figure 8: Synthetic (opto-) genetic toolbox for <i>U. maydis</i> .	19
Figure 9: Enzymatic activity of quantitative reporter genes.	21
Figure 10: Western Blot analysis of <i>U. maydis</i> reporter strains.	22
Figure 11: SEAP activity of AB33 and P _{O2tef} -SEAP.	23
Figure 12: Fast-screening assays for luciferases.	24
Figure 13: Normalization of gene expression in <i>U. maydis</i> .	26
Figure 14: Establishment of IRES sequences in <i>U. maydis</i> .	29
Figure 15: Establishment of bidirectional promoters in <i>U. maydis</i> .	31
Figure 16: DNA binding protein – operating sequence analysis.	33
Figure 17: Pristinamycin based gene expression regulation in <i>U. maydis</i> .	35
Figure 18: Strength comparison of synthetic (orthogonal) promoters for <i>U. maydis</i> .	36
Figure 19: UV-B light regulated gene expression in <i>U. maydis</i> .	38
Figure 20: Confocal microscopy analysis of the localization of GAI, RGA, COP1 and SPA1 in animal cells.	42
Figure 21: Quantification of speckle formation by the COP1/SPA1 complex with DELLA proteins.	42
Figure 22: COP1/SPA1/DELLA interaction studies with a mammalian 2- and 3-hybrid system.	44
Figure 23: ABA-based stabilization of PYL8 in <i>A. thaliana</i> wt protoplasts.	46
Figure 24: ABA-based stabilization of PYL8 after downregulation by RFA4 in <i>A. thaliana</i> wt protoplasts	46
Figure 25: Design of the pifold (potential-induction-fold-determination) gene expression system in plants.	48
Figure 26: AQUA 2.0 Cloning work-flow.	49
Figure 27: Potential-induction-fold-determination for ratiometric degradation-based biosensors in <i>A. thaliana</i> wt protoplasts.	50

Abbreviations

ABA	abscisic acid
ABI	ABA-insensitive
AFU	absolute fluorescence units
ALU	absolute luminescence units
ASK1	ARABIDOPSIS SKP1-related
COP1	CONSTITUTIVELY PHYTOMORPHOGENIC 1
CUL1	CULLIN 1
FLuc	firefly luciferase
GA	gibberellin
GAI	GA-insensitive
GAL4 _{BD}	GALACTOSE-RESPONSIVE TRANSCRIPTION FACTOR 4 binding domain
GID1	GIBBERELLIN INSENSITIVE DWARF 1
GLuc	gaussia luciferase
HA	hemagglutinin
HEK	human embryonic kidney
HTS	high-throughput screening
IRES	internal ribosome entry site
NES	nuclear exclusion signal
NLS	nuclear localization signal
OD	optical density
PCB	phycocyanobilin
PhyB	Phytochrome B
PIF6	PHYTOCHROME INTERACTING FACTOR 6
PIP	PRISTINAMYCIN-INDUCED PROTEIN
PIR	pristinamycin resistance gene operating sequence
pNPP	para-nitrophenyl phosphate
PP2C	PROTEIN PHOSPHATASE 2C
PYL8	PYR1-LIKE 8
PYR1	PYRABACTIN RESISTENCE 1
RFA4	RING-FINGER ABA-RELATED 4
RGA	REPRESSOR-OF-ga1-3
RLuc	renilla luciferase
SEAP	human secreted embryonic alkaline phosphatase
SLY1	SLEEPY 1
SM	sensor module
SnRK2	SNF1-RELATED PROTEIN KINASE 2
SPA1	SUPPRESSOR OF phyA-105
TF	transcription factor
UAS _G	GAL4 upstream activating sequence
UV-B	ultraviolet B
UVR8	UV RESISTANCE LOCUS 8
WT	wild type

Summary

Production of pharmaceutically relevant substances is traditionally realized by chemical synthesis with several drawbacks such as limited product diversity, accumulation of toxic waste and low outcome despite high costs. For these reasons, more and more compounds are produced biotechnologically and new production platforms are constantly needed to be able to satisfy the increasing demands of society. The dimorphic basidiomycete fungus *Ustilago maydis* is used as a model organism for many biological processes, and more recently, a biotechnological role, as a production platform for high value compounds, is emerging.

During this work, several basic and advanced tools for the pathway engineering in *U. maydis* were constructed and tested. The functionality of the quantitative luminescent reporters FLuc, RLuc and GLuc was proven. With their help, a fast screening platform for the efficient generation of *U. maydis* strains was established. Additionally, their use as a normalization element was demonstrated in an induction-based gene expression quantification system. They were further applied for the testing and characterization of several synthetic tools, such as IRES sequences and bidirectional promoters, but also DNA-binding protein – DNA operating sequence interactions, and chemical as well as light regulated gene expression. While IRES sequences and chemical and UV-B-light regulated gene expression are, at this stage, not yet functional, two bidirectional promoters, several orthogonal unidirectional promoters and the PIP-PIR₃ system, as the base for split transcription factor systems, have shown to be functional and useful in *U. maydis*.

In the second part of this work, certain aspects of phytohormone signalling have been analysed in more detail. Fluorescence microscopy studies have proven the interaction of the DELLA proteins RGA and GAI with the COP1/SPA1 complex, and shown that mainly SPA1 is responsible for this interaction.

Moreover, the functionality of induction-based, ratiometric, luminescent phytohormone biosensors was demonstrated on the example of the abscisic acid receptor PYL8, which is upregulated upon hormone perception. Efficiency of this sensor was increased by downregulation of the receptor protein level by co-expression of the E3 ubiquitin ligase RFA4 before hormone treatment.

Lastly, a potential-induction-fold-determination-vector was constructed using an updated version of AQUA cloning, with which dynamic ranges of phytohormone biosensors can be estimated in several organisms.

1. Introduction

1.1 Engineering and implementation of synthetic (opto-) genetic tools for *Ustilago maydis*

1.1.1 Emerging role for *Ustilago maydis* as a production host for high value compounds

The dimorphic basidiomycete fungus *Ustilago maydis* is a phytopathogene, infecting *Zea mays* and causing the corn smut disease. It is used as a model organism for several biological processes such as DNA recombination, cell signaling and fungal mating, when grown in its yeast-like form. In its filamentous growth form, on the other hand, it serves in the investigation of mRNA long distance transport and plant pathogen interactions (León-Ramírez et al., 2014; Bösch et al., 2016; Müller et al., 2019). Lately, a biotechnological role is emerging, as it naturally produces value-added chemicals like polyols, organic acids like itaconic acid and malic acid and glycolipids such as ustilagic acid (Guevarra and Tabuchi, 1990; Feldbrügge et al., 2013). Moreover, for the production of these substances, it can degrade renewable non-food biomass and metabolize carbohydrate originated poly- and monomers (Couturier et al., 2012; Geiser et al., 2013). Recently, *U. maydis* has successfully been shown to serve as a production host for medium scale itaconate synthesis (Hosseinpour Tehrani et al., 2019; Becker et al., 2020). In combination with an unconventional secretion pathway, which is also beneficial for the expression of heterologous proteins, this organism is biotechnologically highly interesting (Stock et al., 2012; Feldbrügge et al., 2013). As the synthesis pathway for these substances is in most cases complex and involves several enzymatic reactions, they need to be optimized for higher output (Hewald et al., 2006; Teichmann et al., 2007). Genetic manipulation of *U. maydis* for the purpose of gene function characterization, by deletion and overexpression mutants, is easily done with the available genome sequence and an efficient homologous recombination system. Fluorescent tags as well as constitutive and inducible promoters are commonly used as well (Banks et al., 1993; Bottin et al., 1996; Spellig et al., 1996; Brachmann et al., 2004; Zarnack et al., 2006; Terfrüchte et al., 2014; Schuster et al., 2016). What is missing, are genetic tools for the simultaneous expression of several genes encoding e.g. enzymes from a synthesis pathway, and the ability to regulate them in a high spatiotemporal

resolution while being noninvasive for the organism itself. For this reason, a synthetic (opto-) genetic toolbox for pathway engineering in *U. maydis* is highly desirable. This toolbox should comprise 2A-peptides, internal ribosome entry site (IRES) sequences and bidirectional promoters as basic tools to build multicistronic vectors on the one hand, and options for gene expression regulation either through chemicals or by light on the other hand. As these genetically encoded tools come in a great and redundant number, the most efficient and robust working systems need to be determined. Therefore, quantifiable reporter genes with high selectivity and specificity have to be established in *U. maydis*.

The challenge, and probably the reason why thus far not many synthetic tools have been engineered for *U. maydis* will be, that strain generation is, by far, more labor intensive than the work with e.g. plant protoplasts and mammalian cells. In this project, more than 60 strains are planned to change this circumstance. The first and main part of this work therefore concentrates on the establishment of a synthetic (opto-) genetic toolbox in *U. maydis*.

1.1.2 Quantitative reporter genes

Quantitative reporter genes are commonly used to analyze promoter activity, DNA binding specificities of proteins, and to screen a large number of substances for their activity in so called high-throughput screenings (HTS). Fluorescent reporters are most frequently used, although luciferases have been discovered almost 70 years earlier than the green fluorescent protein (Dubois, 1885; Shimomura et al., 1962; Thorne et al., 2010). Another widely used reporter mechanism is measuring the absorbance of light by a product of an enzymatic reaction as in phosphatase-, ATPase- and β -glucuronidase assays, where the increase in absorbance is equivalent to e.g. promoter activity (Jefferson et al., 1987; Lavery et al., 2001; Briciu-Burghina et al., 2015).

The major aspects for reporter genes used in this work will be discussed in the following sections.

1.1.3 Bioluminescent reporter genes

Luciferases have been used for about 21% of all HTS assays listed in the PubChem library in 2010 (Thorne et al.), and therefore play an important role in the collection of quantitative reporter genes. They are oxidative enzymes, which catalyze the reaction from a substrate like D-luciferine or Coelenterazine to oxyluciferin or coelenteramide,

respectively (Verhaegen and Christopoulos, 2002; Fan and Wood, 2007). As a byproduct of these reactions light of a specific wavelength is emitted. Some of the most popular ones are firefly luciferase (FLuc) from *Photinus pyralis*, renilla luciferase from *Renilla reniformis* and gaussia luciferase (GLuc) from *Gaussia princeps* (Table 1).

Table 1: Overview of luciferases employed in high-throughput screening assays

Luciferase	Species	emission wavelength	Substrate	Secreted?	Protein half life
Firefly (FLuc)	<i>Photinus pyralis</i>	550-570 nm	D-Luciferin/ATP	No	3h
Modified Firefly (Ultra-Glo)	<i>Photuris pennsylvanica</i>	550-570 nm	D-Luciferin/ATP	No	N/A
Click beetle (CBLuc)	<i>Pyrophorus plagiophtalamus</i>	Green: 537 nm Red: 613 nm	D-Luciferin/ATP	No	7h
Sea pansy (RLuc)	<i>Renilla reniformis</i>	480 nm	Coelenterazine	No	4.5h
Copepod crustacean (GLuc)	<i>Gaussia princeps</i>	460 nm	Coelenterazine	Yes	6 days (in cell media)
Ostracod crustacean (CLuc)	<i>Cypridina noctiluca</i>	465 nm	Vargulin (= Cypridina luciferin)	Yes	53 h (in cell media)

Modified from Thorne et al., 2010

Firefly luciferase catalyzes a two-step reaction using one ATP molecule to transform D-luciferin into an enzyme bound intermediate, luciferyl-AMP, that reacts with O₂ (Figure 1A). Oxyluciferin in a high energy state is the resulting product which then transitions to its ground state, thereby emitting yellow-green light (Brown and Rogers, 1957; DeLuca and McElroy, 1978; DeLuca and McElroy, 1984). In 1987, de Wet and others expressed firefly luciferase in mammalian cells and indicated that it could be used as a fast and inexpensive reporter for promoter activity assays (de Wet et al., 1987).

The reaction that is catalyzed by renilla luciferase was characterized by Matthews and others in 1977 and uses coelenterazine as substrate. In an oxidative decarboxylation CO₂ is released and a coelenteramide anion in excited state is produced (Figure 1B). Relaxation to the ground state emits blue light of 480 nm wavelength *in vitro*, whereas *in vivo*, energy is transferred to a close by GFP protein, that gets excited and as a result, emits green fluorescence (Matthews et al., 1977; Lorenz et al., 1991). Renilla luciferase has been recombinantly expressed successfully in *E. coli* in 1991 by Lorenz et al., and since then, became a marker for gene expression also in plants and mammalian cells (Mayerhofer et al., 1995; Lorenz, 1996).

As renilla and firefly luciferases do not use the same substrate, and emit light at different wavelengths, they can be combined to monitor e.g. the drug activity on two receptors simultaneously in a so-called dual glow-signal luciferase reporter assay (Parsons et al., 2000). In other applications one luciferase is used as a normalization element and internal control, while the other one represents the degradation of a protein upon specific treatments (Samodelov et al., 2016).

Gaussia luciferase was first cloned by Bryan and Szent-Gyorgyi in 2001 and recombinantly expressed and used as a reporter gene only one year later (Bryan and Szent-Gyorgyi, 2001). It catalyzes the same reaction as renilla luciferase, but unlike renilla and firefly, it is secreted into the surrounding medium, which can be advantageous for several applications (Verhaegen and Christopoulos, 2002).

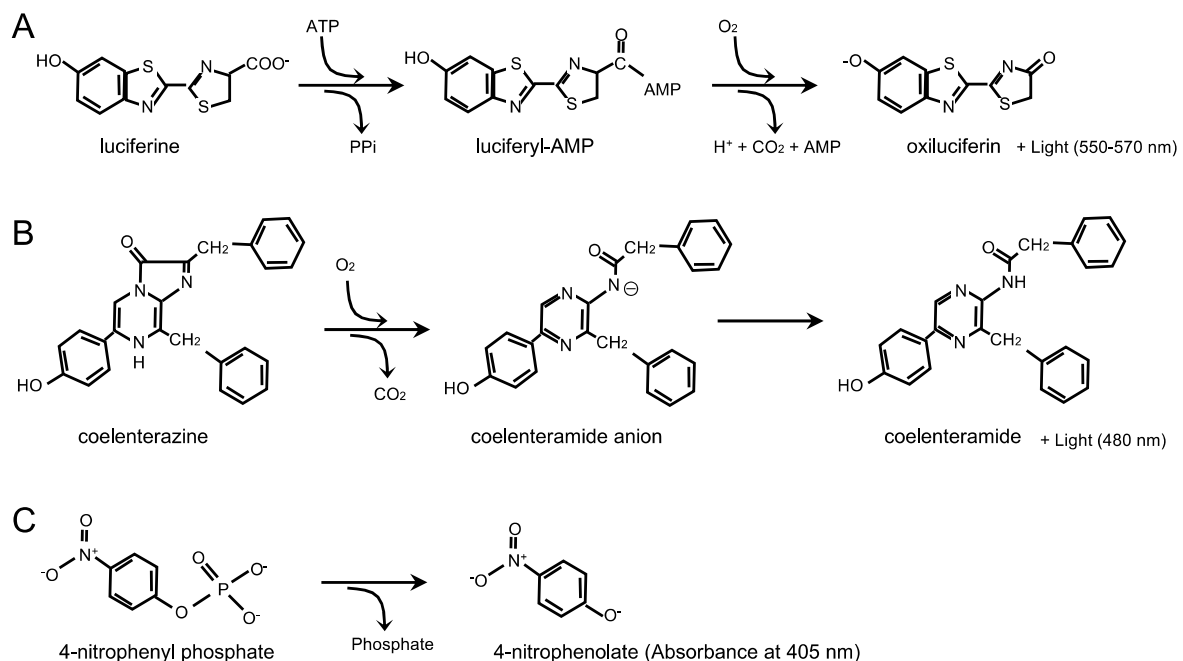


Figure 1: Enzymatic reactions catalyzed by quantitative reporters.

(A) Firefly luciferase catalyzes a two-step reaction from luciferin over luciferyl-AMP to oxyluciferin, thereby using one ATP molecule and O₂. The resulting oxyluciferin is in a high energy state and transitions to its ground state, while emitting yellow-green light. (B) Renilla and gaussia oxidatively decarboxylate coelenterazine to the coelenteramide anion, which subsequently relaxes into its ground state, resulting in coelenteramide and the emission of blue light. (C) Secreted alkaline phosphatase (SEAP) dephosphorylates 4-nitrophenyl phosphate to 4-nitrophenolate, which has an absorption maximum at 405 nm.

1.1.4 SEAP

The human secreted embryonic alkaline phosphatase (SEAP) has been used as an intracellular reporter gene in assays over the last 50 years (McComb and Bowers, 1972). It catalyzes the hydrolysis of para-nitrophenyl phosphate (pNPP) to para-nitrophenolate (pNP), which is a yellow, water soluble substance with an absorption

maximum at 405 nm (Figure 1C). Therefore, unlike with luciferases, the expression is equal to the increase in light absorbance at the given wavelength (McComb and Bowers, 1972). Enzyme activity is calculated following Lambert-Beer's law, where the extinction coefficient for pNP is approximately $18,600 \text{ M}^{-1} \text{ cm}^{-1}$ (Robinson and Biggs, 1955). Before determining SEAP activity, background signals produced by other endogenous phosphatases are eliminated via heat inactivation of them at 65°C , while SEAP is heat stable (Berger et al., 1987). A secreted version of SEAP was generated and is used as quantitative reporter for gene expression in eukaryotic cells since many years (Berger et al., 1988).

1.1.5 Tools for bicistronic vectors

The ability to express two or more proteins from one open reading frame (ORF) is sometimes desirable when it comes to ratiometric expression thereof, or when vectors get too big for sufficient transformation or transfection. Therefore, application of tools to engineer bicistronic expression vectors is widely used in synthetic biology. These tools comprise mostly virus derived 2A-peptides and IRES sequences, as well as bidirectional promoters, which can be endogenous or synthetically engineered. They are presented in more detail in the following paragraphs.

1.1.5.1 2A-peptides

2A-peptides are the smallest in this work presented tools for bicistronicity. They are about 60 to 90 bp long and have a conserved NPG↓P cleavage site at the C-term (Luke et al., 2008). A classical construct including a 2A-peptide would encode a first protein where the stop codon has been removed, followed by a 2A-peptide and a second protein of interest, all under the control of only one promoter. During translation, ribosomes process the first sequence including the 2A-peptide until they reach the cleavage site, where the amino acid chain is released from the complex (Figure 2A). Then translation continues with the second sequence. In this way, both proteins are expressed ratiometrically. However, as a potential drawback both proteins carry additional amino acids (De Felipe et al., 2003). Furthermore, the cleavage efficiency of the most commonly used 2A peptides is around 80-99%, which means that there will always be a percentage of probably unfunctional fusion proteins (Luke et al., 2008). 2A-peptides have successfully been applied in several mammalian cell types, plants, fungi and insects (Ryan and Drew, 1994; Roberts et al., 1997; Gopinath et al., 2000; Suzuki et al., 2000; Thomas and Maule, 2000;

Varnavski et al., 2000; Chng et al., 2015). Intensive literature research has been conducted to identify multiple 2A-peptides to be tested in *Ustilago maydis*. Accordingly, ten 2A-peptides from the list presented in Luke et al. (2008) have been chosen. They were cloned into constructs, encoding the red fluorescent protein mKate2 fused to an HA-tag in the first cistron and eGFP fused to an NLS in the second cistron, separated by the 2A-peptide. With this set-up, western blot analysis, microscopy studies and FRET-measurements can be performed. *U. maydis* strains for all ten 2A-peptides and a negative control, where the C-terminal proline of F2A has been removed, were generated.

The establishment of 2A-peptides and their characterization in terms of functionality and cleavage efficiency in *U. maydis* are not further discussed in this work. For more information refer to Kira Müntjes, institute for microbiology of the Heinrich-Heine-University, Düsseldorf.

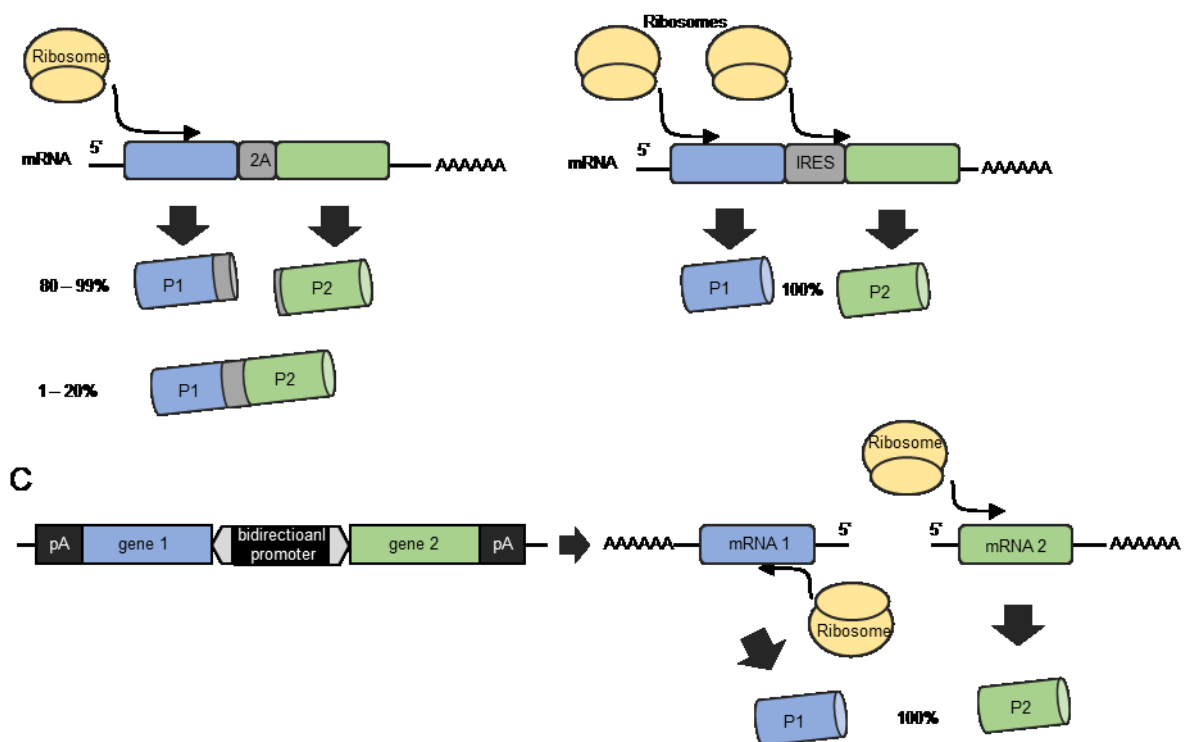


Figure 2: Mechanism of tools for the construction of bicistronic expression vectors.

(A) 2A-peptides have autocatalytic properties at a conserved NPG↓P cleavage site at their c-term. During translation from one mRNA encoding two proteins, the ribosome encounters this cleavage site, releases the first amino acid chain and continues with the translation of the second protein. The resulting proteins are present stoichiometrically and carry additional amino acids originated from the 2A-peptide. Cleavage efficiency lies between 80 and 99% for most 2A-peptides. (B) Internal ribosome entry sites (IRES) form secondary structures in mRNA to which ribosomes can bind independently from a 5'-cap. Bicistronic vectors based on IRES sequences result in 100% separated proteins, but the abundance of IRES originated proteins is lower than 5'-cap-originated proteins from the same construct. (C) Bidirectional promoters lead to transcription of genes upstream and downstream of the promoter sequence, resulting in two individual mRNAs. Translation therefore gives rise to 100% separated proteins.

1.1.5.2 IRES sequences

Internal ribosome entry sites (IRES) form secondary structures in mRNA to which ribosomes can bind (Figure 2B). Both sequences are then individually translated, leading to 100% separated proteins (Thompson et al., 2001). IRES are larger than 2A-peptides, with around 400-650 nucleotides in length, but the general construction of vectors is the same with both tools (Jang et al., 1988; Pelletier and Sonenberg, 1988; Belsham and Brangwyn, 1990). One difference is, that both gene sequences carry a stop codon in IRES constructs. Another major difference compared to 2A-peptides is that the proteins are not synthesized in equal amounts. Expression from an IRES leads to 10%-40% protein in comparison to the amount of 5'-cap-controlled protein from the same construct (Dorokhov et al., 2002). IRES sequences find application in the expression of split transcription factors, where potential fusion proteins, as in the case of 2A-peptides, would lead to leakiness of the whole system (Müller et al., 2013a).

1.1.5.3 Bidirectional promoters

Bidirectional promoters efficiently activate the expression of genes upstream and downstream of the promoter sequence. They occur naturally in several organisms, but can also be engineered synthetically (Baron et al., 1995; Liu et al., 2008; Reyes-Dominguez et al., 2008). In that case, the common structure features a central enhancer or enhancer repeats, flanked by two minimal promoters pointing in opposite directions. Similar as with IRES sequences the resulting proteins are never present as fusions and the expression is not necessarily ratiometric (Figure 2C). Studies have shown, that the minimal promoter that lies in the same direction as the enhancer is more efficiently activated than the minimal promoter that lies upstream (Andersen et al., 2011). Two individual proteins could of course be expressed by applying two unidirectional promoters, but the advantage of bidirectionality is that it most probably saves space on the expression vectors.

1.1.6 Regulation of gene expression

Regulating the expression of certain genes of interest can be achieved in several ways. For constitutive gene expression, promoters of different strength can be used. In the case of mammalian cells e.g. SV40, CMV-IE, EF1 α and PGK are applied. Constitutive expression can also be achieved synthetically by co-expressing the reporter plasmid with an operating sequence and minimal promoter together with a

DNA binding protein - transactivation domain fusion. Another option involves more complex systems, where gene expression is actively turned on or off by the application of chemicals or light. Representative examples will be discussed in more detail.

1.1.6.1 DNA-binding proteins and their operating sequences – constitutive and chemically regulatable gene expression

Constitutive expression from a synthetic operating sequence - minimal promoter system can be achieved with the GALACTOSE-RESPONSIVE TRANSCRIPTION FACTOR GAL4 binding domain (GAL4_{BD}) from *Saccharomyces cerevisiae* and the respective upstream activating sequence (UAS_G) (Fields and Song, 1989). Five repeats of the UAS_G are therefore cloned upstream of a minimal TATA-box promoter or P_{hCMVmin}, while the GAL4_{BD} is fused to a transactivation domain, like the virus derived VP16 (Figure 3A). The described parts can also serve as a base for split transcription factors in light regulated gene expression, which will be discussed later (Sadowski et al., 1988; Triezenberg et al., 1988; Müller et al., 2013b).

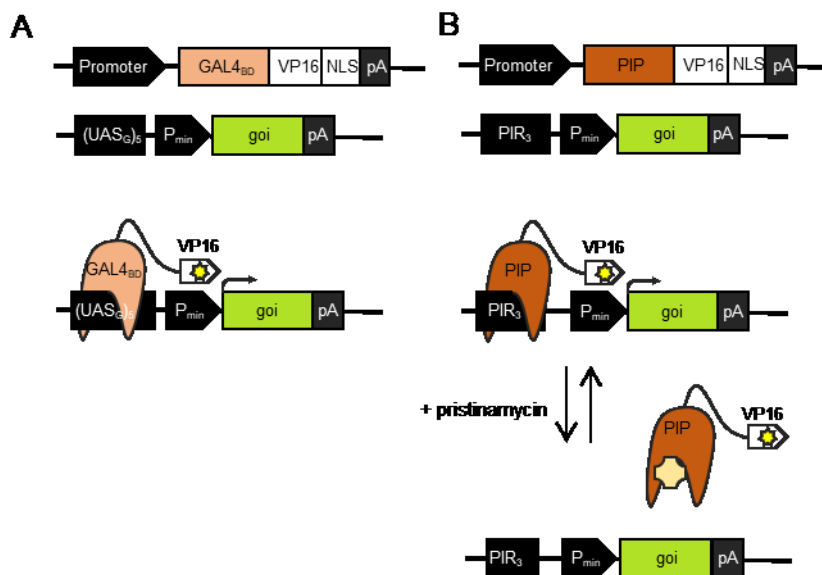


Figure 3: Mechanism of synthetic constitutive and chemically regulatable gene expression systems.

(A) The GAL4_{BD}-based, synthetic, constitutive gene expression system is encoded on two vectors. One comprises the DNA binding GAL4_{BD} fused to the transactivation domain VP16 and an NLS, under the control of a constitutive promoter. The second vector carries the (UAS_G)₅ operating sequence upstream of a minimal promoter, controlling a gene of interest (goi). GAL4_{BD} binds to its operating sequence, which brings the VP16 in close proximity to the minimal promoter, activating it and leading to constitutive expression of the goi. (B) The PIP-based, synthetic, chemically regulatable gene expression system is encoded on two vectors. One comprises the DNA binding protein PIP fused to the VP16 transactivation domain and an NLS, under the control of a constitutive promoter. The second vector carries the PIR₃ operating sequence upstream of a minimal promoter, controlling a goi. PIP binds to its operating sequence, which brings the VP16 in close proximity to the minimal promoter, activating the expression of the goi. Upon addition of pristinamycin binding of PIP is inhibited by the antibiotic and expression of the goi stops. Removal of pristinamycin reactivates the expression.

A similar set up can be found in the chemically regulatable PIP-PIR system. In this case the DNA binding protein is PRISTINAMYCIN-INDUCED PROTEIN (PIP) from *Streptomyces coelicolor*, which binds to three repeats of the pristinamycin resistance gene promoter (P_{ptr}) operating sequence PIR₃ (Figure 3B). In contrast to the GAL4_{BD}-(UAS_G)₅ system, binding of PIP to PIR₃ can be reversibly inhibited by pristinamycin, an antibiotic in the family of streptogramins. Therefore, the PIP-PIR system can be used for chemically regulated gene expression, but also in the same manner as GAL4_{BD} as part of a split transcription factor (Salah-Bey and Thompson, 1995; Fussenegger et al., 2000).

1.1.6.2 Light regulated gene expression

Photoreceptors are light-sensitive proteins which react to light of a certain wavelength, thereby changing their conformation, and as a consequence interact with e.g. transcription factors or other proteins. This interaction leads to differential gene expression in the host organism, mostly followed by developmental changes. Light regulated gene expression is based on these photoreceptors, which mainly originate from plants and bacteria, and that have been engineered into opto-switches. To do so, an output module, e.g. a transcriptional activation domain or repressor domain, is fused to the photoreceptor, influencing the expression of the target gene. To date, photoreceptors for gene expression control cover the whole extended spectrum of visible light from Ultraviolet B (UV-B) to Far-Red (Figure 4A). Commonly used photoreceptors are UV RESISTANCE LOCUS 8 (UVR8); Cryptochromes and light-oxygen-voltage (LOV) domains as well as plant and algal phytochromes (Ziegler and Möglich, 2015). Additionally, a green light responsive expression system has been published based on the bacterial light sensing transcription factor CarH (Chatelle et al., 2018).

UV-B light regulated gene expression is based on the *Arabidopsis thaliana* photoreceptor UVR8, involved in photomorphogenesis (Favory et al., 2009). In the absence of UV-light it homodimerizes and therefore is inactive. Upon illumination with light of 311 nm wavelength homodimers dissociate and UVR8 binds its interaction partner CONSTITUTIVELY PHOTOMORPHOGENIC 1 (COP1). This process does not rely on cofactors or substrates of any kind (Christie et al., 2012; Di Wu et al., 2012; Heijde and Ulm, 2013).

In synthetic biology distinct parts of these two proteins, namely amino acids (AA) 12—381 of UVR8 and the WD40 domain of COP1 are used in a split transcription

factor system to regulate gene expression with UV light (Figure 4B). In detail, UVR8 is fused to a DNA binding protein, whereas the WD40 domain of COP1 is fused to a transactivation domain. Upon light induction UVR8 homodimers dissociate and bind WD40. This interaction brings the transactivation domain in close proximity to a minimal promoter downstream of the operating sequence where the DNA binding protein is located, leading to expression of any gene of interest. The system is reversible in the absence of UV-light (Müller et al., 2013b).

A popular red-light sensitive gene expression regulation system is similarly constructed. The photoreceptor in this case is the *A. thaliana* phytochrome B (PhyB). Its functionality is dependent on the presence of the chromophore phytychromobilin which is covalently bound to the protein (Wagner et al., 1996). PhyB is sensitive to two distinct wavelengths of light. Illumination with red light of 660 nm leads to a conformational change of the chromophore and, in consequence, to a conformational change of PhyB as well (PhyB_{Pfr}). In this state it can interact, among others, with PHYTOCHROME INTERACTING FACTOR 6 (PIF6), a transcription factor regulating hypocotyl cell elongation. The interaction can be actively abolished by illumination with far red light of 740 nm or by dark reversion. Both options lead to the biologically inactive Pr form of PhyB (Eichenberg et al., 2000; Khanna et al., 2004).

For the split transcription factor gene expression system, the first 100 AA of PIF6 are fused to a DNA binding protein, while the first 650 AA of PhyB, containing the relevant domains, are fused to a transactivation domain (Figure 4C). Gene expression is then regulated by illumination with the respective wavelengths (Müller et al., 2013a).

While the chromophore phytychromobilin is naturally available in plants, it has to be added in sufficient amounts for e.g. use in mammalian cells. In that case, the culture medium is supplemented with a derivative, phycocyanobilin (PCB) extracted from cyanobacteria. As an alternative for use in mammalian cells, co-transfection with an expression vector for the conversion of heme to PCB is possible (Müller et al., 2013c).

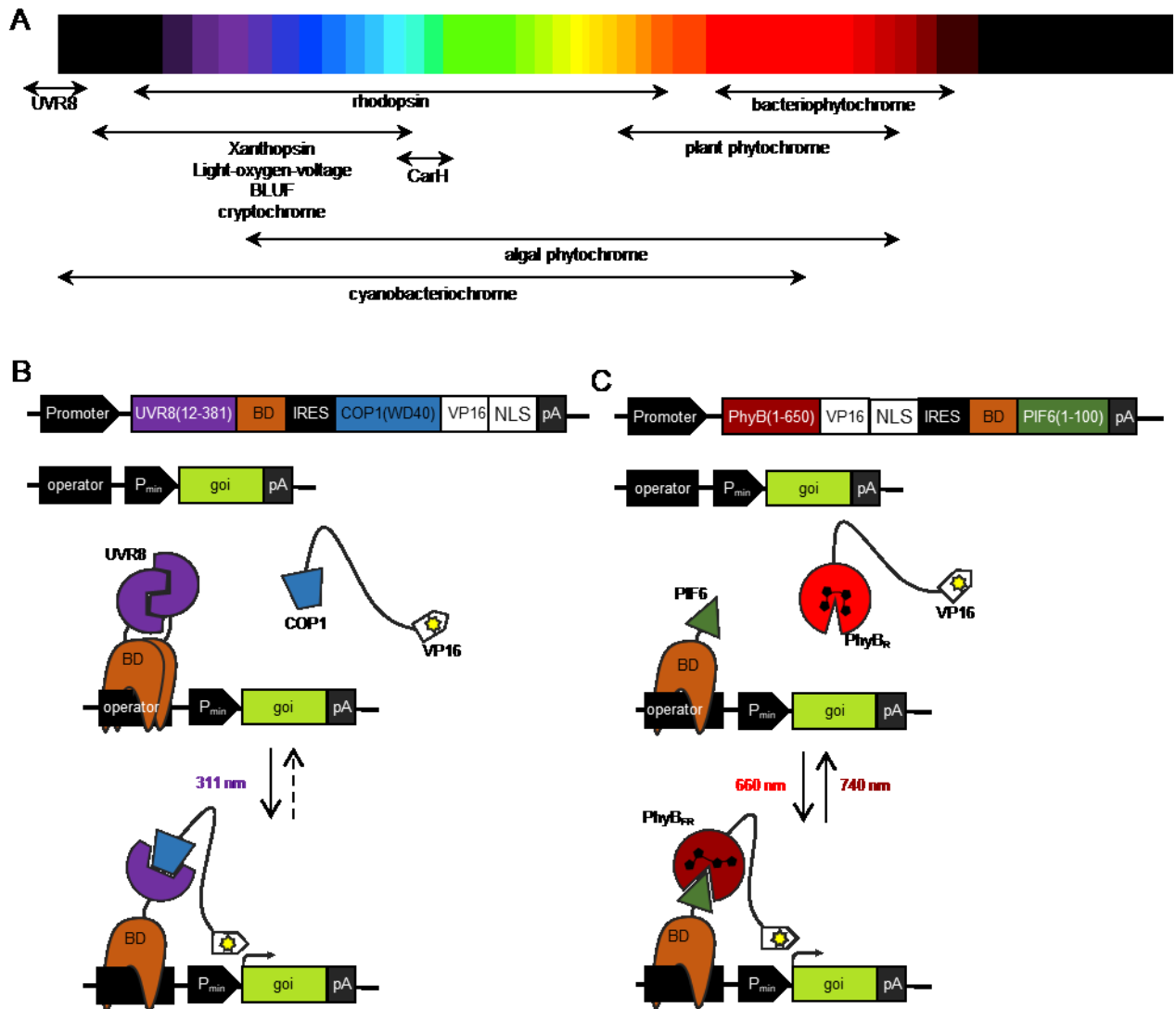


Figure 4: Spectral sensitivity of photoreceptors and mechanisms of light regulated gene expression.

(A) The spectral sensitivity of light sensing proteins ranges from the UV to the near-infrared region of the electromagnetic spectrum. (B) Design and function of a UV-B light regulated gene expression system. The building blocks are encoded on two vectors. The bicistronic vector encodes a split transcription factor consisting of the photoreceptor *Arabidopsis thaliana* UVR8 fused to a DNA binding protein and the *A. thaliana* COP1 WD40 domain fused to a VP16 transactivation domain. Expression of the second part is realized by an internal ribosome entry site. The second vector of the system carries an operating sequence upstream of a minimal promoter, controlling the expression of a *goi*. The DNA binding protein constantly binds to its respective operating sequence. The fused UVR8 forms homodimers in the absence of UV-B light. Upon illumination with light of 311 nm wavelength, the UVR8 homodimers dissociate and the COP1 WD40 domain can bind. As a consequence, the VP16 gets in close proximity to the minimal promoter, which is activated and expression of the *goi* is initiated. The mechanism is reversible in the absence of UV-B light. (C) Design and function of a red light regulated gene expression system. The building blocks are encoded on two vectors. The bicistronic vector encodes a split transcription factor, consisting of the photoreceptor *A. thaliana* PhyB fused to the VP16 transactivation domain and a DNA binding protein fused to *A. thaliana* PIF6. Expression of the second part is realized by an internal ribosome entry site. The second vector of the system carries an operating sequence upstream of a minimal promoter, controlling the expression of a *goi*. The DNA binding protein constantly binds to its respective operating sequence. In its biologically inactive form PhyB_R it can sense red light of 660 nm. This leads to a conformational change of its chromophore phytochromobilin/PCB and as a consequence also to a conformational change of PhyB. PhyB_{FR} binds to PIF6, which brings the VP16 transactivation domain in close proximity to the minimal promoter, thereby initiating gene expression. Upon illumination with far red light the conformational change is reversed, PhyB dissociates from PIF6 and expression is abolished.

1.2 Reconstruction of Phytohormone signaling pathways in plant and orthogonal cell systems

As plants are sessile organisms, they cannot avoid unfavorable growth conditions like changing light, temperature and humidity, lack of growth space and threats by pathogens. Therefore, they developed highly sensitive and specialized mechanisms to react and adapt to these changing stimuli (Koornneef and Pieterse, 2008; Depuydt and Hardtke, 2011). Many of them are based on phytohormones, which have been described first by Julius von Sachs and Charles Darwin, simultaneously (Darwin and Darwin, 1880). Phytohormones serve several purposes e.g. regulating seed germination, vegetative growth, flowering, development and responses to biotic and abiotic stress factors (Bernier and Périlleux, 2005; Gazzarrini and Tsai, 2015; Verma et al., 2016). Their structures are diverse and range from diterpenes over isoprenoids to aromatic compounds. Until now, a total of ten classes of phytohormones have been identified: auxins, abscisic acid (ABA), brassinosteroids, cytokinins, ethylene, gibberellins (GAs), jasmonate, nitric oxide, salicylic acid and strigolactones (Santner et al., 2009). Some of them, for example ABA and ethylene, comprise only of this one substance, while others like GAs and cytokinines comprise a larger family of molecules (Santner et al., 2009). For most phytohormones, several receptors or Co-receptors, as well as transcriptional repressors or activators exist in the genome of *A. thaliana*. To date, 29 Aux/IAAs as transcriptional regulators of auxin signaling are known and ABA perception is realized by a family of 14 receptors (Raghavendra et al., 2010; Wu et al., 2017). These are only two examples underlining the complexity of phytohormone signaling. Another layer of complexity is added by the fact that several signaling pathways are intertwined, like ABA, auxin, cytokinine and ethylene, which are all involved in abiotic stress responses (Sheen, 2010). With the help of molecular biology tools, specific aspects and components of the complex phytohormone signaling pathways can be analyzed and characterized quantitatively in minimal systems like protoplasts. By transferring parts of the pathways into orthogonal systems, even the availability of redundant proteins and crosstalk between pathways can be avoided, which is not possible in the host organism. The second part of this work concentrates on very few specific points in the signaling of GA and ABA, which are shortly presented in the following paragraphs.

1.2.1 Giberellins

Giberellins control processes like seed germination, vegetative growth and flowering, and therefore regulate several aspects of development and growth in general (Yamaguchi, 2008; Daviere and Achard, 2013). In *A. thaliana*, three GA receptors, GIBBERELLIN INSENSITIVE DWARF1 (GID1) -a, -b and -c, perceive the phytohormone upon which they associate with GA response proteins (Figure 5). Consequently, these so-called DELLA proteins (GA-INSENSITIVE, GAI; REPRESSOR-of-ga1-3, RGA; RGA-LIKE1, RGL1; RGL2 and RGL3) get polyubiquitinated by the SCF_{SLY1} E3 ubiquitin ligase complex, consisting of the F-Box protein SLEEPY1 (SLY1), the Arabidopsis SKP1-related (ASK1), and CULLIN1 (CUL1) (Dill et al., 2004; Daviere and Achard, 2013). This leads to proteasomal degradation of the DELLAs, which can no longer physically interact with transcriptions factors (TFs), resulting in changed regulation of target gene expression.

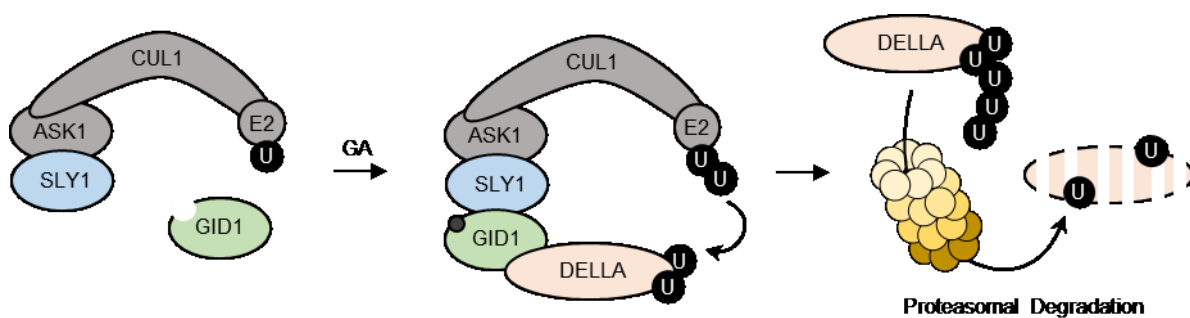


Figure 5: Gibberellin signaling components and perception in *Arabidopsis thaliana*.

Gibberellin perception is realized through a three-component perception complex. The mechanism relies on an SCF perception complex comprising the F-Box protein SLY1, ASK1, Cullin (CUL1), and an E3 ubiquitin ligase (containing an E2 ubiquitin-conjugating enzyme loaded with ubiquitin residues (U)). The Co-receptor GID1 perceives GA and associates with the perception complex through SLY1. Subsequently response proteins of the DELLA family bind to the SCF_{F-Box} complex, where they get polyubiquitinated and are sent for proteasomal degradation. As the DELLA proteins no longer bind to downstream transcription factors, target gene expression is altered.

One group of TFs influenced by GA signaling are PIFs. Their transcriptional activity is inhibited by DELLAs, especially during illumination, as DELLA levels increase with light. Upon GA perception and during shade phases or night, DELLA levels decrease, leading to the expression of genes involved in hypocotyl and/or petiole elongation by PIFs (Alabadí et al., 2007; Djakovic-Petrovic et al., 2007; Arana et al., 2011). The E3 ubiquitin ligase COP1 counteracts these processes. It promotes proteasome-dependent degradation of the respective TFs and gets inactivated by light perceived by certain photoreceptors. For COP1 to be active *in vivo*, it needs to

associate in a complex together with SUPPRESSOR OF phyA-105 proteins (SPA1 to 4) (Lu et al., 2015; Sheerin et al., 2015; Hoecker, 2017). As GA and COP1 signaling seem to act on opposite sides of growth regulation, the relation of DELLAs and the COP1/SPA1 complex has been analyzed in more detail in this work.

1.2.2 Abscisic Acid

The phytohormone Abscisic Acid is involved in growth, stomatal aperture, hydraulic conductivity and seed dormancy in response to drought and salt stress (Hubbard et al., 2010; Raghavendra et al., 2010; Gonzalez-Guzman et al., 2012). It is synthesized mostly in vascular tissues and then transported to the site of action, where it is actively taken up by ATP-dependent ABC-transporters (Kang et al., 2010; Kuromori et al., 2010). Its perception (Figure 6) is realized by a 14-member family of ABA receptors, namely the PYRABACTIN RESISTANCE1 (PYR1)/ PYR1-LIKE (PYL)/ REGULATORY COMPONENTS OF ABA RECEPTORS (RCAR)-Proteins (Raghavendra et al., 2010). While some members of this family are present as dimers (PYR1, PYL1, and PYL2), others have been shown to only act as monomers (e.g., PYL5, PYL6, and PYL8) (Dupeux et al., 2011; Hao et al., 2011). ABA-perception leads to interaction with PROTEIN PHOSPHATASE 2Cs (PP2Cs; clade A phosphatases type 2C) like ABA-insensitive1 (ABI1) and Hypersensitive to ABA1 (HAB1), upon which inactivation of SNF1-RELATED PROTEIN KINASE 2s (SnRK2s) is abolished (Park et al., 2009; Vlad et al., 2009). As a consequence, active SnRK2s phosphorylate target proteins, leading to differential gene expression, the production of second messengers and regulation of ion transporter activity (Hubbard et al., 2010).

In a recent study, it has been shown that specifically the receptor PYL8 is upregulated upon ABA perception, whereas all other tested receptors are targeted for proteasomal degradation. This upregulation seems to rely on elevated protein stability due to abolished polyubiquitination, but not on increased PYL8 mRNA (Belda-Palazon et al., 2018).

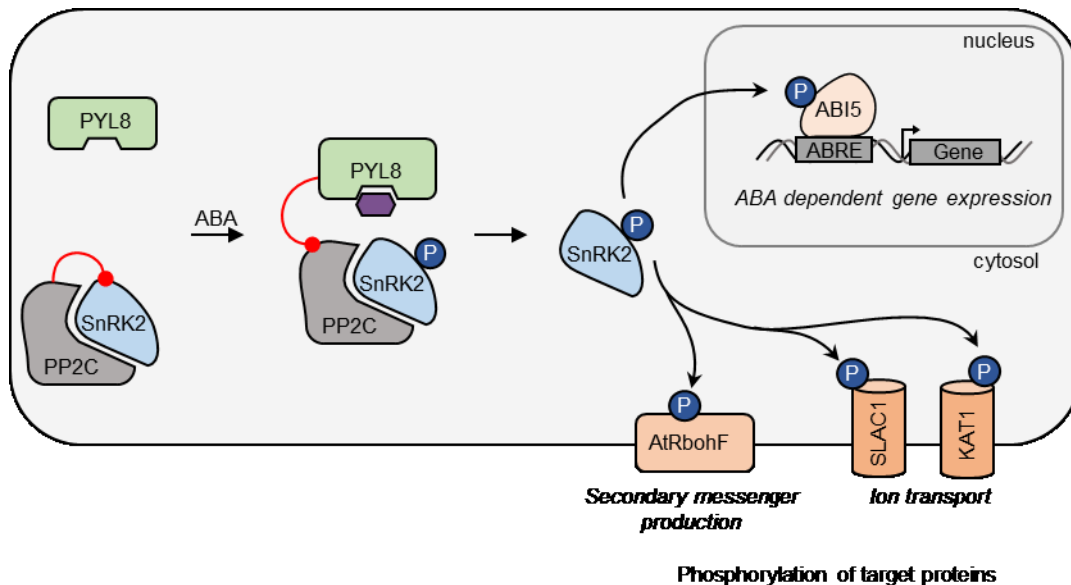


Figure 6: Abscisic acid signaling components and perception in *Arabidopsis thaliana*.

ABA receptors of the PYR/PYL/RCAR-protein family reside as monomers or dimers in the cell, while PP2Cs inhibit the phosphorylating activity of SnRK2s. Upon ABA perception, the receptor interacts with the PP2Cs. As a consequence, inactivation of SnRK2s is abolished, which now transfer phosphate (P) to target proteins, leading to differential gene expression, the production of second messengers and regulation of ion transporter activate (modified from Hubbard et al., 2010).

1.2.3 Ratiometric biosensors and the development of a cloning method for integration of short sequences

Luminescent, degradation-based, quantitative, ratiometric phytohormone biosensors have been developed by Wend et al., in 2013 and were first applied for characterization of auxin signaling. The sensor is engineered as a bicistronic expression vector, encoding renilla luciferase as an internal normalization element and a sensor module (SM) fused to firefly luciferase as the readout (Wend et al., 2013). The SM is commonly a regulator protein which is degraded upon perception of its respective phytohormone. A 2A-peptide located between the normalization element and SM-firefly ensures the stoichiometric co-expression of both proteins. In 2016, Samodelov et al., showed the applicability of this sensor for strigolactone signaling by incorporating SMXL6 as the regulated protein. Very recently Andres et al., have rebuilt the biosensor to investigate the role of all five DELLA proteins in gibberellin signaling more closely (manuscript in preparation).

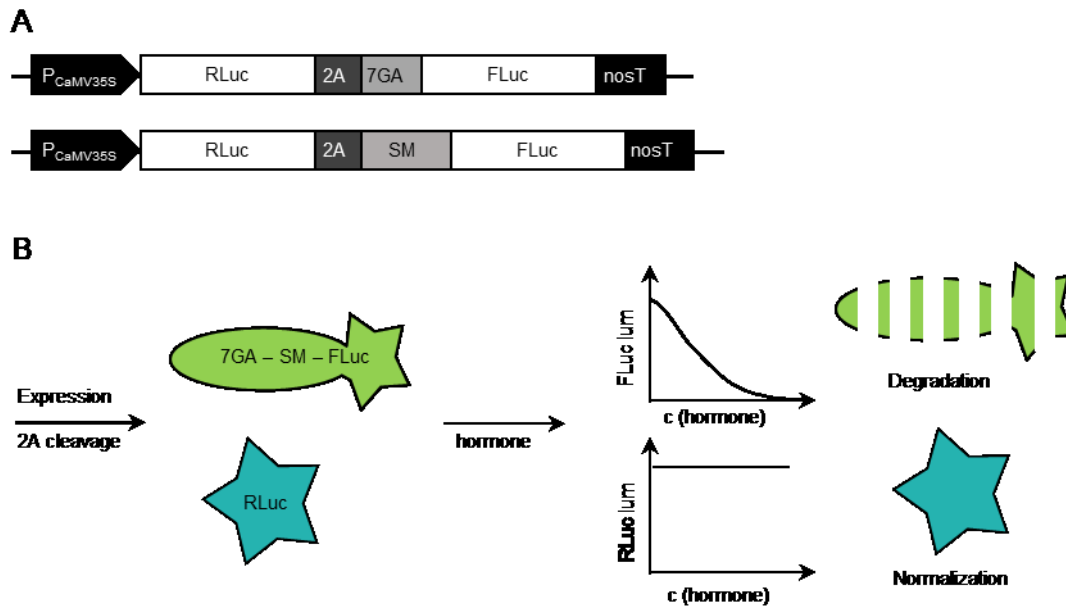


Figure 7: General genetically encoded, ratiometric, degradation-based phytohormone biosensor design. The biosensor construct expresses a renilla luciferase (RLuc) connected via a 2A peptide to a sensor module (SM) fused to a firefly luciferase (FLuc). The 2A peptide leads to the stoichiometric co-expression of the RLuc, as a normalization element, and the SM-FLuc fusion. Upon hormone induction, SM-FLuc becomes polyubiquitinated and is sent for proteasomal degradation, whereas RLuc expression remains constant resulting in a decrease in FLuc/RLuc ratio (modified from Samodelov et al., 2016).

In this work, a luminescent induction-based genetically encoded biosensor was constructed to analyze the effect of ABA on its receptor *PYL8* in *A. thaliana* mesophyll protoplasts. The design followed the discussed principle of Wend et al. (2013). Decreasing the endogenous ABA levels of protoplasts was applied to see more drastic changes after ABA induction. With the sensor modules tested so far, the induction fold between conditions varies to great extent. To assess the maximum potential induction fold of a degradation-based biosensor, the pifold vector was constructed, using a newly developed add-on to AQUA cloning, for the incorporation of short sequences into existing expression vectors.

2. Aims

In this work a synthetic toolbox for pathway engineering in *U. maydis* was constructed and implemented. Additionally, specific parts of the abscisic acid and gibberellin phytohormone signaling pathways were addressed in orthogonal systems. Hence, the aims of this work can be separated into two topics.

The main part of this work was dedicated to the implementation of synthetic tools in *U. maydis* as a work package of the Bioeconomy Science Center focus lab CombiCom. First of all, three luciferases and an alkaline phosphatase were tested as quantitative, enzymatic reporter genes and subsequently used for the characterization of further tools. In a second step, tools for the construction of bicistronic expression vectors, specifically IRES sequences and bidirectional promoters, were tested for their functionality and efficiency. The third aim was to find DNA binding protein – DNA operating sequence combinations, which should serve as the basis for split transcription factors for chemically regulatable gene expression systems. Lastly, the before mentioned tools were combined to generate light regulated gene expression systems for non-invasive regulation of gene expression, in a high spatiotemporal resolution.

The second part of this work focused on the study of molecular mechanism of phytohormone signaling by pathway reconstruction in *A. thaliana* protoplasts and mammalian cells. In detail, interaction of DELLA proteins with the COP1/SPA1 complex were studied in an orthogonal system microscopically and using the mammalian 2-/3-hybrid method. Finally, an induction-based, ratiometric phytohormone biosensor was established to characterize the behavior of the ABA receptor PYL8.

3. Results and Discussion

3.1 Engineering and Implementation of a synthetic (opto-) genetic toolbox for *Ustilago maydis*

The planning and experimental procedures of sections 3.1.1 (including 3.1.1.1 and 3.1.1.2) and 3.1.2.1 were executed in collaboration with Lisa Hüsemann and are therefore also discussed in her PhD thesis.

Production of pharmaceutically relevant substances is traditionally realized by chemical synthesis with several drawbacks. First of all, the novelty and diversity of products is limited due to the amount of reactions and reagents that can be handled. Secondly, many synthesis processes involve multiple protection/deprotection steps, harsh conditions and toxic organic solvents, while byproducts need to be disposed as chemical waste. Lastly, the costs can be relatively high for low yields.

For these reasons more and more compounds are produced biotechnologically and new production platforms are constantly needed to be able to satisfy the increasing demands of society. In 2018, 58% of the newly accepted pharmaceuticals in Germany were the result of biotechnology (<https://de.statista.com/>). Accordingly, the aim of the Bioeconomy Science Center, NRW in the course of the CombiCom focus lab among others, was the establishment of several new platforms for the production of high value compounds. One of them is the basidiomycete fungus *Ustilago maydis*. For the efficient production of these compounds, pathway engineering is one of the major tasks. Therefore, the engineering and implementation of a synthetic, (opto-) genetic toolbox is highly desirable. Figure 8 gives an overview of tools that have been engineered, tested and characterized in the following sections. As a start, enzymatic, quantitative reporter genes were implemented, which have been used to characterize all following tools. Subsequently tools for the construction of bicistronic expression vectors were tested in parallel with DNA binding proteins and their operating sequences, to be used as the basis for split transcription factor systems in light regulated gene expression.

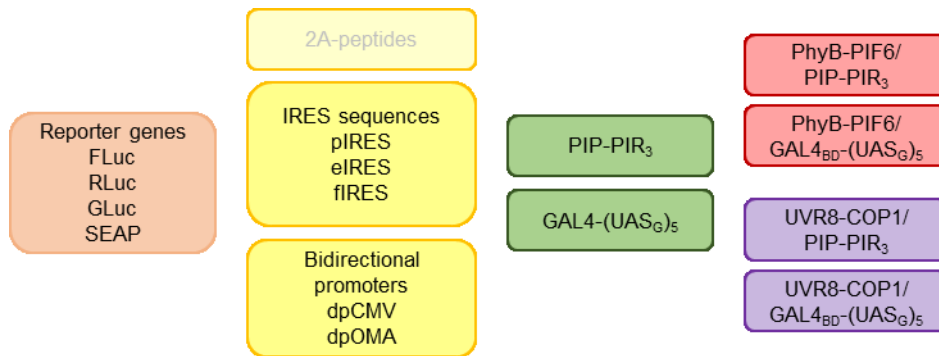


Figure 8: Synthetic (opto-) genetic toolbox for *U. maydis*.

In the course of this work, several synthetic (opto-) genetic tools for the regulation of gene expression in *U. maydis* were engineered and tested, including quantitative reporter genes, IRES sequences and bidirectional promoters and DNA binding proteins and their respective operating sequences. On the basis of these parts, light regulated gene expression systems were built and tested.

3.1.1 Establishment of enzymatic, quantitative reporter genes in *Ustilago maydis*

Quantitative reporter genes are not necessarily needed for pathway engineering, but they are essential for the characterization and comparison of several synthetic tools. Accordingly, three luciferases, namely firefly luciferase (FLuc), renilla luciferase (RLuc) and gaussia luciferase (GLuc), as well as the human secreted placental alkaline phosphatase (SEAP) were chosen for testing in *Ustilago maydis*. To start off with, the gene sequences were dicodon usage optimized, using an online tool by Finkernagel et al., 2011 (<http://dicodon-optimization.appspot.com/>) and ordered from Invitrogen GeneArt. They were cloned into an expression vector under the control of the strong constitutive promoter P_{O2tef} and C-terminally fused to an HA-tag (Figure 9A). For stable expression, constructs were integrated into the *upp3* locus of the *U. maydis* genome by transformation of strain AB33. Transformants were tested by antibiotic selection and counterselection before verification by southern blot analysis. In contrast to the usual culture volumes for cultivation of *U. maydis*, which start at a minimum volume of 20 ml in Erlenmeyer flasks, experiments were conducted in small scale of 3 to 6 ml culture in 15 ml glass reaction tubes, for several reasons. First of all, many variants of most tools were to be tested and experiments would get extensive and cumbersome. With smaller cultures, a higher throughput was possible. Second, as this work focused on the characterization of functionality, and not so much on the behavior and health state of *U. maydis*, small volumes were sufficient for our purposes. Lastly, in this way many resources such as space on shaking incubators and culture medium ingredients and time for the preparation of media,

could be saved. Therefore, most experiments were performed in small scale, if not indicated otherwise.

Enzymatic activity of the reporters was measured in the lysate and supernatant of over-night cultures of an $OD_{600} = 0.5$ for AB33, representing the wild type (WT) and each reporter strain (Figure 4B-E). While AB33 showed only background signals in firefly luminescence, around 100,000 absolute luminescence units (ALU) could be detected for the lysate of the FLuc-HA strain. The supernatant was also free from luminescence signal (Figure 4B). Renilla activity was very high with 800,000 ALU in lysates of the RLuc-HA strain, whereas the supernatant showed only around 3,000 ALU. Renilla luminescence was not detectable in the supernatant of AB33 and showed background signals of about 1,500 ALU in the lysates (Figure 4C).

The overall GLuc luminescence was very low compared to RLuc and FLuc with values between 2,000 and 2,500 ALU in lysate and supernatant of the GLuc-HA strain. The background signal in AB33 was even lower with 500 ALU in the lysate and almost no luminescence in the supernatant (Figure 4D). SEAP activity was not detectable either in the lysate or the supernatant of the SEAP-HA strain, which resembled the results for AB33 (Figure 4E).

Taken together FLuc and RLuc activity was very high in cell lysates, while GLuc showed less, but still detectable signals. Both RLuc and GLuc seem to be secreted into the culture medium by *U. maydis*, although RLuc is secreted to a much lesser extent. Secretion of RLuc was not expected, as it does not possess any signal peptides for secretion and this has not been observed before. It is most probably not an active secretion of the protein. As the general expression of RLuc-HA seems to be extremely high, it could be that a certain amount of protein is leaking out of the cells during cell division. Another possible reason could be that cell contents are released into the supernatant upon apoptosis or mechanical disruption of cells, and therefore a certain amount of functional RLuc-HA is residing in the culture medium.

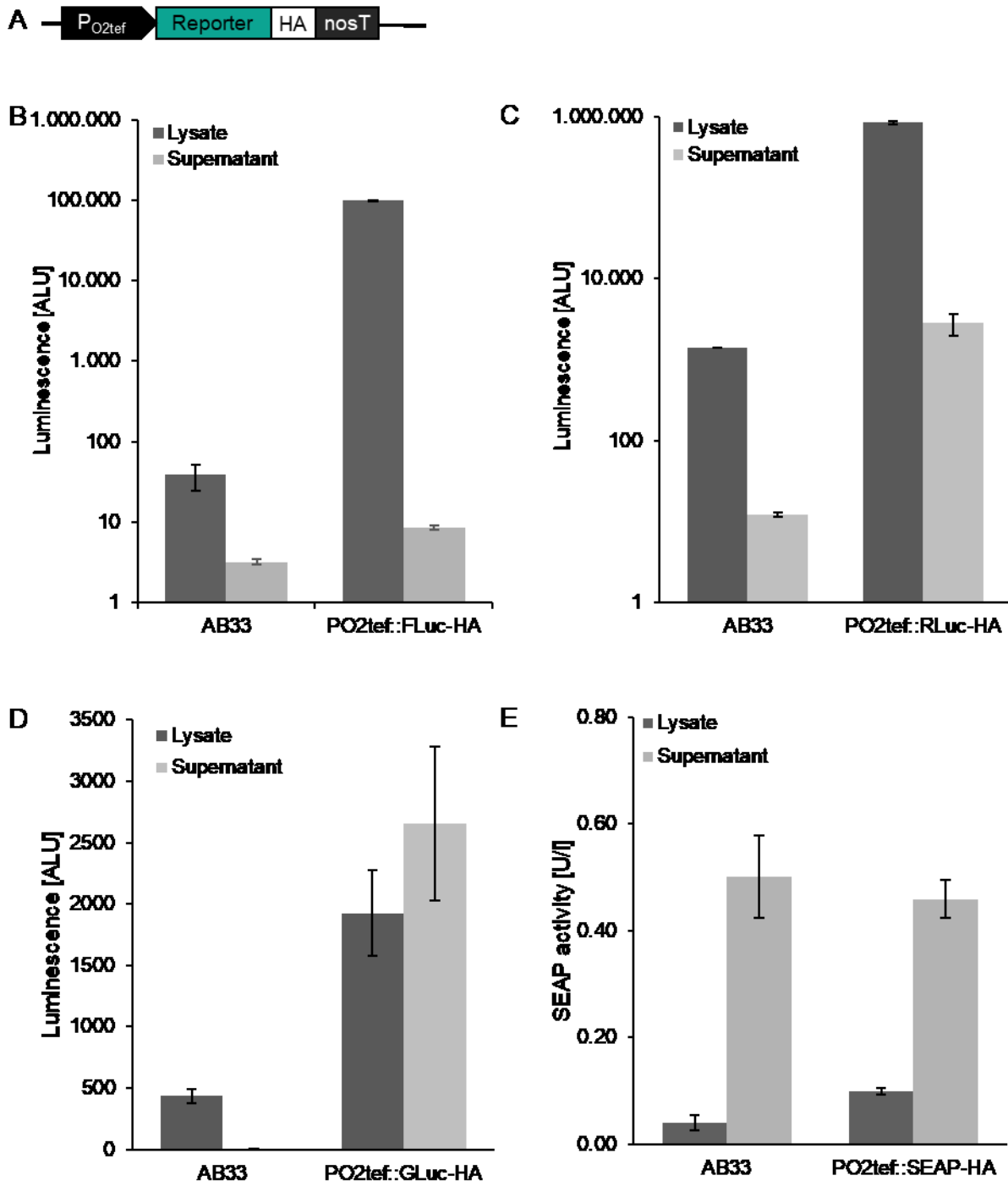


Figure 9: Enzymatic activity of quantitative reporter genes.

Whole cell lysates and culture supernatants of *U. maydis* cultures of an $OD_{600} = 0.5$ were analyzed for enzymatic activity of reporter genes. (A) Configuration of the constructs that have been transformed for stable integration into the *upp3* locus of the AB33 wild type strain. (B) FLuc luminescence of AB33 and FLuc-HA strain after addition of D-luciferin. (C) RLuc luminescence of AB33 and RLuc-HA strain after addition of 1:15 diluted Coelenterazine in PBS. (D) GLuc luminescence of AB33 and GLuc-HA strain after addition of 1:250 diluted Coelenterazine in PBS. (E) SEAP activity of AB33 and SEAP-HA strain after addition of 4-nitrophenyl phosphate. Luminescence is given as absolute luminescence units (ALU). The error bars represent the SEM of this individual experiment with $n=6$.

SEAP seems to not be functional in *U. maydis* in the presented configuration. This could be due to three reasons. First: SEAP might not be expressed in sufficient amounts or was too diluted to reach the threshold that can be measured in the assay,

which could be tested by RT-qPCR. Second: The polypeptide might not get folded properly, resulting in unfunctional protein. Third: The C-terminal HA-Tag might change the protein 3D structure or somehow inhibit binding of the substrate, leading to no activity.

Due to time and material limitations, a RT-qPCR was not possible. Experiments to confirm or discard any of the other options were carried out. To test if full length SEAP protein is present in the SEAP-HA strain, a western blot was performed (Figure 10). Strong bands for FLuc-HA and RLuc-HA could be detected at the expected sizes of 142 and 80 kDa, respectively. A slight band was also visible for GLuc-HA in the lysate at the expected size of approximately 48 kDa, but not in the supernatant, probably due to low protein concentrations, which resembles the lower luminescence measured for this reporter. SEAP on the other hand, was neither detectable in the lysate or in the supernatant at an expected size of 130 kDa. Thus, the amount of SEAP protein is too low to be detected in a western blot, if present at all.

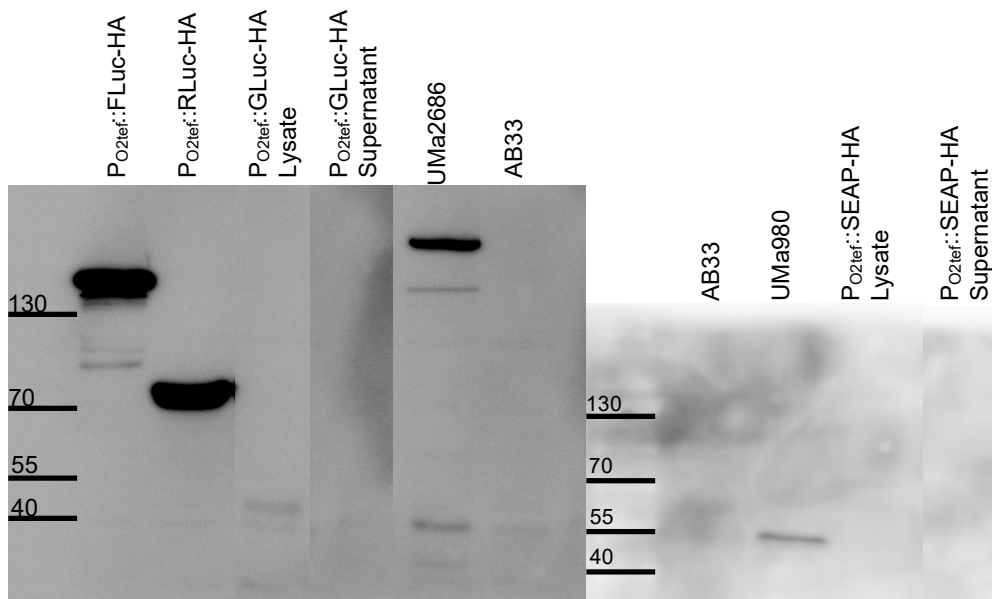


Figure 10: Western Blot analysis of *U. maydis* reporter strains.

10 μ g protein from whole cell lysates and TCA-precipitated protein of culture supernatant of the indicated strains were run on a 10% SDS gel, blotted onto a PVDF membrane and labeled with a mouse-anti-HA antibody as first antibody and an HRP-conjugated anti-mouse antibody as secondary antibody. Detection with an ImageQuant LAS 4000 was performed after incubation with ECL detection substrate for five minutes. FLuc-HA, RLuc-HA and GLuc-HA were detected at their expected sizes of 142, 80 and 48 kDa, respectively, in the cell lysates. GLuc-HA was not detectable in the culture supernatant. SEAP-HA was not detectable in cell lysates or supernatant. AB33 serves as the WT negative control. UMA2686 and UMA980 are HA-positive controls. Results represent two individual blots; Membrane parts have been arranged for better order of samples. Size standard is given in kDa.

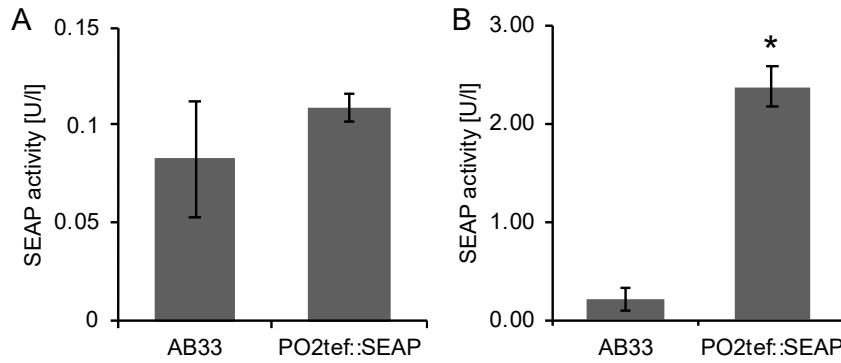


Figure 11: SEAP activity of AB33 and P_{O2tef}-SEAP.

SEAP activity was determined in 100 µg protein of whole cell lysates and the supernatant of cultures with an OD₆₀₀ = 0.5. (A) SEAP activity of AB33 and P_{O2tef}-SEAP in the culture supernatant after addition of 4-nitrophenyl phosphate. (B) SEAP activity of AB33 and P_{O2tef}-SEAP in whole cell lysates after addition of 4-nitrophenyl phosphate. The error bars represent the SEM of this individual experiment with n=3. (*) indicates statistically significant difference between the strains with p<0.005 (students t-test).

Next, a strain was generated that expressed SEAP under the control of the same constitutive promoter, also in the *upp3* locus, but without the C-terminal HA-tag. A SEAP assay was performed with samples from culture supernatant, where no SEAP activity could be measured (Figure 11A). Furthermore, cell lysates of this strain were tested for SEAP activity, to see if it resides inside the cells (Figure 11B). Here, a slight SEAP activity of about 2.5 U/l was measured, which was significantly higher than for AB33.

In conclusion, all three luciferases are functional in *U. maydis* and can be used as quantitative reporter genes for the characterization of other tools. While RLuc and FLuc are more sensitive and smaller variations in gene expression can be visualized with their help, GLuc can be measured very fast and easy as it is secreted into the culture medium. SEAP is not secreted from *U. maydis* cells and the general protein abundance is very low. Hence, it is not qualified for use as a quantitative reporter gene in *U. maydis*.

3.1.1.1 A fast screening platform for the generation and characterization of *U. maydis* strains

The generation of *U. maydis* strains is relatively time consuming, compared to transient transformation of e.g. plant leaf material and plant protoplasts or transfection of mammalian cells, where synthetic tools can be tested in less than a week, once the plasmid encoding the tool is available. Additionally, most of the tools to be established come in many variants, which gives rise to a long list of strains, that need to be generated. The previous experiments have shown that the substrates D-

luciferin and coelenterazin are very specific for their enzymes and have a low background signal in *U. maydis* culture medium, compared to the actual enzymatic signal. This led us to the idea for using them as a fast screening system in the generation of strains, as most of the ones produced in this work, would carry at least one of the reporters along with other tools to be tested. To save even more time, the measurability of luciferase activity in the pure untreated cultures was tested. Cultures were grown over-night to an $OD_{600} = 0.5$ and whole cell lysates of 2 ml of each culture were produced. Cell lysates were analyzed for their luciferase activity over 20 minutes, in parallel with the untreated cultures, from which the lysates originated (Figure 12).

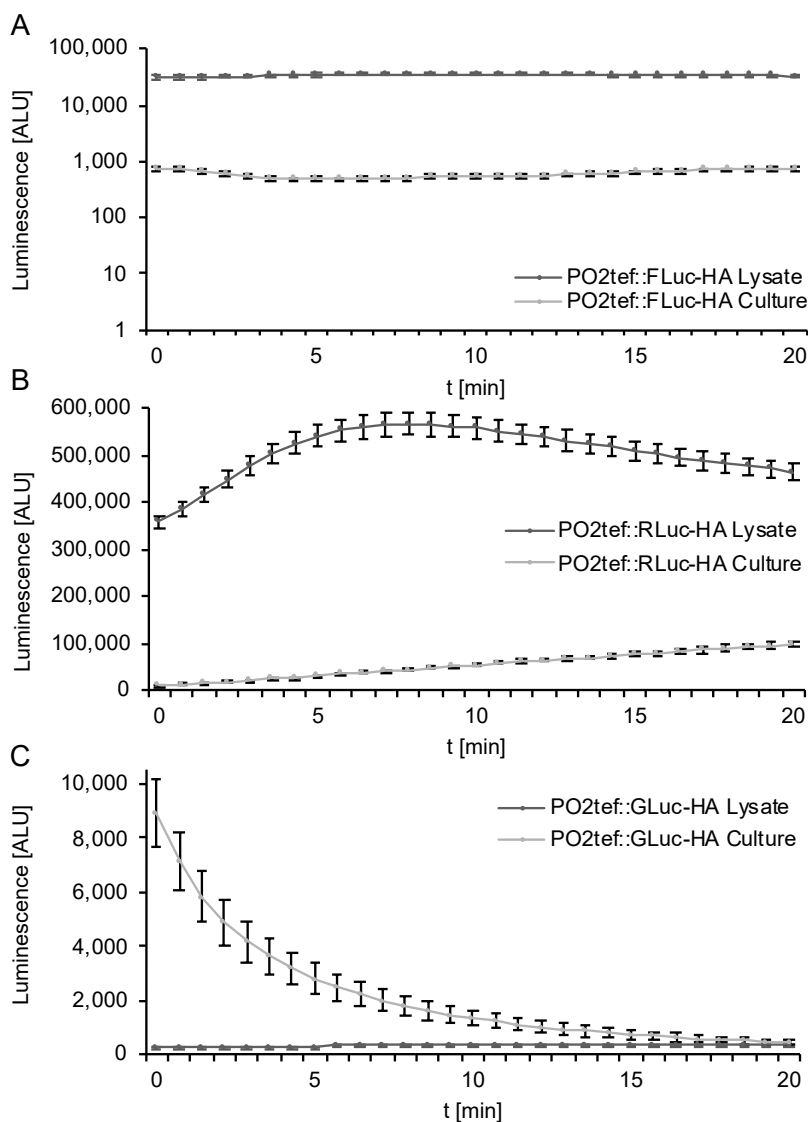


Figure 12: Fast-screening assays for luciferases.

Whole cell lysates of 2 ml culture and the respective cultures with an $OD_{600} = 0.5$ of constitutively expressing luciferase strains were analyzed for their luminescence over 20 minutes after addition of substrates. (A) FLuc luminescence. (B) RLuc luminescence. (C) GLuc luminescence. Luminescence is given in absolute luminescence units. Error bars represent the SEM for this individual experiment with $n=3$

FLuc luminescence was constant in the lysate with over 30,000 ALU and varied slightly in the culture between 470 ALU and 750 ALU (Figure 12A). RLuc luminescence increased over the first 7 min from 360,000 ALU to 567,000 ALU and then slowly decreased again to around 465,000 ALU in the lysate. Contrary, the signal in the supernatant started out with only 11,000 ALU and constantly increased over time to 97,000 ALU (Figure 12B). When the mean values over the whole 20 min are calculated and the luminescence in the lysate is set to 100 %, the supernatant of FLuc and RLuc strains showed 1.75 % and 10.5 % luminescence signal, respectively. As it was previously shown that GLuc is secreted into the supernatant, it was no surprise that it was also measurable in the untreated cultures, whereas the lysate exhibited no more than background signal (Figure 12C). The general GLuc abundance is quite low and the catalyzed reaction is relatively fast, which is why the strongest signal and therefore the optimal measuring time point are the first 5 min after substrate addition.

In summary, all three luciferases can be used to quickly screen transformants for their expression by simply adding substrate to the cultures and analyze the samples in a plate reader.

3.1.1.2 Gene expression normalization with quantitative reporter genes

One common application of quantitative reporter genes is the use as a normalization element of one reporter, while the second reporter serves as a readout for the change of expression, protein interaction or protein abundance upon a specific stimulus. Thus, independent experiments can be compared without the influence of biological fluctuations of the organism. Especially ratiometric phytohormone biosensors and light regulated gene expression systems make use of this mechanism, but also the efficiency of IRES sequences and bidirectional promoters can be assessed in this way.

To test if this can also be applied in *U. maydis*, a strain was generated, expressing FLuc under the control of the inducible CRG promoter, which is activated upon change of carbon source, and RLuc under the control of the constitutive O2tef promoter, both in the *upp3* locus (sNH039; Figure 13 A). The absolute FLuc and RLuc luminescence of whole cell lysates from 2 ml culture of the normalization strain, the constitutively expressing RLuc strain (sLHNNH005) and an inducible FLuc strain (UMa3212) was measured every hour over 8 hours after shifting the cultures from CM-Glucose to CM-Arabinose for induction of P_{CRG1} or CM-Glucose as a control and

normalized to an $OD_{600} = 0.5$ (Figure 13C). The actual optical density of the cultures was monitored over time, to ensure that they were in the exponential growth phase during the experiment (Figure 13B).

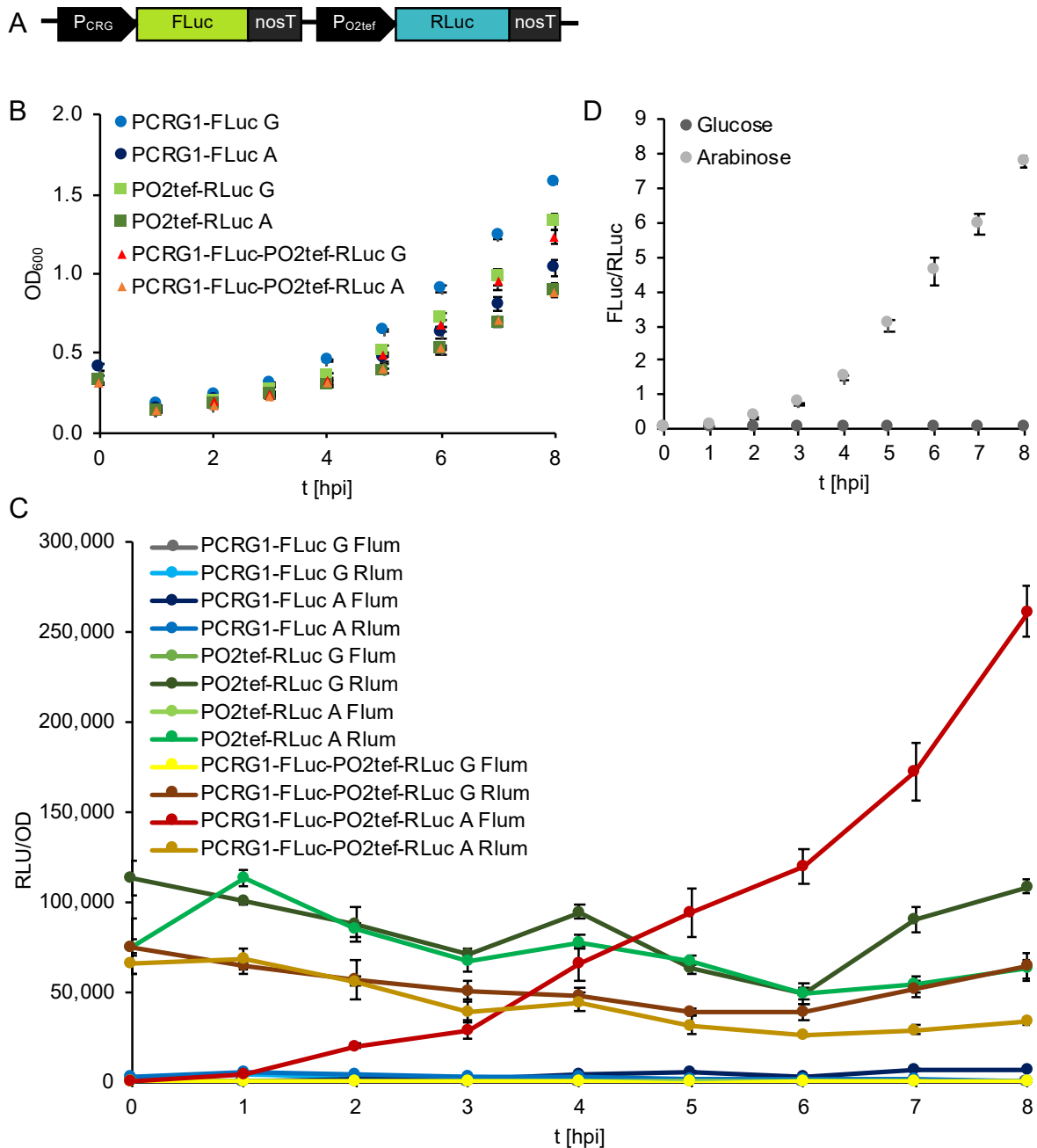


Figure 13: Normalization of gene expression in *U. maydis*.

(A) Configuration of the construct that has been transformed into the *upp3* locus of AB33 for generation of the normalization strain sNH039. (B) OD_{600} of the indicated strains. (C) Absolute luminescence of whole cell lysates from 2 ml culture of the indicated strains is shown normalized to an $OD_{600} = 0.5$. Cultures have been grown overnight in CM medium supplemented with 1% Glucose (G) and were shifted to CM medium supplemented with 1% Arabinose (A) or 1% Glucose at timepoint 0. Samples have been taken every hour, lysed all at once and analyzed for FLuc luminescence (Flum) and RLuc luminescence (Rlum). (D) Absolute FLuc to RLuc ratio of the normalization strain over time. Error bars represent the SEM of this individual experiment with $n=3$.

RLuc luminescence was relatively constant in sLHNH005 and sNH039 over 8 h under both sugar conditions, with 30,000 to 100,000 ALU depending on the strain (Figure 13C). Both strains only showed background signals for FLuc luminescence, as was expected. While sNH039 and UMa3212 showed no FLuc luminescence in Glucose supplemented medium, it steadily increased over time in medium with 1% Arabinose. Unfortunately, the increase of FLuc luminescence in UMa3212 (dark blue) is not as noticeable as in sNH039 (bright red). Comparing the values from t0 and t8, UMa3212 shows a 400-fold induction, while sNH039 shows almost 3,700-fold induction in CM-Arabinose. The absolute FLuc to RLuc luminescence ratio was calculated for the normalization strain for every timepoint (Figure 13D). FLuc expression is increasing over time relative to the constitutively expressed normalization element RLuc, which was expected to happen after induction of the FLuc controlling promoter. This experiment nicely demonstrates the use of a normalization element that is not reacting to the stimulus of interest in *U. maydis* cultures.

3.1.2 Implementation of tools for bicistronic expression in *U. maydis*

The generation of stably expressing *U. maydis* strains is time consuming and involves several steps from transformation of protoplasts to the verified strains compared to a simple transfection of mammalian cells. For the integration of more than one construct into this fungus, intermediate strains have to be generated, one for each construct. Due to the fact that stable strains are always used for *U. maydis*, and co-transformation is very inefficient, a maximum of two constructs to be integrated into the genome is advantageous, as it saves time and material. For the engineering of light regulated gene expression systems, which are based on split transcription factors, three parts are actually needed, hence two of the parts, namely the split transcription factor (TF), is normally encoded on a bicistronic expression vector. Additionally, for tight regulation systems it is also necessary to have the certainty of unfused proteins for the split TF.

In this section, only expression tools which lead to 100% separated proteins, specifically IRES sequences and bidirectional promoters, will be discussed.

3.1.2.1 IRES sequences

Three commonly used IRES sequences from *human poliovirus*, *encephalomyocarditis virus* and *foot-and-mouth-disease virus* have been chosen for

testing in *U. maydis* (Figure 14B). Constructs were designed both with the fluorescence proteins mKate2 and eGFP, fused to a NES and NLS respectively, and with FLuc and RLuc. eGFP-NLS and FLuc were always under the control of the IRES sequences (Figure 14A) while mKate2-NES and RLuc were constitutively expressed. For fluorescence analysis, the strains were grown over night in CM-Glucose, samples were taken and fluorescence was measured in a plate reader, before shifting the cultures to NM-Glucose for the induction of filamentous growth. Six hours later, samples of filamentous cultures were again analyzed in the plate reader as well as under the microscope. AB33 and strains for the constitutive expression of eGFP and mKate2 were used as the controls. AB33 showed low auto-fluorescence in the eGFP channel, visible under the microscope (Figure 14C) and in the plate reader (Figure 14D), and even lower auto-fluorescence in the mKate2 channel, which was only detectable with the plate reader. The positive controls showed high fluorescence levels between 9,000 and 26,000 absolute fluorescence units (AFU), with filaments showing more fluorescence than sporidia in both channels. IRES-containing strains showed a generally low fluorescence, both microscopically and in the plate reader. mKate2 fluorescence in the IRES strains was between 3 and 11 times higher than in AB33 while it was almost 200 times higher in the positive control. Moreover, eGFP fluorescence of the IRES strains was comparable to the auto-fluorescence observed in AB33. Similar results were obtained with luciferases as the reporter. While AB33 showed the usual low background signal, the positive controls, constitutive FLuc and RLuc, exhibited between 400,000 and 500,000 ALU. RLuc luminescence was between 11,000 ALU and 146,000 ALU but FLuc luminescence of all three IRES stains resembled that of the wt.

To enhance the expression of IRES constructs, they have been re-cloned with the very strong constitutive promoter pOMA, which consists of 8 repeats of the prf1 enhancer and the mfa1 minimal promoter (A. Brachmann, unpublished data). It was not possible to generate strains with these constructs. Only very few transformants were obtained to begin with, probably due to toxicity, and the ones obtained were identified as false positives after the counterselection process.

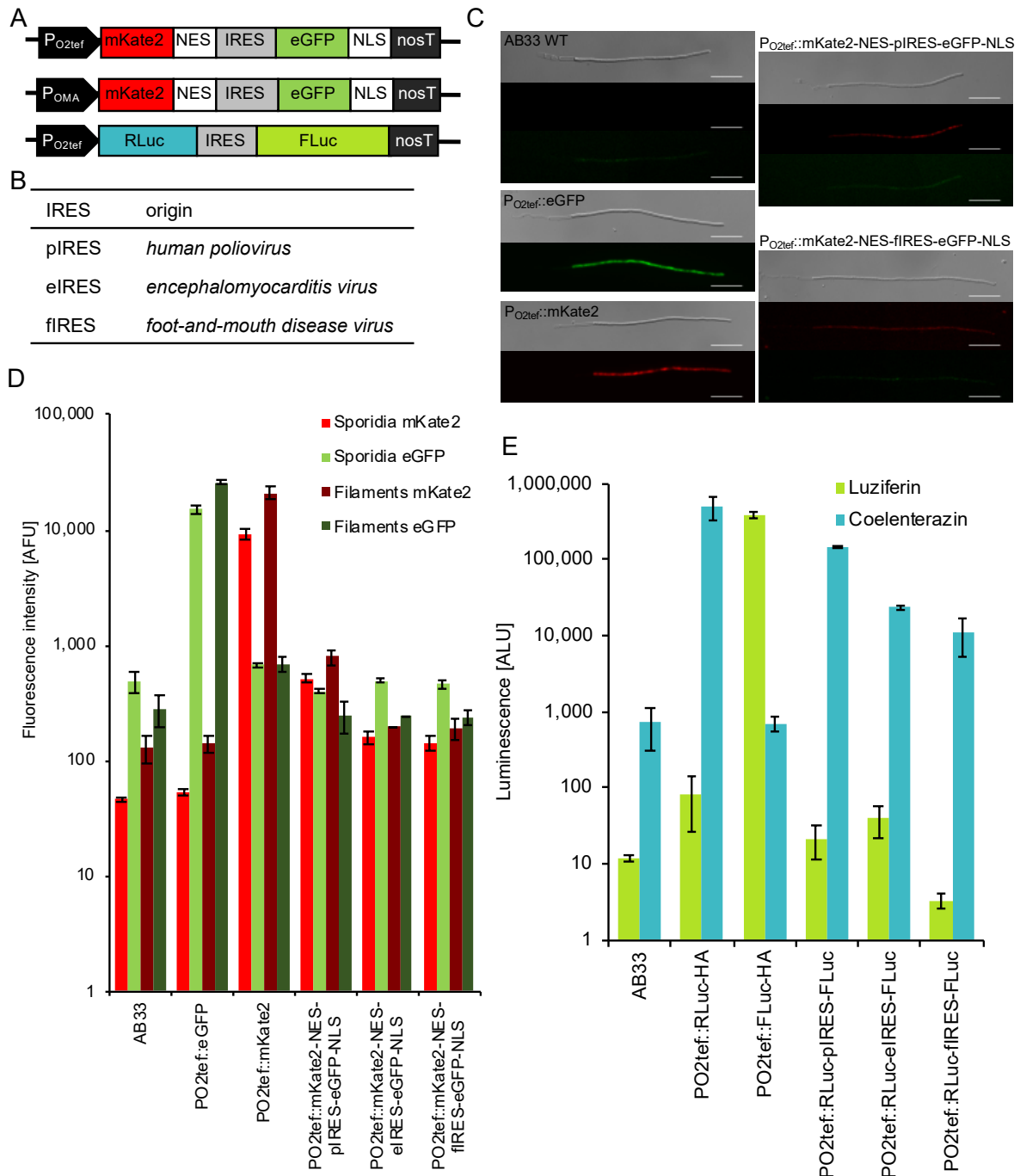


Figure 14: Establishment of IRES sequences in *U. maydis*.

(A) Configuration of the vectors that have been transformed into the *upp3* locus of AB33 with the IRES sequences listed in (B). (C) Microscopic analysis of WT AB33, mKate2 and eGFP positive controls and piRES and fiRES strains six hours after induction of filamentous growth. Scalebars represent 20 μm . (D) Fluorescence intensity of controls and IRES strains measured in cultures of an $\text{OD}_{600} = 0.5$ in sporidia and six hours after induction of filamentous growth in a plate reader is given in absolute fluorescence units (AFU). (E) Absolute luminescence of whole cell lysates from 2 ml culture with an $\text{OD}_{600} = 0.5$ of the indicated strains is shown. Error bars represent the SEM of the individual experiments with $n=3$.

The IRES sequences were not codon optimized before cloning, as they are not translated. Potentially the sequences contain unfavorable dicodons, which lead to inefficient transcription of eGFP-NLS and FLuc due to premature mRNA

polyadenylation, which was observed before, for non-dicodon-optimized heterologous sequences (Zarnack et al., 2006). If that was the problem, at least mKate2-NES and RLuc should be detectable in significantly higher amounts, comparable to the positive controls, as they are under the control of the same constitutive promoter. To exclude this possibility, the constructs would have to be re-cloned with dicodon usage optimized IRES sequences and tested again. More likely, the whole mRNA containing the IRES is detected as harmful to the cells, by whichever complex that could potentially bind to the secondary structures of the IRES, and lead to degradation of the mRNA, resulting in a generally low expression from these constructs. This hypothesis is supported by the fact that stronger expression of the IRES sequence seems to be toxic and strains transformed with the pOMA-IRES constructs are not viable. RT-qPCRs would clarify this.

In conclusion, the current amount of proteins in strains carrying IRES constructs is not sufficient for biotechnological applications or synthetic expression systems.

3.1.2.2 Bidirectional promoters

The alternative to IRES sequences for the expression of split transcription factors from a bicistronic construct are bidirectional promoters. In the course of this work, two synthetic bidirectional promoters have been constructed and tested in *U. maydis*. They comprised a central enhancer region or repeats of an enhancer and a minimal promoter on either side of it. The first one was designed as shown in Andersen et al., 2011, with the CMV immediate early promoter enhancer surrounded by two CMV minimal promoters. Following this design, a second promoter was constructed using endogenous parts, in case the CMV promoter might not be functional in *U. maydis*. To this end, four repeats of the *prf1* enhancer were used as the core, surrounded by two *mfa1* minimal promoters (Figure 15A and C). Both bidirectional promoters, further called dP_{CMV} and dP_{(prf)4}, were cloned either with mKate2-NES and eGFP-NLS or FLuc and RLuc as reporters. Additionally, two versions of each were cloned in a way that once either eGFP or FLuc were located downstream, and mKate2 or RLuc upstream relative to the enhancer, and once inverted, so that mKate2 or RLuc were located downstream of the enhancer. These versions are further called dP_{CMV}-A and dP_{CMV}-B, as well as dP_{(prf)4}-A and dP_{(prf)4}-B.

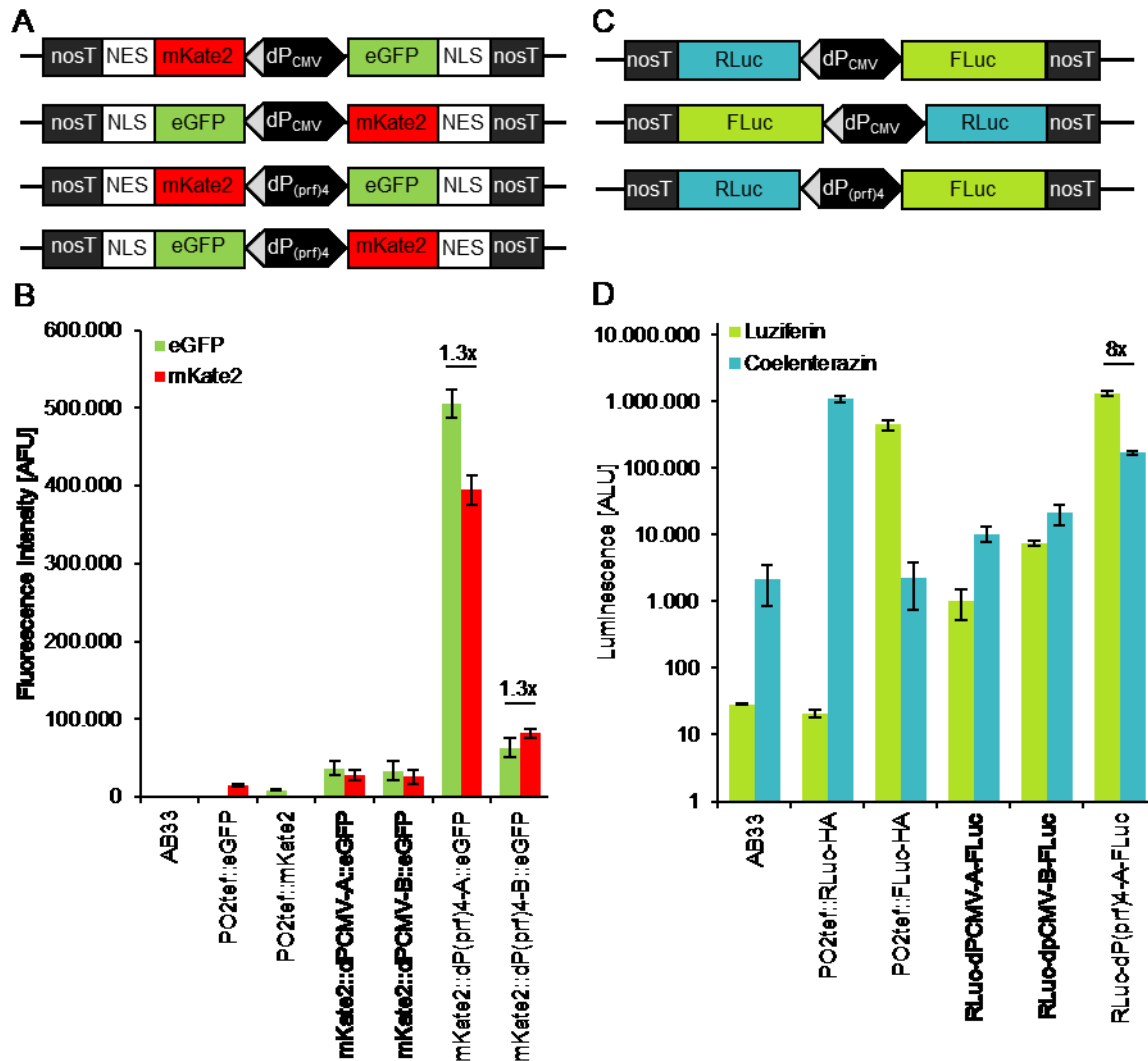


Figure 15: Establishment of bidirectional promoters in *U. maydis*.

(A + C) Configuration of constructs that have been transformed into the *upp3* locus of AB33. The minimal promoter that is located upstream of the enhancer is on the light grey end of the bidirectional promoter (bP). (B) Fluorescence intensity of controls and bP strains measured in cultures of an $OD_{600} = 0.5$ in a plate reader is given in absolute fluorescence units. (D) Absolute luminescence of whole cell lysates from 2 ml culture with an $OD_{600} = 0.5$ of controls and bP strains is shown. Error bars represent the SEM of the individual experiments with $n=3$.

Seven strains were generated, carrying the various versions of bidirectional promoters, and analyzed for their fluorescence or luminescence, respectively. The dP_{CMV}-A and -B strain both showed about 35,000 absolute fluorescent units (AFU) of eGFP and around 27,000 AFU of mKate2, which is approximately 2.5 to 3 times more than the positive controls (Figure 15B). The fluorescence intensities measured for dP_{(prf)4}-A and -B differ quite a lot. While dP_{(prf)4}-A showed over 500,000 AFU in the eGFP channel and almost 400,000 AFU for mKate2, dP_{(prf)4}-B only exhibited 82,000 and 63,000 AFU for mKate2 and eGFP, respectively. Nonetheless, for the two versions of dP_{(prf)4} the relative amount of expressed protein is 1.3 times more of that

located downstream of the enhancer, than of the one upstream to it. This resembles the results obtained by Andersen et al., who showed that the minimal promoter, that lies aligned to the naturally occurring orientation with the enhancer, is activated more efficiently than the one opposite to it. dP_{CMV}-A and -B did not show such a behavior, which could be due to the relatively low fluorescence intensities with high SEM. While the fluorescent version showed more eGFP in both orientations, in the luminescent dP_{CMV}-A and -B RLuc was the more abundant signal (Figure 15D). Moreover, dP_{CMV} driven expression was less efficient for luciferases than for fluorescent proteins, when compared to their respective positive controls. The FLuc luminescence for dP_{(prf)4}-A was almost 8 times higher than RLuc with 1.35 million to 170,000 ALU, respectively. Unfortunately, a luminescent dP_{(prf)4}-B could not be tested, due to cloning issues. Consequently, it cannot be said if the changed orientation would have also changed the luminescence ratio of FLuc and RLuc as it did in the fluorescent versions. Additionally, FLuc and RLuc luminescence highly depend on their enzymatic properties, which is why they can't necessarily be compared 1:1 as the fluorescence signals from two fluorescent proteins.

Generally, one can conclude that both engineered bidirectional promoters are functional in *U. maydis*. The lowest achieved expression, which was FLuc under the control of dP_{CMV}-A was still 36-fold higher than the background signal measured in AB33. While this is more suitable for testing synthetic tools, the engineered dP_{(prf)4} could be an interesting candidate for use in biotechnology with very strong constitutive expression at a non-toxic level.

3.1.3 DNA binding protein – operating sequence interaction studies

After establishing bidirectional promoters for the construction of bicistronic vectors, the next part on the way of building a light regulated gene expression system was to find a suitable DNA-binding protein – operating sequence pair as the basis for the split transcription factor. Requirements thereof are a minimum of leakiness from the operating sequence - minimal promoter combination and a high induction fold of expression when including the DNA binding protein - transactivation domain fusion. Accordingly, two DNA binding proteins and their respective operating sequences, namely PIP and PIR₃ as well as GAL4_{BD} and (UAS_G)₅, have been characterized (Figure 16A). To obtain the optimal combination of minimal promoter and transactivation domain with the two systems, they were cloned with either the

orthogonal $P_{hCMVmin}$ or the endogenous $P_{mfa1min}$ and with the p65 transactivation domain or a short version of the VP16 transactivation domain, hereafter called VP16ff. Reporter constructs were again integrated into the *upp3* locus, while the transactivation domain containing parts were integrated into the *cco1* locus in the AB33 background.

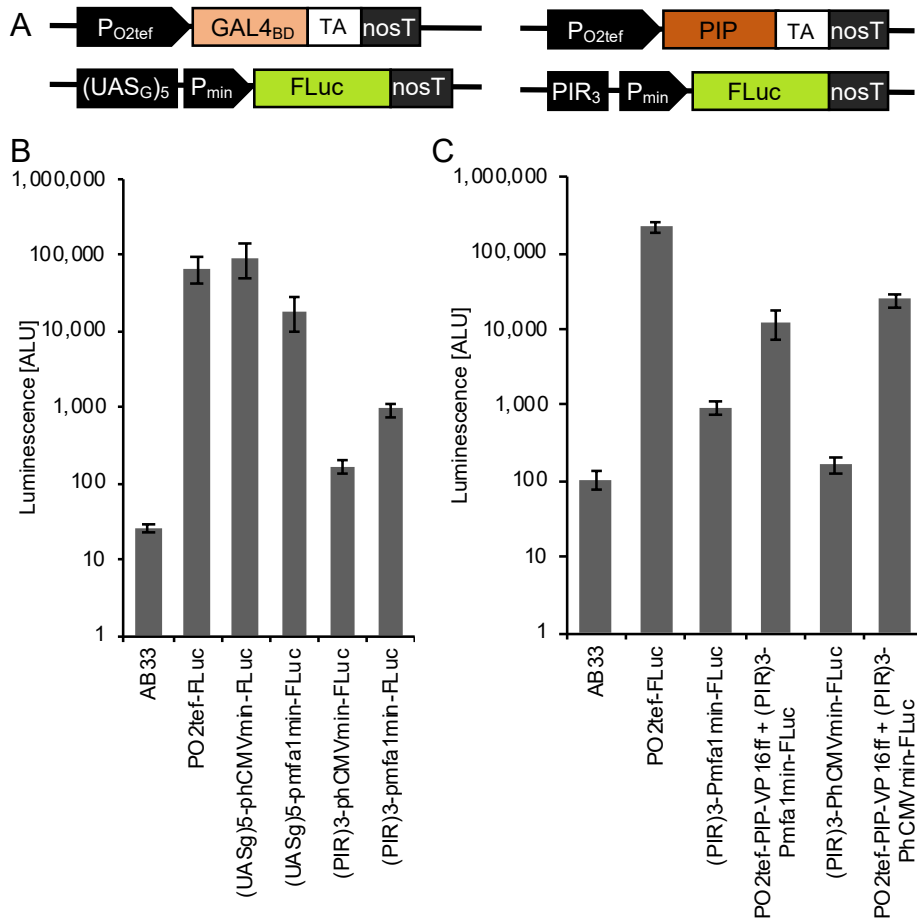


Figure 16: DNA binding protein – operating sequence analysis.

(A) Configuration of constructs that have been transformed into the *cco1* and *upp3* locus of AB33. (B) Cultures of an $OD_{600} = 0.5$ of transformants carrying the indicated reporter constructs in the *upp3* locus have been analyzed for their FLuc luminescence to estimate leakiness of the operating sequence – minimal promoter combinations. Error bars represent the SEM of this individual experiment with $n=10$. (C) Cultures of an $OD_{600} = 0.5$ of transformants carrying the indicated reporter constructs in the *upp3* locus or the reporter constructs in *upp3* and the DNA-binding protein – transactivation domain fusion in the *cco1* locus to estimate the induction fold of the complete PIP-PIR₃ based systems. Error bars represent the SEM of this individual experiment with $n=5$ (AB33 and P_{O2tef} -FLuc) and $n=10$ (half and complete systems).

To start with, strains with the different operating sequence – minimal promoter combinations were generated and analyzed for their FLuc luminescence to get an idea of their leakiness (Figure 16B). Both combinations harboring the $(UAS_G)_5$ showed similarly high FLuc luminescence as the positive control and 3600 and 700 times more FLuc signal than AB33 with $P_{hCMVmin}$ and $P_{mfa1min}$, respectively. As GAL4

and its operating sequence (UAS_G)₅ are *S. cerevisiae* derived parts and *U. maydis* is a fungus itself, it is most likely that it inherits at least one TF that is structurally similar to GAL4 and can bind to the (UAS_G)₅ resulting in expression of FLuc. Nevertheless, both PIR₃ combinations exhibited only minor FLuc signals being 1.6 and 9.2 times higher than AB33. Accordingly, the PIR₃-P_{min}-FLuc strains were transformed with PIP-p65 or PIP-VP16ff constructs. It was not possible to generate viable strains with p65 as the transactivation domain and therefore only two strains with the complete PIP-PIR₃-System carrying the VP16ff as transactivation domain were characterized further (Figure 16C). The strain with P_{O2tef}-PIP-VP16ff-PIR₃-P_{mfa1min}-FLuc (sNH058) showed a 14 times induction fold compared to the respective reporter strain, which corresponds to 5.6% of constitutive FLuc expression. The combination harboring the P_{hCMVmin} (sNH056) on the other hand, had an induction fold of 146 compared to the respective reporter strain resembling almost 11% of the constitutive FLuc expression. Taken together, sNH056 showed less leakiness, higher expression and higher induction fold as sNH058 and was therefore chosen as the pristinamycin-based gene expression system and as the basis for the split TF-based light regulated gene expression systems.

3.1.3.1 Pristinamycin-based chemical regulation of gene expression

FLuc expression in the strain sNH056 should be regulatable by the addition of the antibiotic pristinamycin to the culture medium (Figure 17A). To test this, sNH056 and appropriate controls were grown for 24 h in culture medium supplemented with 200 µg/ml pristinamycin, which corresponds to the amount used in plant protoplast experiments (Müller et al., 2014), or with respective amounts of DMSO as mock treatment. FLuc luminescence was determined in whole cell lysates of 2 ml cultures of an OD₆₀₀ = 0.5. The negative control only expressing the PIR₃-P_{hCMVmin}-FLuc reporter construct (sNH030) showed the expected low background signal while a strain without the PIR₃ operating sequence (P_{hCMVmin}-FLuc; sNH041) gave almost 50 times more FLuc luminescence in mock treated samples. For the constitutive positive control around 72,000 ALU were measured, while the PIP system showed almost 41,000 ALU. Opposite to what was expected, addition of pristinamycin increased FLuc luminescence in all four strains to 2.5 to 5 times more than in the respective mock treated samples. Different pristinamycin concentrations were tested to see a potential dose dependency, however only a toxic effect of the amount of DMSO needed for the highest pristinamycin concentration was observed.

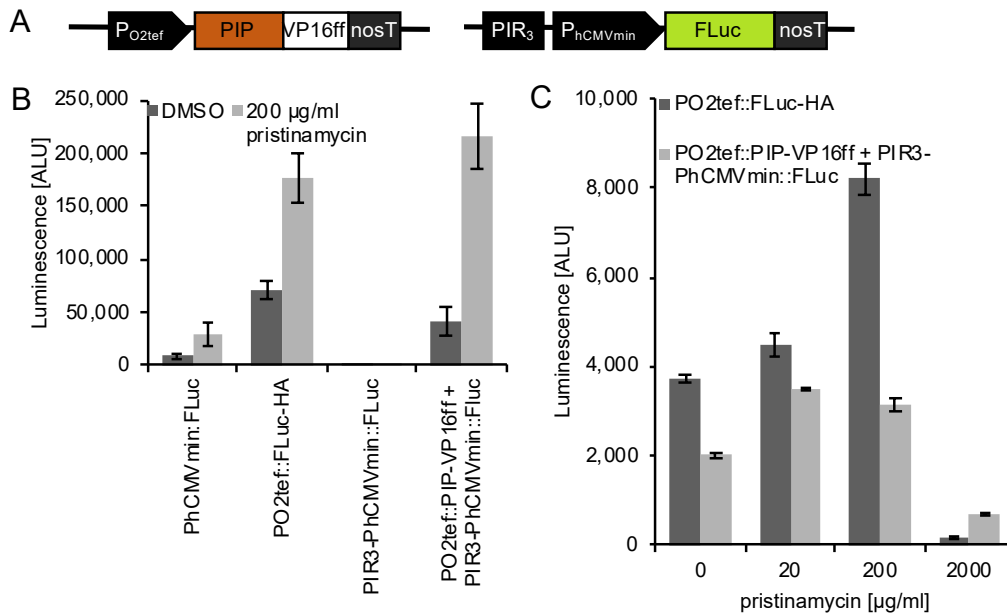


Figure 17: Pristinamycin based gene expression regulation in *U. maydis*.

(A) Configuration of the constructs that have been transformed into the *cco1* and *upp3* locus of AB33. (B) Whole cell lysates of 2 ml culture of an $\text{OD}_{600} = 0.5$ of the indicated strains were analyzed for their FLuc luminescence after growing for 24 h in CM-Glucose supplemented with 200 $\mu\text{g/ml}$ pristinamycin or mock treated with respective amounts of DMSO. Error bars represent the SEM of this individual experiment with $n=3$. (C) cultures of the indicated strains with an $\text{OD}_{600} = 0.5$ were analyzed for their FLuc luminescence after growing 24 h CM-Glucose supplemented with indicated amounts of pristinamycin. The amount of DMSO for a concentration of 2000 $\mu\text{g/ml}$ pristinamycin seems toxic as these cultures contained almost no viable cells. Error bars represent the SEM of this individual experiment with $n=3$.

It seems that the general protein expression of *U. maydis* is increased upon treatment with pristinamycin, independently of any part of the PIP-system, as the constitutive strain showed higher FLuc luminescence compared to untreated cultures as well. Functionality of the pristinamycin used in these experiments was verified in plant protoplast experiments simultaneously by a colleague. As this pristinamycin is obtained from commercially available pyostacin pills, which are used as an oral antibiotic for humans, several additives are mixed with the active ingredient: Silica crystals, dextrans, gelatin, magnesium stearate, hypromellose and titanium dioxide are also present in the antibiotic. Especially the dextrans, which are low-molecular weight carbohydrates, and the hypromellose, as partly methylated cellulose, could serve as a good carbon source for the metabolism of *U. maydis*. To prove this, the experiments would need to be repeated with pure pristinamycin which is unfortunately only available in large amounts from China with very long delivery times. Alternative streptogramin type antibiotics, such as virginiamycin are readily available but extremely cost intensive, with around 25,000 €/experiment in the required size.

In summary, the PIP-system is not applicable at this stage of research, regarding chemical regulation of gene expression.

3.1.4 Orthogonal promoters for *U. maydis*

Along with the establishment of the above described synthetic tools, several synthetically engineered promoters have presented themselves to be functional in *U. maydis*. To get an idea about their strength, they were compared with the regularly used P_{O2tef} (Figure 18). To this end, the FLuc luminescence of cultures of an $OD_{600} = 0.5$ of the respective strains was measured and their strength calculated relative to P_{O2tef} which was set to 1. The weakest promoter was dP_{CMV-A} , with only 4% of the FLuc luminescence of P_{O2tef} . Both $(UAS_G)_5$ -Pmin strains showed 60% and 40% of the P_{O2tef} derived expression. $dP_{(prf)4}$ was the only promoter with a higher FLuc expression than P_{O2tef} , being 4.3 ± 1.7 times stronger.

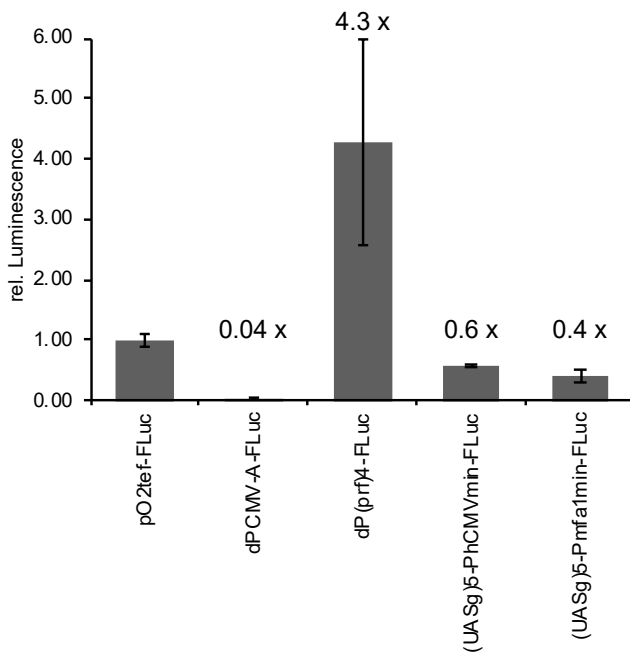


Figure 18: Strength comparison of synthetic (orthogonal) promoters for *U. maydis*.

The various synthetic promoters established in this work have been tested for their strength compared to P_{O2tef} . Therefore, cultures of an $OD_{600} = 0.5$ were analyzed for their FLuc luminescence. The strength of the indicated promoters was calculated relative to P_{O2tef} which was set to 1. Error bars represent the SEM of this individual experiment with $n=5$

Depending on the purpose, all four synthetic promoters can be used for the expression of genes of interest in *U. maydis*. They will most likely not be affected by biological changes of *U. maydis*, as endogenous promoters might be and therefore crosstalk between the exogenous system to be studied and endogenous changes are avoided. While $dP_{(prf)4}$ might be more biotechnologically relevant, the less

expressing promoters could be used for pathway finetuning, and the expression of transcription factors.

3.1.5 Light regulated gene expression in *U. maydis*

After establishing bidirectional promoters as a means for bicistronic expression, and the PIP protein with its operating sequence PIR₃ as the base for a split transcription factor in *U. maydis*, UV-B and red-light responsive gene expression systems were constructed. Unfortunately, only a strain carrying the complete UV-B system could be generated, due to cloning issues with the red system.

The configuration of constructs that have been transformed into AB33 to generate a strain with the UV-B system are shown in Figure 19A. The reporter construct comprising the PIR₃ operating sequence upstream of P_{hCMVmin} controlling FLuc expression was integrated into the *upp3* locus (sNH030). The light responsive split transcription factor parts UVR8-PIP and COP1(WD40)-VP16ff-NLS are encoded on a bicistronic construct under the control of dP_{CMV-A} and were subsequently transformed into the *cco1* locus of sNH030 resulting in sNH034.

To test the light responsiveness of the strain, cultures were dark adapted for 3 h and then grown for 14 h of alternating 15 min illumination with 10 $\mu\text{mol m}^{-2} \text{s}^{-1}$ UV-B light (310 nm) and 15 min dark or 14 h dark, respectively (Figure 19B). Whole cell lysates of 2 ml of cultures with an OD₆₀₀ = 0.5 have been analyzed for their FLuc luminescence. The negative control PIR₃-P_{hCMVmin}-FLuc and sNH034 showed equally low FLuc signals with 250 and 290 ALU, respectively. The positive control, expressing a PIP-VP16ff-NLS fusion together with the reporter construct (sNH056) displayed almost 14,000 ALU. Illumination with UV-B light had no effect on the viability of the cells and the FLuc signal of the negative control hardly changed (400 ALU). Surprisingly, the positive control showed 2.6 times more FLuc luminescence than the corresponding dark samples. In contrast to that, the samples for the UV-B system stayed as unchanged as the negative control with only 440 ALU. Longer illumination (20 h of alternating 30 min illumination with 10 $\mu\text{mol m}^{-2} \text{s}^{-1}$ and 15 min dark) did not improve the results, but only increased the FLuc luminescence of sNH056 to 6 times more than the respective dark samples (data not shown).

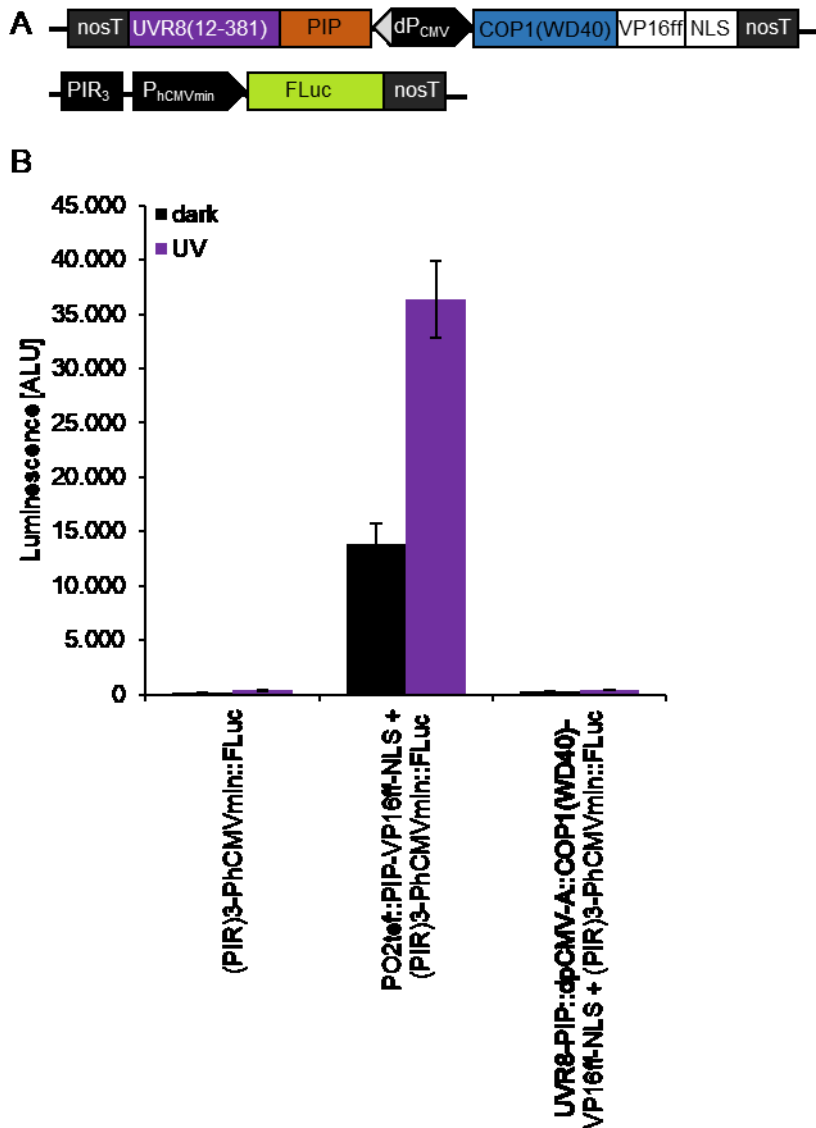


Figure 19: UV-B light regulated gene expression in *U. maydis*.

(A) Configuration of the constructs that have been transformed into the *cco1* and *upp3* locus of AB33. (B) Whole cell lysates of 2 ml of a culture with an $OD_{600} = 0.5$ have been analyzed for their FLuc luminescence after growing in the dark for 3 h followed by 14 h of alternating 15 min illumination with $10 \mu\text{mol m}^{-2} \text{s}^{-1}$ UV-B light (310 nm) and 15 min dark or 14 h dark. Error bars represent the SEM of this individual experiment with $n=4$.

In the preceded experiments PIP was fused to the VP16ff and an NLS. In the UV-B system, the UVR8-PIP fusion does not have such a localization tag. Consequently, it could be that the UVR8-PIP fusion is only present in the cytosol and therefore, PIP cannot bind to its operating sequence and only the COP1(WD40)-VP16ff-NLS half of the split TF is located at the site of action. This would also explain the complete lack of leakiness of the system in *U. maydis*, whereas most light systems in other organisms show at least small amounts of leakiness. To verify this hypothesis, a strain would have to be generated where the UVR8-PIP fusion is tagged with an NLS.

3.2 Reconstruction of phytohormone signaling pathways

In this section, specific aspects of two phytohormone signaling pathways, namely the interaction of the COP1/SPA1 complex with DELLA proteins of the gibberellin response, and the regulation of the phytohormone receptor PYL8 by abscisic acid, will be discussed. Moreover, the establishment of an enzyme-free assembly cloning method for the integration of short sequences into existing vectors will be presented. The method was tested for the construction of the potential-induction-fold-determination vector (pifold), to estimate potential phytohormone biosensor degradation.

3.2.1 Interaction studies of the COP1/SPA1 complex with proteins of the Gibberellin signaling pathway

Parts of this chapter are based on a manuscript accepted in PNAS, Appendix 7.2.

The order of complex formation for the perception of a phytohormone, as well as the complexes involved in signal transduction and processing can give a clue about the functions and relevance of the involved proteins, but the high complexity and redundancy among plant proteins makes it difficult to study *in planta*. In order to circumvent this, synthetic biology approaches use orthogonal platforms like mammalian cells to specifically analyze certain parts of a pathway, only including the proteins of interest and excluding crosstalk with other pathways. DELLA proteins from the gibberellin signaling pathway are involved in signal transduction in response to environmental changes controlling growth. Recent results also suggest that they are influenced by shade and warm temperature and that this is realized through the E3-ubiquitin ligase COP1. If this is true, COP1 and the DELLA proteins most probably interact physically. To prove this hypothesis, the interaction of the COP1/SPA1 complex with the DELLA proteins RGA and GAI was analyzed more closely in Human Embryonic Kidney 293T (HEK293T) cells by classical fluorescence-based microscopy and with mammalian 2-/3- hybrid systems developed by J. Andres in our lab. In this way, side effects from GA-signaling, which might disturb the potential interaction *in planta*, are excluded. Additionally, the order of complex formation can easily be reconstructed.

3.2.1.1 Microscopy studies

For microscopy studies, the two DELLA proteins GAI and RGA were tagged with mCherry, while COP1 and SPA1 were fused to mVenus and mCerulean, respectively. SPA1 was additionally tagged with an NLS to facilitate the localization and interaction studies. All constructs were transfected either on their own or in several combinations into HEK293T cells. After two days of incubation, cells were fixed on microscopy slides and analyzed for their fluorescence (Figure 20).

RGA-mCherry and GAI-mCherry were mostly present outside the nucleus and accumulated in certain spots in the cytosol. mVenus-COP1 was localized exclusively in the nucleus and formed speckle-like structures, while mCerulean-SPA1-NLS was distributed throughout the whole nucleus except nucleoli (Figure 20A-D). When mVenus-COP1 and mCerulean-SPA1 were co-transfected, SPA1 was relocated to the same speckle-like structures and colocalized with mVenus-COP1 (Figure 20E). Co-expression of mVenus-COP1 and either RGA-mCherry or GAI-mCherry did not change the original localization of the proteins (Figure 20F and I), while co-expression of the DELLA proteins with mCerulean-SPA1-NLS lead to a partial relocation of RGA and GAI to the nucleus (Figure 20G and J). Co-expression of RGA-mCherry or GAI-mCherry with both mVenus-COP1 and mCerulean-SPA1-NLS partially recruited the DELLA proteins into the speckle-like structures in the nucleus that were formed by mVenus-COP1 (Figure 20H and K). In the case of RGA-mCherry, cytosolic localization was completely abolished.

Next, the strength of co-localization was quantified by comparing RGA-mCherry or GAI-mCherry fluorescence in the speckle-areas in co-transfected cells to 10 random spots in the nucleus of single-transfected cells (Figure 21). While co-transfection of RGA-mCherry and mVenus-COP1 lead to no relocation of RGA, as seen in the pictures, mVenus-COP1 indeed recruited GAI-mCherry to the speckle-like structures. Co-transfection with mCerulean-SPA1-NLS increased this significantly. Additionally, RGA-mCherry fluorescence was significantly higher in the speckle-like structures of mVenus-COP1 - mCerulean-SPA1-NLS co-transfected cells.

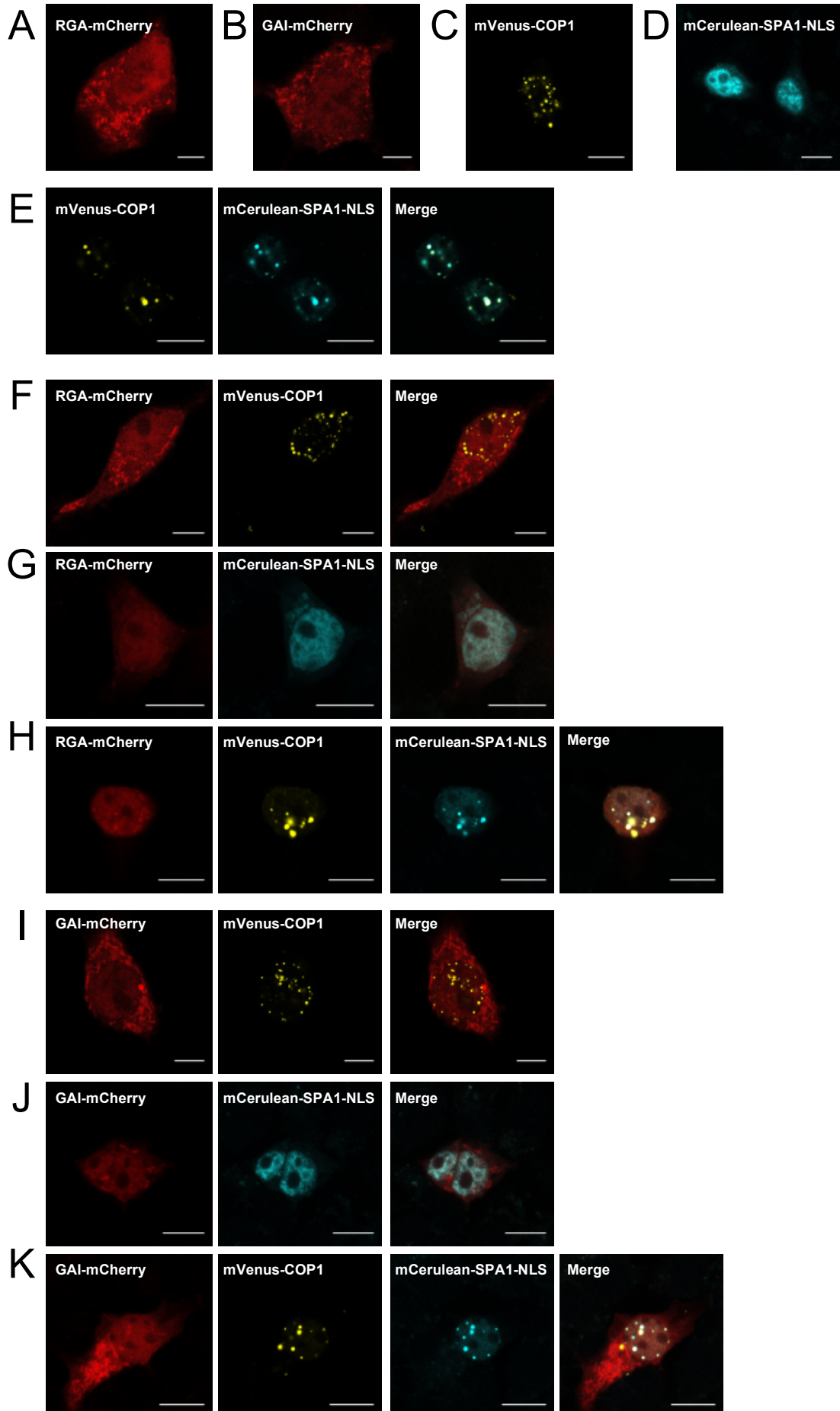


Figure 20: Confocal microscopy analysis of the localization of GAI, RGA, COP1 and SPA1 in animal cells. (A-D) The fusion proteins RGA-mCherry (A), GAI-mCherry (B), mVenus-COP1 (C) and mCerulean-SPA1-NLS (D) were transfected into Human Embryonic Kidney 293T (HEK-293T) cells. GAI and RGA are distributed throughout the whole cell. mVenus-COP1 localizes to nuclear speckle-like structures. mCerulean-SPA1-NLS localizes to the nucleus. (E-K) HEK-293T cells were co-transfected with mVenus-COP1 and mCerulean-SPA1-NLS (E), RGA-mCherry and mVenus-COP1 (F), RGA-mCherry and mCerulean-SPA1-NLS (G), RGA-mCherry, mVenus-COP1 and mCerulean-SPA1-NLS (H), GAI-mCherry and mVenus-COP1 (I) GAI-mCherry and mCerulean-SPA1-NLS (J) or GAI-mCherry, mVenus-COP1 and mCerulean-SPA1-NLS. Representative cells are shown. Scale bars represent 10 μm .

In summary, RGA-mCherry seems to only interact with mCerulean-SPA1-NLS, while GAI-mCherry interacts to a certain extent with mVenus-COP1 on its own, and also with mCerulean-SPA1-NLS. Therefore, the interaction of GAI with the whole COP1/SPA1 complex is even stronger. The interaction of GAI and RGA with COP1 and SPA1 was also proven in a yeast-2-hybrid assay, although this was performed with truncated versions of the DELLA proteins, which otherwise would lead to strong self-activation and false positives (Blanco-Touriñán et al., 2020). Pull down assays in *Nicotiana benthamiana* leaves, on the other hand, showed the same interaction pattern as the colocalization studies in mammalian cells presented above. The truncated version of GAI did interact with COP1 on its own, and interaction was increased by co-expression of SPA1, while the truncated RGA only showed interaction when SPA1 was present.

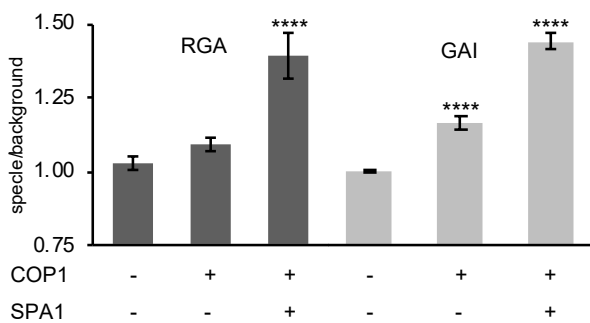


Figure 21: Quantification of speckle formation by the COP1/SPA1 complex with DELLA proteins.

Fluorescence intensities of GAI-mCherry and RGA-mCherry in the nucleus of control cells and in speckle-like structures in cells co-expressing mVenus-COP1 or mVenus-COP1 and mCerulean-SPA1-NLS from 10-13 transfected cells. (****) indicates statistically significant difference between co-transfected and respective single-transfected cells (Students t-test; $P < 0.0001$).

3.2.2 Mammalian 2- and 3-hybrid

The quantification of microscopy pictures can be complicated and time consuming, as for some ways of analysis, this has to be done by hand. Therefore, and also to have means of generating complementary information, other methods in mammalian cells have been developed which result in easier-to-process data. The mammalian 2-

and 3-hybrid (M2H/M3H) systems are based on a split TF mechanism (Figure 22A). One protein of interest (P1) is fused to the Tet repressor (TetR) while the second protein (P2) is fused to a VP16 transactivation domain. P1 is bound to the DNA of the reporter plasmid through TetR which is binding to 13 repeats of its operating sequence tetO. Upon interaction of P1 and P2, the VP16 gets in close proximity to the minimal promoter ($P_{hCMVmin}$) that is located downstream of tetO₁₃ and recruits the transcription initiation complex. Transcription from $P_{hCMVmin}$ is thereby activated and leads to expression of SEAP as the reporter. If P1 and P2 do not interact on their own, a third protein, P3 could potentially interact with both of them and result in SEAP expression as well.

For this experiment, RGA and GAI were fused to the VP16 transactivation domain, while COP1 or SPA1 were fused to TetR. All possible combinations were transfected into HEK293T cells together with the SEAP reporter plasmid and analyzed for their SEAP activity 24h after transfection. The combinations VP16-SPA1 + TetR-COP1 and VP16-COP1 + TetR-SPA1 showed half and a quarter of SEAP expression of the positive control, respectively. Unfortunately, none of the tested RGA or GAI combinations showed more SEAP activity as the negative control. It could be that the combination of the DELLA proteins together with COP1 or SPA1 or both of them forms a complex that is sterically hindering activation of $P_{hCMVmin}$ by the VP16. To test this, truncated versions of COP1 and SPA1 only including the domains which are most probably responsible for interaction with other proteins, would need to be cloned into the M2H/M3H systems.

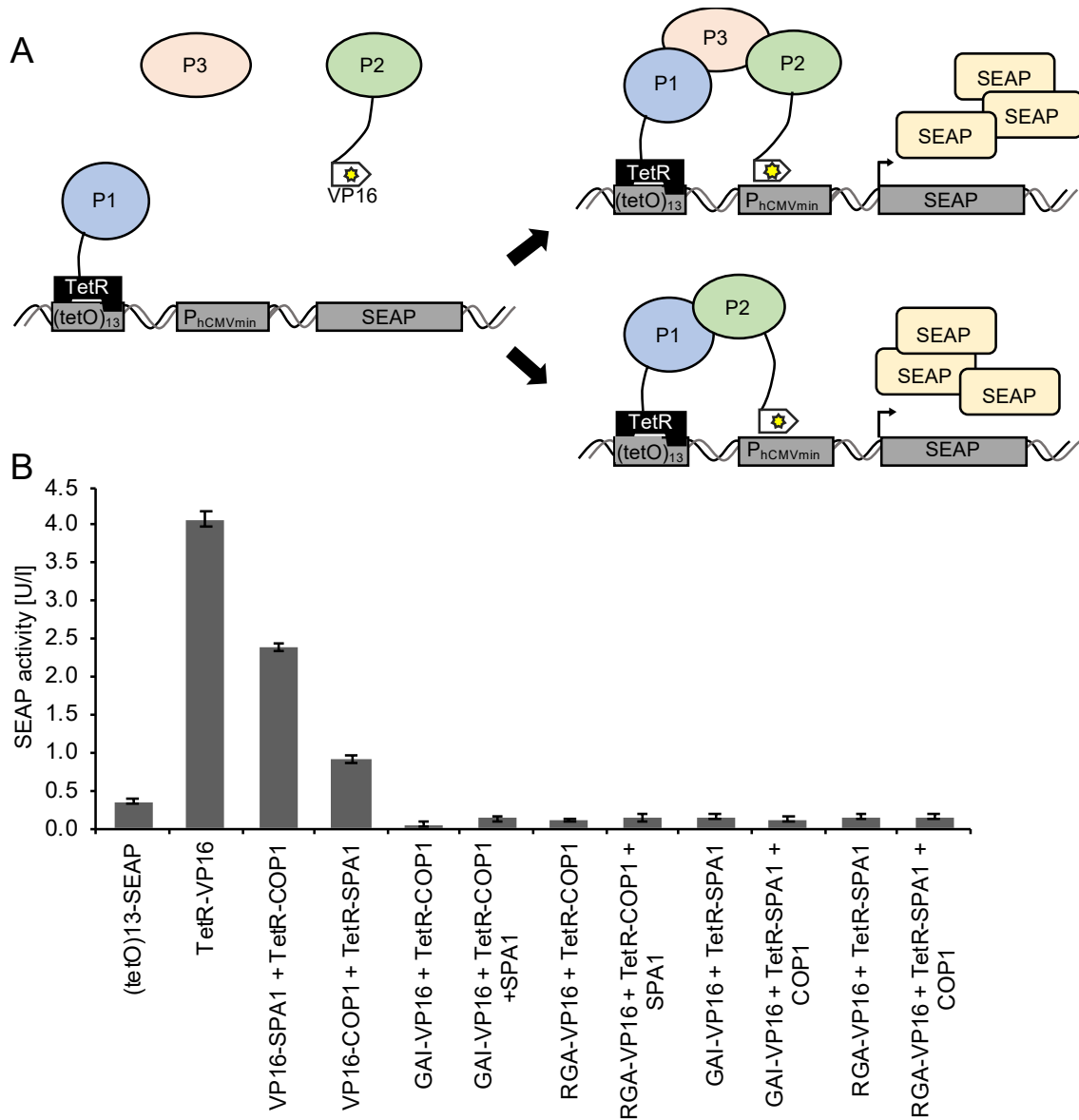


Figure 22: COP1/SPA1/DELLA interaction studies with a mammalian 2- and 3-hybrid system.

(A) Mode of function of the split TF system. The two building blocks for the split TF system are encoded on a bicistronic expression vector under the control of the P_{SV40} . In the first cistron, a protein of interest (P1) is fused to a VP16 transactivation domain and an NLS. In the second cistron, a tetracycline repressor (TetR) is N-terminally fused to the second protein of interest (P2). A polioviral internal ribosome entry site, pIRES, induces the translation of the second cistron. The response vector comprises 13 repeats of the TetR-specific operator tetO. One protein is bound via TetR to the tetO₁₃ operating sequence. If P1 and P2 interact individually or upon coexpression with a third protein of interest (P3), VP16 recruits the transcription initiation complex and thereby activates transcription of SEAP expression via $P_{hCMVmin}$. (B) HEK293T cells were transfected with the indicated configurations in combination with the response vector. After incubation for 24 h SEAP activity was quantified. The positive control contains a TetR-VP16 fusion under the control of P_{SV40} with the response plasmid. The response plasmid alone serves as negative control. Error bars represent the SEM of this individual experiment with $n=4$.

3.2.3 Quantitative analysis of increased PYL8 after ABA sensing in *Arabidopsis thaliana* mesophyll protoplasts

Quantitative, ratiometric phytohormone biosensors have been used for the characterization of receptor degradation in the auxin and strigolactone signaling pathways, and most recently also for gibberellins (Wend et al., 2013; Samodelov et al., 2016; Andres et al., manuscript in preparation). In all of them the sensor module is degraded upon perception of the respective phytohormone. Biosensors can give information about the specificity towards derivatives and metabolites of a phytohormone, which in some cases have many biologically active forms. Additionally, they showcase the strength of degradation, which depends on the derivative and concentration thereof. ABA receptors are degraded upon ABA treatment as well, with only one exception. Specifically, the PYL8 protein was shown to be upregulated upon ABA perception due to less degradation by the 26S proteasome (Belda-Palazon et al., 2018). Using an induction-based, ratiometric biosensor with the same configuration as previously presented for auxin, strigolactone and gibberellin, the ABA receptor PYL8 could be analyzed more closely. Therefore, in this section, the ABA induced upregulation of PYL8 was quantified using the receptor as the sensor module, to test if induction can also be quantified in this manner.

The previously published CtrlQuant and the PYL8 sensor were transformed into *A. thaliana* wt protoplasts. 20 h post transformation, protoplasts were induced with a dilution series of ABA and incubated either for 30 or 120 min before measuring luminescence. The change of FLuc to RLuc ratio relative to the lowest concentration of ABA is shown in Figure 23. After 30 minutes of ABA induction, no significant change was observed in PYL8 abundance (Figure 23A) whereas after 120 min, PYL8 increased gradually with increasing ABA concentrations and was significantly upregulated by 1000 μ M ABA compared to 0.1 μ M and less (Figure 23B). At the highest concentration, the relative amount of PYL8 was almost 70% more than without addition of the hormone.

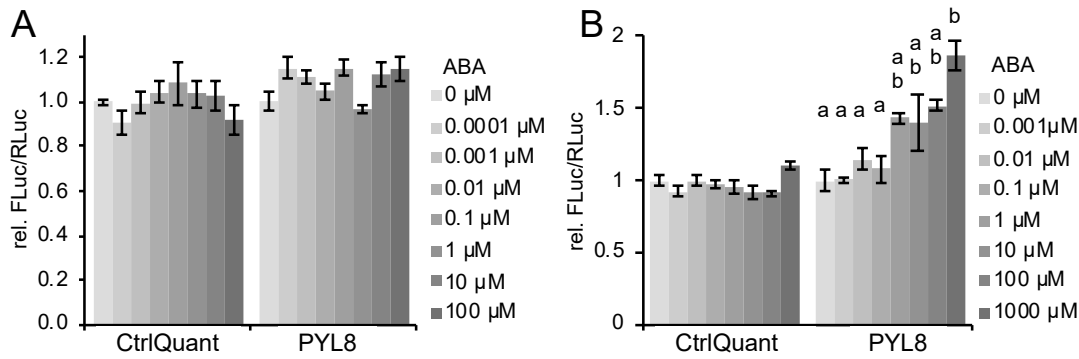


Figure 23: ABA-based stabilization of PYL8 in *A. thaliana* wt protoplasts.

A. thaliana wt protoplast were transformed with either CtrlQuant or the PYL8 biosensor and induced with ABA 20 h post transformation. After hormone incubation for 30 min (A) or 120 min (B) luciferase activity and subsequently the FLuc/RLuc ratios were determined and shown as relative FLuc/RLuc ratios compared to the lowest ABA concentration which was set to 1. The statistical significance between the different ABA concentrations is indicated in lower case letters, where “a” significantly differs from “b”. One-way analysis of variance (ANOVA) was performed with $p < 0.05$. Error bars represent the SEM of this individual experiment with $n = 6$.

Recently it was shown that the RING FINGER ABA-RELATED 4 (RFA4; At2G21420) interacts among others with ABA receptors like PYR1, PYL4 and PYL8 and promotes their proteasomal degradation (Fernandez et al., 2019). In consequence, overexpression of RFA4 should decrease the PYL8 level, so that stabilization by ABA perception gets more prominent. This could indeed be observed when the PYL8 biosensor was co-expressed with RFA4 in plant protoplasts (Figure 24). The relative PYL8 protein abundance increased by 90% with 1000 μM ABA compared to no ABA induction already after 30 min of incubation.

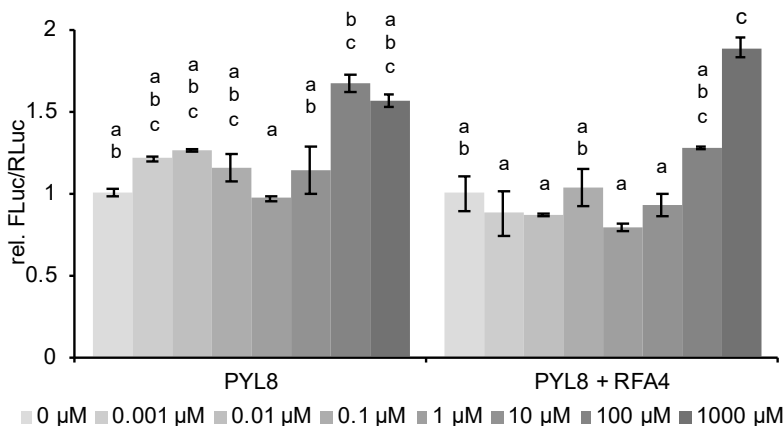


Figure 24: ABA-based stabilization of PYL8 after downregulation by RFA4 in *A. thaliana* wt protoplasts

A. thaliana wt protoplast were transformed with either the PYL8 biosensor or the PYL8 biosensor and RFA4 and induced with ABA 20h post transformation. After hormone incubation for 30 min luciferase activity and subsequently the FLuc/RLuc ratios were determined and shown as relative FLuc/RLuc ratios compared to the lowest ABA concentration which was set to 1. The statistical significance between the different ABA concentrations is indicated in lower case letters, where “a” significantly differs from “b” and “b” from “c”. One-way analysis of variance (ANOVA) was performed with $p < 0.05$. Error bars represent the SEM of this individual experiment with $n = 6$.

In summary, a stabilization-based, quantitative, ratiometric phytohormone biosensor was generated, demonstrating the increase of the ABA receptor PYL8 after hormone treatment. Additionally, the efficiency of the sensor was increased by downregulation of the receptor by the E3 ubiquitin ligase RFA4.

With the help of this sensor, a comprehensive analysis of PYL8 can be performed, giving insights into the fine tuning of the signaling pathway, the regulation of target genes and the resulting developmental changes. Although there is only one naturally occurring ABA, and target specificity of the receptor is therefore not relevant, the combination of different ABA concentrations and abiotic stresses, such as high salinity, drought and heat stress, would be of great interest, especially for the engineering of more resistant food crops in a changing world climate.

3.2.4 Development of pifold and an upgrade to AQUA

In this section, two methodical aspects of synthetic biology are presented in the background of degradation-based, quantitative, ratiometric phytohormone biosensors. These sensors can be used in several plant platforms such as *A. thaliana* or *N. benthamiana* protoplasts, but also e.g. in mammalian cells. As all of these platforms exhibit differences in their translation and degradation kinetics, they will most certainly also display different dynamic ranges, when analyzing a sensor module of choice, especially as plant platforms exhibit endogenous phytohormones, additionally to the ones, applied for specific experiments. To estimate the potential dynamic range or induction fold of a platform, the lowest possible abundance of the SM-FLuc fusion has to be determined. Therefore, a PEST sequence was integrated into CtrlQuant right between the 7GA linker and FLuc, which will lead to fast proteasomal degradation of the SM-Fluc fusion (Figure 25). The PEST sequence used for the construction of this vector is only 126 bp in length and cloning such short sequences into a 7 kb vector has shown itself to be relatively inefficient with assembly cloning methods. Moreover, the sequence is too long to be integrated into oligonucleotide overhangs. Therefore, an update to AQUA cloning was developed for the integration of short sequences without the need of re-cloning a complete vector.

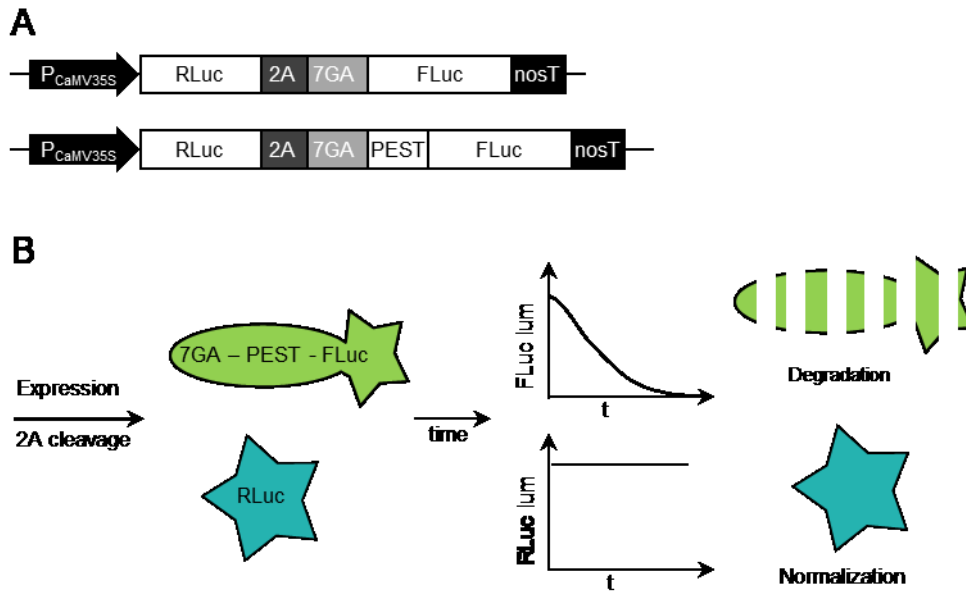


Figure 25: Design of the pifold (potential-induction-fold-determination) gene expression system in plants. (A) Configuration of the vectors. (B) Mode of function. Pifold construct expressing a renilla luciferase (RLuc; blue) connected via a 2A peptide to the degradation module (PEST) fused to a firefly luciferase (FLuc; green), under the control of a constitutive 35S promoter. The 2A peptide in the synthetic construct leads to stoichiometric coexpression of RLuc (normalization element) and PEST-FLuc. PEST-FLuc becomes degraded, whereas RLuc expression remains constant, leading to a decrease in the FLuc/RLuc ratio.

The cloning strategy is shown in Figure 26. Briefly, the sequence to be integrated is split into around 70 bp long nucleotide sequences including 20 bp homologous overhangs to the adjacent sequences. All parts are synthesized in forward and reverse orientation and pre-annealed in complementary pairs according to the oligo-annealing protocol presented by sigma (<https://www.sigmaaldrich.com/technical-documents/protocols/biology/annealing-oligos.html>), while the vector backbone is cut open by restriction enzymes and subsequently purified. The digested backbone and double stranded oligonucleotides are mixed in H_2O in a total volume of 10 μ l and incubated at room temperature for 1 h prior to transformation into chemically competent *E. coli*. Finally, obtained colonies are confirmed for correct assembly by standard methods such as analytical PCR, restriction digest, or comprehensive sequencing.

To verify the functionality of the designed potential-induction-fold-determination vector *A. thaliana* wt protoplasts were either transformed with CtrlQuant or pifold and analyzed for their FLuc and RLuc expression after 20 h (Figure 27). The relative FLuc/RLuc ratio was decreased to 0.4% due to PEST induced degradation of FLuc, which corresponds to a dynamic range of 250.

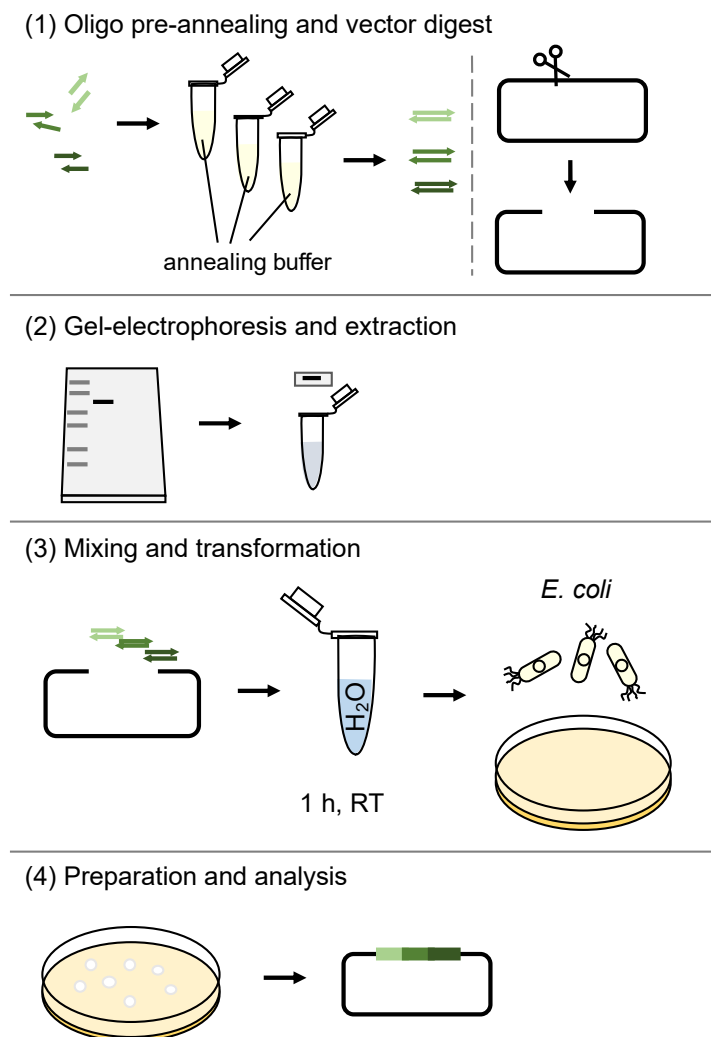


Figure 26: AQUA 2.0 Cloning work-flow.

(1) DNA parts are generated by Oligo pre-annealing and PCR amplification or restriction digest. (2) Vector backbone is purified by gel-electrophoresis. (3) Pre-annealed oligos and digested plasmid are mixed and incubated in H₂O prior to transformation into chemically competent *E. coli* Top10 cells for *in vivo* assembly. (4) Finally, obtained colonies are confirmed for correct assembly by standard methods such as analytical PCR, restriction digest, or comprehensive sequencing.

To summarise, the functionality of both the new cloning approach and the pifold vector were presented, as tools for synthetic biology approaches. AQUA 2.0 will be especially helpful for the cloning of libraries of truncated versions of any gene of interest or single domains thereof, which might be too short for conventional cloning methods. More specifically, versions of phytohormone sensor modules could be cloned in this way to uncover binding domains more easily than with complicated and labor-intensive methods such as protein crystallography.

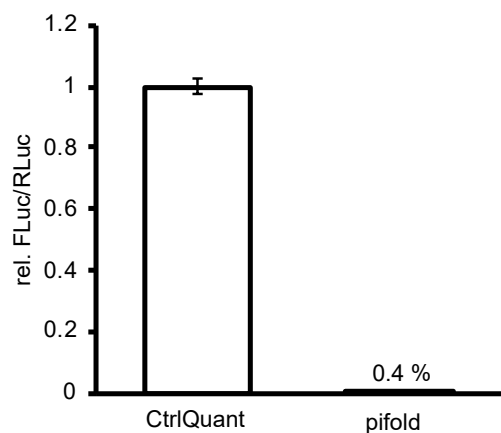


Figure 27: Potential-induction-fold-determination for ratiometric degradation-based biosensors in *A. thaliana* wt protoplasts.

Protoplasts were isolated from wt seedlings and transformed with the respective plasmid. Twenty-four hours after transformation, luciferase activity was determined. Results are averaged FLuc/RLuc ratios, normalized to the sample without PEST sequence. The data shown correspond to one representative experiment. Error bars represent SEM from the individual experimental data shown with $n = 12$.

4. Conclusion

In conclusion, several basic and advanced synthetic tools were designed, constructed and tested in the basidiomycete fungus *Ustilago maydis*:

First, easy to measure, enzymatic, quantitative reporter genes, namely firefly luciferase, renilla luciferase and gaussia luciferase, were tested for their general functionality and were then applied for the characterization of other tools, but also used in a fast screening system for efficient strain production. This system will be particularly helpful in the future for faster strain generation, as the substrates are highly specific and actual enzymatic signal can easily be distinguished from background, while selection markers still lead to false positives in this task and southern blots are rather labor-intensive and error prone. Moreover, especially firefly and renilla have proven themselves to be useful as readout and normalization element for inducible expression systems. While the establishment of IRES sequences for bicistronic expression of genes needs closer examination, two bidirectional promoters were successfully engineered and implemented in *U. maydis*, to serve the same purpose. One limitation of bidirectional promoters certainly is their complexity in cloning compared to IRES sequences and future work should also concentrate on them. Until then, bidirectional promoters will be the tool of choice for the engineering of split transcription factor-based expression systems.

The operating sequences (UAS_G)₅ and PIR₃ were tested for their leakiness in combination with minimal promoters and further analyzed for activation by respective binding proteins GAL4_{BD} and PIP. The PIP-system is very promising with extremely low leakiness and good induction folds. Although it is not regulatable with the usual pyostacine pills, it still serves a base for light regulated, split transcription factor gene expression systems and it might be regulatable with pure pristinamycin, which remains to be examined. With the methods established in this work, more chemically inducible expression systems can be tested and characterized faster and in a more quantitative manner than with so far existing protocols. On that base, also UV-B and red-light systems can be examined further, for regulated gene expression with high spatiotemporal resolution, whereas inducible gene expression in *U. maydis* is classically realized by changing the carbon or nitrogen source by change of the culture medium. These conventional procedures require more materials and are by far more cumbersome than switching on light of the respective wavelength to induce gene expression.

Additionally, several unidirectional synthetic promoters of various strength are now available for the controlled expression of any gene of interest, avoiding the influence of endogenous stimuli. The tools presented in this work will be of great use in biotechnology applications of *U. maydis* as well as basic research in this well-established model organism.

Second, specific parts of the gibberellin and abscisic acid signaling pathways have been reconstructed and were characterized and partially quantified in orthogonal systems. Simultaneously, a ratiometric, quantitative, genetically encoded biosensor was constructed following the design by Wend et al. (2013) and applied to monitor PYL8 increase in ABA treated *Arabidopsis thaliana* protoplasts. While all previous biosensors of this type were degradation-based, the PYL8 biosensor is the first that senses protein increase. With this tool available, open questions on the connection between ABA and abiotic stresses can be investigated quantitatively in a minimal plant system. All information that can be gained from these investigations might be of great value for the engineering of high-performance food crops.

Finally, an updated protocol for AQUA cloning was presented, that facilitates the integration of short sequences into large vectors. The method was applied to integrate a PEST sequence into a phytohormone biosensor control vector, resulting in a potential-induction-fold-determination vector for use in plants. Moreover this cloning method will facilitate the generation of large libraries of sensor modules, domains and truncated versions of proteins in any research area.

5. Material and Methods

5.1 Establishment of a synthetic toolbox in *Ustilago maydis*

5.1.1 Plasmid generation

Design and construction of plasmids for synthetic (opto-) genetic tools for *Ustilago maydis* is described in 5.4, with oligos listed in 5.5

5.1.2 Strains and growth conditions of *Ustilago maydis*

All strains described in this work are listed in 5.6 and were produced in the AB33 background (Brachmann et al., 2001) either in the *upp3* or *cco1* locus. For all experiments strains were cultivated as liquid cultures under aerobic conditions and at 28°C in complete medium (CM; Holliday, 1974: 0.25 % (w/v) Casamino acids; 0.1 % (w/v) Yeast extract; 1.0 % (v/v) Vitamin solution (Holliday, 1974); 0.05 % (w/v) Salmon sperm DNA; 6.25 % (v/v) Salt solution (Holliday, 1974); 0.15 % (w/v) NH₄NO₃) supplemented with 1% Glucose after autoclaving, if not indicated otherwise. For induction of either the P_{crg} promoter or the P_{nar} promoter cells were pelleted, washed twice with sterile H₂O and resuspended in CM supplemented with 1% Arabinose or nitrate minimal medium (NM; 0,3% (w/v) KNO₃; 6,25% (v/v) salt solution (Holliday, 1974)) supplemented with 1% Glucose at an OD₆₀₀ = 0.5. For chemical regulation of gene expression, CM-Glucose medium was supplemented with indicated concentrations of pristinamycin from a 50 mg/ml stock solution in DMSO.

5.1.3 Preparation of chemically competent *Ustilago maydis* protoplasts

Protoplasts were prepared according to the basic protocol of Tsukuda et al 1988. Briefly, 50 ml cultures were grown to an OD₆₀₀ between 0.6 – 1 and harvested for 5 min at 3000 rpm. Cells were washed with 20 ml SCS (Solution I: 20 mM tri-sodium citrate*2 H₂O; 1 M sorbitol; Solution II: 20 mM citric acid*H₂O; 1 M sorbitol; ratio of solution I to solution II approximately 5:1; pH 5.8) and pelleted again. Protoplasting was carried out at room temperature in freshly prepared and filter sterilized SCS supplemented with 100 mg Lysing Enzymes from *Trichoderma* (Sigma L1412) and observed microscopically. The reaction was stopped by adding 10 ml cold SCS buffer. Protoplasts were washed twice more with cold SCS buffer and once with cold STC buffer (50% (v/v) 2 M Sorbitol; 1% (v/v) 1 M Tris-HCl pH 7,5; 10% (v/v) 1 M

CaCl₂). The final pellet was resuspended in 1 ml cold STC buffer and stored at -80°C as 100 µl aliquots.

5.1.4 Transformation of *Ustilago maydis*

For the generation of new strains, protoplasts were transformed by adding 1 µl 15 mg/ml Heparin and about 4 µg linearized plasmid DNA before incubating the mixture on ice for 10 minutes. 500 µl STC/PEG (60% (v/v) STC; 40% (w/v) PEG 3350) were added and incubation on ice continued for another 15 minutes. Protoplasts were plated on Reg.-light agar plates (1.0% (w/v) yeast extract; 0.4% (w/v) peptone; 0.4% (w/v) sucrose; 18.22% (w/v) sorbitol; 1.5% (w/v) agar;) containing a gradient of the appropriate selective antibiotics and grown at 28°C for 5-10 days.

	stock solution	Reg.-light agar (bottom)	
	mg/ml	µg/ml	µl/100 ml
Carboxin (Cbx)	5	4	80
Hygromycine (Hyg)	50	400	800
Nourseothricin (Nat)	200	300	150
Genitacin (G418)	50	1000	2000

5.1.5 Extraction of genomic DNA from *Ustilago maydis*

For the extraction of genomic DNA from *Ustilago maydis* 2 ml of a 3 ml small culture were pelleted at 13,000 rpm for 2 min and the supernatant was discarded. About 200 µl of 0.4 – 0.6 mm Ø glass beads and 500 µl of a 1:1 mixture of gDNA lysis buffer (10mM Tris-Cl (pH 8,0); 100 mM NaCl; 1% SDS; 2% Triton X100; 1mM EDTA) and TE (1.31 mM Tris-Base; 8.69 mM Tris-HCl; 10 mM Na₂-EDTA*2H₂O; pH 8) were added to the pellet. Cells were disrupted for 15 min in a thermoshaker at RT and 1,400 rpm and then incubated at 65 °C for 20 min. After a 5 min incubation on ice, 100 µl 8 M potassium acetate were added and the mixture inverted 8 to 10 times. Glass beads and cell debris were pelleted by centrifugation for 15 min at 13,000 rpm and 450 µl of the supernatant were transferred into new reaction tubes containing 500 µl isopropanol for DNA precipitation. The genomic DNA was pelleted for 15 min at 13,000 rpm, washed once with 70% EtOH and resuspended in 50 µl TE/RNase

(50 μ l RNaseA (10 mg/ml) in 50 ml TE; final concentration 10 μ g/ml) for 60 min at 50°C and 600 rpm.

5.1.6 Genotyping by PCR

Genomic DNA of *Ustilago maydis* was analyzed for correct integration of plasmid DNA by polymerase chain reaction (PCR). Therefore, a PCR reaction was set up with 1.25 U Taq DNA polymerase (New England Biolabs), 2.5 μ l 10X ThermoPol® Buffer, 0.6 mM dNTP Mix (Promega), 2 mM MgCl₂ (New England Biolabs), 4% DMSO (v/v) and 0.2 μ M of each oligonucleotide in a final volume of 25 μ l. Pairs of oligonucleotides were chosen to bind right before the upstream flanking sequence of the *upp3* or *cco1* locus and in the center part of the integrated DNA sequence. After running the given program in a Biometra TAdvanced Twin 48/48G Thermocycler, samples were separated by gel electrophoresis on a 1% Agarose in TAE gel with 30 μ g/100 ml Ethidium bromide and analyzed for correct banding patterns under UV light.

95°C	2 min		
94°C	20 s		
57°C	20 s	$\Delta T -0.5^\circ C$	10 x
72°C	x		
94°C	20 s		
52°C	20 s		15x
72°C	x		
10°C	∞		

5.1.7 DIG-Southern Blot

Strain verification was also performed via Southern Blots on the extracted gDNA of *U. maydis* transformants after antibiotic selection. Therefore, gDNA was digested using appropriate restriction enzymes to generate banding patterns that are distinguishable between transformed and untransformed candidates. The digested gDNA was separated by size on a 0.8% agarose in TAE gel overnight at 20 volts. Subsequently the gel was washed in 0.25 M HCl, DENAT (1.5 M NaCl; 0.4 M NaOH) and RENAT (1.5 M NaCl; 282 mM Tris-HCl; 218 mM Tris-Base) for 20 minutes per solution and brief rinsing with H₂O in-between. DNA fragments were then transferred from the gel onto a Hybond-N-Nylon-membrane for at least 4 hours using capillary

forces in a Whatman paper assembly with 20x SSC buffer (3,0 M NaCl; 0,3 M trisodium citrate). For fixation, the membrane was shortly illuminated with UV light, followed by hybridization with a digoxigenin-labeled DNA probe overnight. For detection, the membrane was incubated with an alkaline phosphatase conjugated polyclonal anti Digoxigenin-AP antibody (Roche), before treating it with the phosphatase substrate CDP-Star® (Roche). Visualization of chemiluminescence was performed with an ImageQuant LAS 4000.

Restriction digests for Southern Analysis were incubated at least 4 hours at 37°C and contained 1x Cut Smart Buffer, 10 µl gDNA and 5 U restriction enzymes in a final volume of 20 µl/reaction.

Digoxigenin-labeled DNA probes were produced via PCR with PCR DIG Labeling Mix (Roche) and linearized DNA containing the flanking sequences for the *upp3* or *cco1* locus. PCR reactions were verified via gel electrophoresis and diluted in 15 ml Southern Hybridization Buffer (26% (v/v) 20x SSPE [3 mM NaCl; 227 mM NaH₂PO₄*H₂O; 20 mM Na₂-EDTA*2H₂O]; 5% (v/v) Denhardt solution [2% (w/v) BSA fraction V; 2% (w/v) Ficoll; 2% (w/v) polyvinyl Pyrrolidone]; 5% (v/v) 10% SDS).

Reaction mix:

5x Q5® Reaction Buffer	10 µl
PCR DIG labeling Mix	5 µl
Primer 1 (10 µM)	1 µl
Primer 2 (10 µM)	1 µl
Q5® high fidelity Polymerase	0,5 µl
DMSO	1.5 µl
DNA	1 µl
H ₂ O	ad 50 µl

The **Whatman assembly** was layered from bottom to top as follows:

Whatman paper soaked in 20x SSC as salt bridge

2 layers Whatman paper soaked in 20x SSC

Agarosegel (face down)

Hybond-N-Nylon-membrane

2 layers Whatman paper soaked in 20x SSC

Paper towels

Plexi glass panel with weight

Membrane incubation was performed at 65°C for the first 5 wash steps and at 35°C for the last 5 wash steps. Incubation with CDP-Star® was carried out at RT.

Hybridization Buffer	(20 ml)	30 min
DIG Probe Solution	(15 ml)	min. 6 h
Southern Wash Buffer I	(15 ml)	15 min
Southern Wash Buffer II	(15 ml)	15 min
Southern Wash Buffer III	(15 ml)	15 min
DIG Wash	(5 ml)	5 min
DIG2	(25 ml)	30 min
Anti-DIG 1:10000 in DIG 2	(25 ml)	30 min
DIG Wash	(15 ml)	15 min
(Re) DIG Wash	(15 ml)	15 min
CDP-Star® 1:100 in DIG3	(8 ml)	5-10 min

5.1.8 Protein isolation from *Ustilago maydis*

Cell extracts for reporter assays were prepared from 2-5 ml cultures by pelleting the cells and adding about 200 µl of 0.4 – 0.6 mm Ø glass beads and 200 µl protein lysis buffer (1 M Tris-HCL pH 7,4; 5 M NaCl; 0.5 M EDTA pH 8; 10% Nonident-P-40; 1 mM PMSF; 1 mM DTT; 2.5 mM Benzamidine; 4% (v/v) 1x complete protease inhibitor cocktail tablet dissolved in 2 ml distilled H₂O) per 1 ml of culture. Cells were disrupted for 25 min at 4°C and 1,400 rpm in a thermoshaker. Glass beads and cell debris were pelleted by centrifugation at 4°C for 5 min and the supernatant transferred to new reaction tubes for storage at -20°C.

5.1.9 Light experiments

Light experiments were carried out under safe light conditions (green light, approximately 520 nm). 6 ml cultures were started from 3 ml pre-cultures in 6-well plates and dark adapted for 3-5 hours. Afterwards cultures were illuminated with UV-B (310 nm) light for up to 20 hours under a UV-B narrowband lamp (Philips, prod. no. PL-S 9W/01). Light of higher wavelengths was eliminated by using a 310-nm bandpass filter (Ashai Spectra, prod. no. ZBPA310). Cultures were illuminated with

10 $\mu\text{mol m}^{-2} \text{s}^{-1}$ intensity before samples were taken for direct luciferase assay or protein extraction.

5.2 Phytohormone signaling

5.2.1 COP1/SPA1/DELLA interactions

5.2.1.1 Plasmid generation

Design and construction of expression plasmids for fluorescently tagged COP1, SPA1 and DELLA proteins is described in 5.4, with oligos listed in 5.5.

5.2.1.2 Mammalian cell culture

Human embryonic kidney cells (HEK-293T, ATCC CRL-11268), were maintained in Dulbecco's modified Eagle's medium (PAN, cat. no. P04-03550), supplemented with 10% fetal calf serum (FCS, PAN, cat. no. P30-3602) and 1% penicillin/streptomycin (PAN, cat. no. P06-07100). For confocal imaging, cells were seeded onto glass coverslips placed in cell culture wells.

5.2.1.3 PEI transfection

For transfection, 40,000 cells per well of a 24-well plate, were transfected using polyethylenimine (PEI, linear, MW: 25 kDa, Polyscience) as described in Müller et al. 2013a. The medium was exchanged 5h post transfection. In co-transfections, all plasmids were transfected in equal amounts (weight-based).

5.2.1.4 Fixing cells for microscopy

For confocal imaging, cells on glass coverslips were fixed with 4% PFA for 10 min on ice followed by 10 min at room temperature. Subsequently, cells were washed once with ice cold PBS. Coverslips were embedded in Mowiol 4-88 (Roth) containing 15 mg/ml 1,4-diazabicyclo[2.2.2]octane (DABCO, Roth) and mounted onto glass microscope slides as in Beyer et al. 2015.

5.2.2 Application of an ABA biosensor and construction of the potential-induction-fold-determination sensor pifold in plant protoplasts

General materials and methods for protoplast experimentation are described in detail in Ochoa-Fernandez et al., 2016.

5.2.2.1 Plasmid generation

Design and construction of ABA-based sensors and pifold is described in 5.4, with oligos listed in 5.5.

5.2.2.2 Plant material

Arabidopsis thaliana col-0 wt seeds were surface-sterilized with 5% (w/v) calcium hypochlorite and 0.02% (v/v) Triton X-100 in 80% (v/v) ethanol solution before seeding. 400 – 600 seeds were seeded in two rows on filter paper strips layered on top of 50 ml SCA (seedling culture Arabidopsis) growth medium [0.32% (w/v) Gamborg B5 basal salt powder with vitamins (bioWORLD), 4 mM $\text{MgSO}_4 \cdot 7\text{H}_2\text{O}$, 43.8 mM sucrose, 0.1% (v/v) Gamborg B5 Vitamin Mix (bioWORLD), and 0.8% (w/v) phytoagar in H_2O (pH 5.8)] per each 12 cm^2 plate (Greiner Bio-One). For protoplast isolation seedlings were grown for 2 weeks in a Sanyo/Panasonic MLR-352-PE growth chamber at 22°C under long day conditions (16h light, 8h dark).

5.2.2.3 Protoplast isolation and transformation

Arabidopsis thaliana protoplasts were isolated and transformed over two days starting with cutting the leaf material with a scalpel in 10 ml MMC (MES, Mannitol, Calcium: 10 mM MES, 40 mM $\text{CaCl}_2 \cdot \text{H}_2\text{O}$, 85 g/l mannitol for an osmolarity of 550 mOsm; pH 5.8) prior to the digestion of the cell wall over night by adding 2 ml of a 5% stock solution of cellulase (Onozuka R10) and macerozyme (R10, SERVA Electrophoresis GmbH, Germany). On the following day, leaf material was homogenized and filtered through a cell strainer with 70 μm pore size. The suspension was centrifuged at 100g for 20 min in a total volume of 50 ml MMC. After removing the supernatant, the pellet was resuspended in 10 ml MSC (MES, Sucrose, Calcium: 10 mM MES, 0.4 M sucrose, 20 mM $\text{MgCl}_2 \cdot 6\text{H}_2\text{O}$, 85 g/l mannitol to obtain an osmolarity of 550 mOsm; pH 5.8) and transferred to a round bottom falcon. The solution was overlaid with 3 ml 3M (MES, Mannitol, Magnesium: 15 mM MgCl_2 , 5 mM MES, 85 g/l mannitol for an osmolarity of 600 mOsm; pH 5.8) and centrifuged for 10 min at 80g. The resulting interphase of protoplasts was collected in W5 solution (2 mM MES, 154 mM glucose; pH 5.8) and the procedure repeated 2 more times. Protoplasts were counted in a Rosenthal chamber and the concentration per ml was calculated.

Subsequently protoplasts were pelleted again and resuspend in 3M solution to a concentration of 500,000 protoplasts/100 μl for transformation. For each transformation, 20 μg of plasmid DNA in a total volume of 20 μl 3M solution were gently mixed with 100 μl protoplast suspension and incubated 5 min at RT. The protoplasts were overlaid with 120 μl freshly prepared PEG_{4000} solution (61.5%

(w/v) PEG₄₀₀₀, 0.3 M mannitol, 0.15 M CaCl₂) and incubated for 9 min at RT. Next, 120 µl of 3M solution were added, directly followed by 1,440 µl PCA (Protoplast Culture Arabidopsis: 0.32 % (w/v) Gamborg B5 basal salt powder with vitamins (bioWORLD), 2 mM MgSO₄·7H₂O, 3.4 mM CaCl₂·2H₂O, 5 mM MES, 0.342 mM l-glutamine, 58.4 mM sucrose, glucose 550 mOsm (ca. 80 g/l), 8.4 µM Ca-pantothenate, 2 % (v/v) biotin from a biotin solution 0.02 % (w/v) in H₂O, 0.1 % (v/v) Gamborg B5 Vitamin Mix; pH 5.8) supplemented with ampicillin (55.6 µg/ml). Protoplasts were left for 24h at 22°C in the dark for sufficient expression of plasmid DNA before hormone treatment and luciferase measurements.

5.2.2.4 Hormone treatment

A 100 mM stock of (+)-ABA (Carbosynth) in MeOH was used for induction experiments for the ABA-biosensors in indicated concentrations and induction times.

5.2.3 Reporter Assays

5.2.3.1 Luciferase Assays

For the determination of reporter luminescence 80 µl of *Ustilago maydis* culture or cell extract or *Arabidopsis thaliana* protoplasts were transferred into a Costar® 96-well flat bottom white plate. Next, 20 µl of the respective substrates for firefly luciferase (20 mM tricine, 2.67 mM MgSO₄·7H₂O, 0.1 mM EDTA·2H₂O, 33.3 mM DTT, 0.52 mM ATP, 0.27 mM acetyl-CoA, 0.47 mM d-luciferin (Biosynth AG), 5 mM NaOH, 264 µM MgCO₃·5H₂O, in H₂O), or renilla and gaussia luciferases (472 mM coelenterazine stock solution in methanol, diluted directly before use, 1:15 for renilla and 1:250 for gaussia in cooled phosphate-buffered saline) were added. Firefly luminescence was determined in a Berthold Technologies Centro XS3 LB 960 Microplate luminometer, while renilla and gaussia luminescence were determined in a Berthold technologies Tristar2S LB942 Multimode Plate Reader. All measurements were conducted with 29 measuring points over 20 min.

5.2.3.2 SEAP reporter Assay

Transfected HEK293T cells or *Ustilago maydis* culture were analysed for SEAP activity in a Berthold technologies Tristar2S LB942 Multimode Plate Reader or in a BMG Labtech ClarioStar Multimode Plate Reader. Therefore, 200 µl of each sample were incubated at 65°C for 60 minutes to inactivate endogenous phosphatases. 80 µl of heat inactivated sample were transferred into 100 µl of SEAP buffer (20 mM L-

homoarginine, 1 mM MgCl₂ 21 % (v/v) diethanolamine) in a transparent 96-well plate. Before the measurement, 20 µl of 120 nM para-nitrophenyl phosphate (pNPP, Sigma-Aldrich) were added and the absorbance was measured at 405 nm for 1 h. SEAP activity [U/l] was determined using the Lambert-Beer's-law:

$$\frac{U}{l} = \frac{E}{\varepsilon * d} * 10^6 * \frac{200}{80}$$

with $\varepsilon = 18,600 \text{ M}^{-1} \cdot \text{cm}^{-1}$, E = increase of *para*-nitrophenolate per minute [$\text{M} \cdot \text{min}^{-1}$], d = length of the light path [cm] = 0,6 cm and $\frac{200}{80}$ = amount of SEAP-containing supernatant / dilution factor of the sample.

5.2.3.3 Fluorescence measurements via Plate Reader

The fluorescence intensity of 80 µl *Ustilago maydis* culture or cell extract or *Arabidopsis thaliana* protoplasts was performed in a Corning® 96-well flat bottom black plate. Fluorescence was determined in a BMG Labtech ClarioStar Multimode Plate Reader. Excitation wavelength for GFP, mCherry and mKate2 were 470, 570 and 588 nm, while emission was measured at 495-535, 600-640 and 605-665 nm, respectively.

5.2.3.4 Fluorescence microscopy

Cells were imaged with a confocal microscope (Nikon Instruments Eclipse Ti with a C2plus confocal laser scanner, 60× oil objective, NA = 1.40). mCherry, mVenus and mCerulean were visualized using excitation lasers of 561, 488, 405 nm and emission filters of 570–620, 535-550, 425–475 nm, respectively.

5.3 Software

Geneious 10.2.2 for cloning

MS PowerPoint 2016 for graphical design

Excel 2016 for graphs and statistical analysis

GraphPad Prism for ANOVA

Fiji 2.0.0 for image analysis and processing

5.4 Plasmids

Table 2: Generation and description of plasmids used in this work.

All plasmids are constructed with AQUA or Gibson assembly cloning (Gibson et al., 2009; Beyer et al., 2015) if not indicated otherwise.

Synthetic Toolbox for <i>Ustilago maydis</i>		
Plasmid	Description	Reference
pUMa047	tetO6-P_{mfa1min}-eGFP-nosT Vector encoding eGFP under the control of a tet operator-mfa1min promoter.	K. Müntjes
pUMa2055	P_{tef}-tetR-CI-VP16ff Vector encoding a tetR-CI-VP16ff fusion under the control of P _{tef} .	K. Müntjes
pUMa2675	prf1₈-P_{mfa1min}-eGFP-nosT Vector encoding eGFP under the control of a prf1 operator-mfa1min promoter.	K. Müntjes
pUMa2977	Storage vector encoding the red fluorescent protein mKate2.	K. Müntjes
pUMa3132	P_{O2tef}-eGFP-nosT-NatR Vector encoding eGFP under the control of P _{O2tef} and the Nourseothricin resistance cassette. The vector carries upstream and downstream flanking sequences for integration into the upp3 locus of <i>Ustilago maydis</i> .	K. Müntjes
pUMa3651	P_{O2tef}-eGFP-nosT Vector encoding eGFP under the control of P _{O2tef} and the Hygromycine resistance cassette. The vector carries upstream and downstream flanking sequences for integration into the cco1 locus of <i>Ustilago maydis</i> .	K. Müntjes
pUMa4175	P_{CRG}-5'UTR-rrm4-eGFP-e'UTR-nosT Plasmid encoding a fusion of rrm4 and eGFP under the control of the inducible CRG promoter.	K. Müntjes
pKM006	tetO13-P_{hCMVmin}-SEAP-pA SEAP reporter plasmid with 13 tetO repeats and a VP16 inducible hCMV minimal promoter.	(Müller et al., 2013b)
pKM022	P_{SV40}-PhyB-VP16-NLS-IRES-TetR-PIF6(1-100)-HA-pA Bicistronic vector encoding PhyB(1-650)-VP16 and tetR-PIF6(1-100) under control of PSV40.	
pKM084	uas_GO5-P_{min}-SEAP-pA SEAP reporter plasmid with 5 UAS _G repeats and a VP16 inducible minimal promoter.	

pKM272	pirO3-P_{HSP70min}-FLuc-pA FLuc reporter plasmid with 3 pirO repeats and a VP16 inducible HSP70 minimal promoter.	
pHB109	P_{CMV-IE}-PhyB-mCherry-NES-pA Vector encoding PhyB-mCherry-NES under the control of the hCMV immediate early promoter.	
pMZ725	P_{SV40}-PIF3-mEGFP-pA Vector encoding PIF3-mEGFP under the control of P _{SV40} .	
pVITRO-HPV68-L1L2	Vector encoding the FMDV IRES	Addgene #52587
R5 EMCV	Vector encoding the EMCV IRES	Addgene #51733
pLHNNH001	P_{O2tef}-GLuc-NLS-nosT Vector encoding GLuc-NLS under the control of P _{O2tef} . pUMA3132 and pLHNNH029 were digested with SfbI and AflIII, and ligated with QuickLigase.	this work, cloned by K. Müntjes
pLHNNH004	P_{O2tef}-SEAPn-term-nosT Vector encoding SEAPn-term under the control of P _{O2tef} . pLHNNH001 was digested with MfeI and BglIII, SEAPn-term was amplified pLHNNH020 with oNH048 and oNH070 and digested with MfeI and BglIII. Fragments were ligated with QuickLigase	this work
pLHNNH017	Vector encoding the synthesized codon optimized FLuc	GeneArt
pLHNNH018	Vector encoding the synthesized codon optimized GLuc	GeneArt
pLHNNH019	Vector encoding the synthesized codon optimized RLuc	GeneArt
pLHNNH020	Vector encoding the synthesized codon optimized SEAP-nTerm	GeneArt
pLHNNH022	Vector encoding the synthesized codon optimized AtCOP1 WD40 domain	GeneArt
pLHNNH024	Vector encoding the synthesized codon optimized ePDZb and PIF6(1-100)	GeneArt
pLHNNH025	Vector encoding the synthesized codon optimized GAL4 _{BD} and KRAB	GeneArt
pLHNNH026	Vector encoding the synthesized codon optimized PhyB(1-650)	GeneArt
pLHNNH027	Vector encoding the synthesized codon optimized UVR8	GeneArt
pLHNNH028	Vector encoding the synthesized codon optimized PIP and LOVpep	GeneArt
pLHNNH029	Vector encoding the synthesized P _{O2tef} and codon optimized GLuc-NLS	GeneArt
pLHNNH030	P_{O2tef}-RLuc-HA-nosT Vector encoding RLuc-HA under the control of P _{O2tef} . pLHNNH001 was digested with MfeI and BglIII, RLuc was amplified from pLHNNH019 with oNH020 and oNH116 adding an HA-tag c-terminally to RLuc.	this work
pLHNNH031	P_{O2tef}-GLuc-HA-nosT Vector encoding GLuc-HA under the control of P _{O2tef} . pLHNNH001 was digested with MfeI and BglIII, GLuc was amplified from pLHNNH018 with oNH016 and oNH117 adding an HA-tag c-terminally to GLuc.	this work

pLHNNH032	P_{O2tef}-SEAP-HA-nosT Vector encoding SEAP-HA under the control of P _{O2tef} . pLHNNH001 was digested with MfeI and BglII, SEAP was amplified from pLHNNH034 with oNH048 and oNH132, adding an HA-tag c-Terminally to SEAP.	this work
pLHNNH033	P_{O2tef}-FLuc-HA-nosT Vector encoding FLuc-HA under the control of P _{O2tef} . pLHNNH001 was digested with MfeI and BglII, FLuc was amplified from pLHNNH017 with oNH012 and oNH119 adding an HA-Tag c-terminally to FLuc.	this work
pLHNNH034	P_{O2tef}-SEAP-nosT Vector encoding SEAP under the control of P _{O2tef} . pLHNNH001 was digested with MfeI and BglII, SEAP n-term was amplified from pLHNNH020 with oLH017 and oLH021, SEAP c-term was amplified from pLHNNH035 with oNH130 and oNH131. SEAP parts were fused via PCR with oNH048 and oNH131.	this work
pLHNNH035	Vector encoding the synthesized codon optimized SEAP-cTerm	GeneArt
pNH001	Gal4UAS₅-P_{hCMVmin}-SEAPn-term-nosT Vector encoding SEAPn-term under the control of VP16ff inducible Gal4UAS ₅ -P _{hCMVmin} . pLHNNH004 was digested with SbfI and MfeI, (UAS _G) ₅ was amplified with oNH090 and oNH082 from pKM084, P _{hCMVmin} was amplified with oNH084 and oNH091 from pKM006, (UAS _G) ₅ and P _{hCMVmin} were fused via PCR with oNH081 and oNH085.	this work
pNH002	Gal4UAS₅-P_{mfa1min}-SEAPn-term-nosT Vector encoding SEAPn-term under the control of VP16ff inducible Gal4UAS ₅ -P _{mfa1min} . pLHNNH004 was digested with SbfI and MfeI, (UAS _G) ₅ was amplified with oNH090 and oNH083 from pKM084, P _{mfa1min} was amplified with oNH086 and oNH092 from pUMa047, (UAS _G) ₅ and P _{mfa1min} were fused via PCR with oNH081 and oNH087.	this work
pNH003	PIR₃-P_{hCMVmin}-SEAPn-term-nosT Vector encoding SEAPn-term under the control of VP16ff inducible PIR ₃ -P _{hCMVmin} . pLHNNH004 was digested with SbfI and MfeI, PIR ₃ was amplified with oNH098 and oNH096 from pKM272, P _{hCMVmin} was amplified with oNH084 and oNH091 from pKM006, PIR ₃ and P _{hCMVmin} were fused via PCR with oNH095 and oNH085.	this work
pNH004	PIR₃-P_{mfa1min}-SEAPn-term-nosT Vector encoding SEAPn-term under the control of VP16ff inducible PIR ₃ -P _{mfa1min} . pLHNNH004 was digested with SbfI and MfeI, PIR ₃ was amplified with oNH098 and oNH097 from pKM272, P _{mfa1min} was amplified with oNH086 and oNH092 from pUMa047, PIR ₃ and P _{mfa1min} were fused via PCR with oNH095 and oNH087.	this work

pNH005	<p>P_{O₂tef}-GAL4_{BD}-p65-NLS-nosT</p> <p>Vector encoding GAL4_{BD}-p65-NLS under control of P_{O₂tef}. pUMa3651 was digested with NcoI and Ascl, the GAL4_{BD} was amplified from pLHNNH025 using oNH104 and oNH105, p65 was amplified from pLHNNH021 using oNH110 and oNH109. GAL4_{BD} and p65 were fused via PCR using oNH166 and oNH120, adding an NLS to the c-term of the fusion.</p>	this work
pNH006	<p>P_{O₂tef}-GAL4_{BD}-VP16ff-NLS-nosT</p> <p>Vector encoding GAL4_{BD}-VP16ff-NLS under control of P_{O₂tef}. pUMa3651 was digested with NcoI and Ascl, the GAL4_{BD} was amplified from pLHNNH025 using oNH104 and oNH105, VP16ff was amplified from pUMa2055 using oNH114 and oNH113. GAL4_{BD} and VP16ff were fused via PCR using oNH166 and oNH121, adding an NLS to the c-term of the fusion.</p>	this work
pNH007	<p>P_{O₂tef}-PIP-p65-NLS-nosT</p> <p>Vector encoding PIP-p65-NLS under control of P_{O₂tef}. pUMa3651 was digested with NcoI and Ascl, PIP was amplified from pLHNNH028 using oNH106 and oNH107, p65 was amplified from pLHNNH021 using oNH111 and oNH109. PIP and p65 were fused via PCR using oNH167 and oNH120, adding an NLS to the c-term of the fusion.</p>	this work
pNH008	<p>P_{O₂tef}-PIP-VP16ff-NLS-nosT</p> <p>Vector encoding PIP-VP16ff-NLS under control of P_{O₂tef}. pUMa3651 was digested with NcoI and Ascl, PIP was amplified from pLHNNH028 using oNH106 and oNH107, VP16ff was amplified from pUMa2055 using oNH115 and oNH113. PIP and VP16ff were fused via PCR using oNH167 and oNH121, adding an NLS to the c-term of the fusion.</p>	this work
pNH009	<p>P_{O₂tef}-mKate2-NES-pIRES-eGFP-NLS-nosT</p> <p>Bicistronic vector encoding mKate2-NES and eGFP-NLS under the control of P_{O₂tef}. pLHNNH001 was digested with MfeI and PacI, mKate2 was amplified from pLHNNH015 with oNH058 and oNH122, eGFP was amplified from pLHNNH015 with oNH205 and oNH057, <i>human polio virus</i> IRES was amplified from pKM006 with oNH124 and oNH125, mKate2, pIRES and eGFP were fused via PCR using oNH008 and oNH123.</p>	this work
pNH010	<p>P_{O₂tef}-mKate2-NES-eIRES-eGFP-NLS-nosT</p> <p>Bicistronic vector encoding mKate2-NES and eGFP-NLS under the control of P_{O₂tef}. pLHNNH001 was digested with MfeI and PacI, mKate2 was amplified from pLHNNH015 with oNH058 and oNH122, eGFP was amplified from pLHNNH015 with oNH205 and oNH057, <i>Encephalomyocarditis virus</i> IRES was amplified from pLHNNH017 with oNH126 and oNH127, mKate2, eIRES and eGFP were fused via PCR using oNH008 and oNH123.</p>	this work

pNH011	<p>P_{O₂ter}-mKate2-NES-fIRES-eGFP-NLS-nosT</p> <p>Bicistronic vector encoding mKate2-NES and eGFP-NLS under the control of P_{O₂ter}. pLHNNH001 was digested with MfeI and PaeI, mKate2 was amplified from pLHNNH015 with oNH058 and oNH122, eGFP was amplified from pLHNNH015 with oNH205 and oNH057, <i>Foot-and-mouth-disease virus</i> IRES was amplified from pLHNNH018 with oNH128 and oNH129, mKate2, fIRES and eGFP were fused via PCR using oNH008 and oNH123.</p>	this work
pNH012	<p>nosT-NES-mKate2-P_{hCMVmin}-CMVenhancer(5'→3')-P_{hCMVmin}-eGFP-NLS-nosT</p> <p>Bicistronic vector encoding mKate2-NES and eGFP-NLS under the control of a bidirectional P_{CMV}. pNH030 was digested with Ascl, eGFP was amplified from pUMa3132 using oligos oNH136 and oNH123. Parts were assembled via AQUA cloning. The resulting plasmid pNH012a was digested with MfeI; mKate2 was amplified from pUMa2977 using oligos oNH139 and oNH141.</p>	this work
pNH013	<p>nosT-NES-mKate2-P_{hCMVmin}-CMVenhancer(5'←3')-P_{hCMVmin}-eGFP-NLS-nosT</p> <p>Bicistronic vector encoding mKate2-NES and eGFP-NLS under the control of a bidirectional P_{CMV} pNH012 was digested with Ascl, mKate2 was amplified from pUMa2977 using oligos oNH657 and oNH658. Parts were assembled via Aqua cloning. The resulting plasmid pNH013a was digested with MfeI, eGFP was amplified from pUMa3132 using oligos oNH659 and oNH660.</p>	this work
pNH014	<p>nosT-NES-mKate2-P_{mfa1min}-(prf1)₄(5'→3')-P_{mfa1min}-GFP-NLS-nosT</p> <p>Bicistronic vector encoding mKate2-NES and eGFP-NLS under the control of a bidirectional P_{(prf1)₄-mfa1min}. pNH032 was digested with MfeI; mKate2 was amplified from pUMa2977 with oNH141 and oNH153, parts were assembled via AQUA cloning. The resulting plasmid pNH014a was digested with Ascl, eGFP was amplified from pUMa3132 with oNH721 and oNH123.</p>	this work
pNH015	<p>nosT-NES-mKate2-P_{mfa1min}-(prf1)₄(5'←3')-P_{mfa1min}-GFP-NLS-nosT</p> <p>Bicistronic vector encoding mKate2-NES and eGFP-NLS under the control of a bidirectional P_{(prf1)₄-mfa1min}. pNH032 was digested with MfeI, eGFP was amplified from pUMa3132 with oNH152 and oNH660. Parts were assembled via AQUA cloning. The resulting plasmid, pNH015a was digested with Ascl, mKate2 was amplified from pUMa2977 with oNH722 and oNH658.</p>	this work
pNH018	<p>Gal4UAS₅-P_{hCMVmin}-GLuc-nosT</p> <p>Vector encoding GLuc under the control of VP16ff inducible Gal4UAS₅-P_{hCMVmin}. pNH001 was digested with MfeI and Ascl, GLuc was amplified from pLHNNH018 using oligos oNH182 and oNH183.</p>	this work

pNH019	Gal4UAS₅-P_{hCMVmin}-FLuc-nosT Vector encoding FLuc under the control of VP16ff inducible Gal4UAS ₅ -P _{hCMVmin} . pNH001 was digested with MfeI and AclI, FLuc was amplified from pLHNNH017 using oligos oNH184 and oNH174.	this work
pNH020	Gal4UAS₅-P_{mfa1min}-GLuc-nosT Vector encoding GLuc under the control of VP16ff inducible Gal4UAS ₅ -P _{mfa1min} . pNH002 was digested with MfeI and AclI, GLuc was amplified from pLHNNH018 using oligos oNH185 and oNH183.	this work
pNH021	Gal4UAS₅-P_{mfa1min}-FLuc-nosT Vector encoding FLuc under the control of VP16ff inducible Gal4UAS ₅ -P _{mfa1min} . pNH002 was digested with MfeI and AclI, FLuc was amplified from pLHNNH017 using oligos oNH186 and oNH174.	this work
pNH022	PIR₃-P_{hCMVmin}-GLuc-nosT Vector encoding GLuc under the control of VP16ff inducible PIR ₃ -P _{hCMVmin} . pNH003 was digested with MfeI and AclI, GLuc was amplified from pLHNNH018 using oligos oNH182 and oNH183.	this work
pNH023	PIR₃-P_{hCMVmin}-FLuc -nosT Vector encoding FLuc under the control of VP16ff inducible PIR ₃ -P _{hCMVmin} . pNH003 was digested with MfeI and AclI, FLuc was amplified from pLHNNH017 using oligos oNH184 and oNH174.	this work
pNH024	PIR₃-P_{mfa1min}-GLuc -nosT Vector encoding GLuc under the control of VP16ff inducible PIR ₃ -P _{mfa1min} . pNH004 was digested with MfeI and AclI, GLuc was amplified from pLHNNH018 using oligos oNH185 and oNH183.	this work
pNH025	PIR₃-P_{mfa1min}-FLuc -nosT Vector encoding FLuc under the control of VP16ff inducible PIR ₃ -P _{mfa1min} . pNH004 was digested with MfeI and AclI, FLuc was amplified from pLHNNH017 using oligos oNH186 and oNH174.	this work
pNH026	P_{O2tef}-RLuc-pIRES-eGFP-FLuc-nosT Bicistronic vector encoding RLuc and FLuc under the control of P _{O2tef} . pLHNNH001 was digested with MfeI and AclI, RLuc was amplified from pLHNNH019 using oligos oLH015 and oNH181, pIRES was amplified from pKM006 using oligos oNH612 and oNH613, RLuc and pIRES were fused via PCR using oligos oNH020 and oNH613. FLuc was amplified from pLHNNH017 using oligos oNH175 and oNH174. FLuc and the RLuc-pIRES fusion were fused via PCR using oligos oNH623 and oNH624.	this work

pNH028	<p>P_{O₂tef}-RLuc-eIRES-eGFP-FLuc-nosT</p> <p>Bicistronic vector encoding RLuc and FLuc under the control of P_{O₂tef}. pLHNNH001 was digested with MfeI and AseI, RLuc was amplified from pLHNNH019 using oligos oLH015 and oNH178, eIRES was amplified from pLHNNH036 using oligos oNH614 and oNH615, RLuc and eIRES were fused via PCR using oligos oNH020 and oNH615. FLuc was amplified from pLHNNH017 using oligos oNH177 and oNH174. FLuc and the RLuc-leIRES fusion were fused via PCR using oligos oNH623 and oNH624.</p>	this work
pNH029	<p>P_{O₂tef}-RLuc-fIRES-eGFP-FLuc-nosT</p> <p>Bicistronic vector encoding RLuc and FLuc under the control of P_{O₂tef}. pLHNNH001 was digested with MfeI and AseI, RLuc was amplified from pLHNNH019 using oligos oLH015 and oNH180, fIRES was amplified from pLHNNH037 using oligos oNH616 and oNH617, RLuc and fIRES were fused via PCR using oligos oNH020 and oNH617. FLuc was amplified from pLHNNH017 using oligos oNH179 and oNH174. FLuc and RLuc-fIRES fusion were fused via PCR using oligos oNH623 and oNH624.</p>	this work
pNH030	<p>nosT-RLuc-P_{hCMVmin}-CMVenhancer(5'→3')-P_{hCMVmin}-FLuc-nosT</p> <p>Bicistronic vector encoding RLuc and FLuc under the control of a bidirectional P_{CMV}. pLHNNH001 was digested with MfeI and AseI; FLuc was amplified from pLHNNH017 using oligos oNH198 and oLH018, P_{CMV} was amplified from pHB109 using oligos oNH137 and oNH135, P_{CMV} and FLuc were fused via PCR using oligos oNH174 and oNH625. Parts were assembled via AQUA cloning. The resulting plasmid pNH030a was digested with SbfI and MfeI, RLuc was amplified from pLHNNH019 using oligos oLH019 and oNH196, a P_{hCMVmin} was added via PCR using oligos oNH197 and oNH140, nosT was amplified from pUMa3132 using oligos oNH158 and oNH144, P_{hCMVmin}-RLuc and nosT were fused via PCR using oligos oNH169 and oNH143.</p>	this work
pNH031	<p>nosT-RLuc-P_{hCMVmin}-CMVenhancer(5'←3')-P_{hCMVmin}-FLuc-nosT</p> <p>Bicistronic vector encoding RLuc and FLuc under the control of a bidirectional P_{CMV}. pNH030 was digested with AseI. RLuc was amplified from pLHNNH019 using oligos oNH646 and oNH645. Parts were assembled via Aqua cloning. The resulting plasmid pNH031a was digested with MfeI. FLuc was amplified from pLHNNH017 using oligos oNH184 and oNH647.</p>	this work

- pNH032 **nosT-RLuc-P_{mfa1min}-(prf1)₄(5'→3')-P_{mfa1min}-FLuc-nosT** this work
- Bicistronic vector encoding RLuc and FLuc under the control of a bidirectional P_{(prf1)₄-mfa1min}. pLHNN001 was digested with PacI and AscI, FLuc was amplified from pLHNN017 with oNH695 and oNH174. Parts were assembled via AQUA cloning. The resulting plasmid pNH032a was digested with MfeI and PacI, pOMA was amplified from pUMa2675 with oNH626 and oNH696 and parts were assembled via AQUA cloning. 4 repeats of the prf1 enhancer were lost during cloning. The resulting plasmid pNH032b was digested with MfeI and SbfI. nosT was amplified from pUMa3132 with oNH144 and oNH142, RLuc was amplified from pLHNN019 with oNH627 and oNH197. nosT and RLuc were fused via PCR using oNH144 and oNH628. The resulting fragment was again amplified using oNH143 and oNH157 to add overhangs to the backbone.
- pNH035 **pA_{SV40}-NES-mCherry-P_{hCMVmin}-CMVenhancer(5'→3')-P_{hCMVmin}-eGFP-NLS-pA_{SV40}** this work
- Bicistronic expression vector coding for mCherry-NES and eGFP-NLS under the control of a bidirectional P_{CMV}. pNH044 was digested with NotI and XbaI. P_{CMV-IE} was amplified from pHB109 with oNH135 and oNH137. eGFP was amplified from pMZ725 with oNH151 and oNH057. P_{CMV-IE} and eGFP were fused via PCR using oNH652 and oNH145. Parts were assembled via AQUA cloning. The resulting plasmid pNH035a was digested with NotI and EcoRI. mCherry was amplified from pMZ333 using oNH146 and oNH150. The resulting fragment was again amplified with oNH147 and oNH140 to add P_{hCMVmin}. pA_{SV40} was amplified from pMZ333 using oNH601 and oNH148. P_{hCMVmin}-mCherry and pA_{SV40} were fused via PCR with oNH149 and oNH653.
- pNH036 **pA_{SV40}-NES-mCherry-P_{hCMVmin}-CMVenhancer(5'←3')-P_{hCMVmin}-eGFP-NLS-pA_{SV40}** this work
- Bicistronic expression vector coding for mCherry-NES and eGFP-NLS under the control of a bidirectional P_{CMV}. pNH035 was digested with BamHI and Sall, mCherry was amplified from pMZ333 using oNH151 and oNH654. Parts were assembled via AQUA cloning. The resulting plasmid pNH036a was digested with AgeI. eGFP was amplified from pMZ725 using oNH655 and oNH656.

pNH037	<p>nosT-RLuc-P_{hCMVmin}-CMVenhancer(5'→3')-P_{hCMVmin}-FLuc-nosT</p> <p>Bicistronic vector encoding RLuc and FLuc under the control of a bidirectional P_{CMV}. pUMa3651 was digested with NcoI and Ascl. FLuc was amplified from pLHNNH017 using oNH198 and oLH018, P_{CMV-IE} was amplified from pHB109. FLuc and P_{CMV-IE} were fused via PCR using oligos oNH625 and oNH174. Parts were assembled via AQUA cloning. The resulting plasmid, pNH037a was digested with SbfI and MfeI. RLuc was amplified from pLHNNH019 using oLH019 and oNH196. The resulting fragment was again amplified using oNH197 and oNH140 to add P_{hCMVmin}. nosT was amplified from pUMa3132 using oNH158 and oNH698. P_{hCMVmin}-RLuc and nosT were fused via PCR using oligos oNH669 and oNH169.</p>	this work
pNH041	<p>P_{OMA}-mKate2-NES-pIRES-eGFP-NLS-nosT</p> <p>Bicistronic vector encoding mKate2-NES and eGFP-NLS under the control of P_{OMA}. pNH009 was digested with SbfI and MfeI, pOMA was amplified from pUMa2675 using oligos oNH621 and oNH622.</p>	this work
pNH042	<p>P_{OMA}-mKate2-NES-eIRES-eGFP-NLS-nosT</p> <p>Bicistronic vector encoding mKate2-NES and eGFP-NLS under the control of P_{OMA}. pNH010 was digested with SbfI and MfeI, pOMA was amplified from pUMa2675 using oligos oNH621 and oNH622.</p>	this work
pNH043	<p>P_{OMA}-mKate2-NES-fiRES-eGFP-NLS-nosT</p> <p>Bicistronic vector encoding mKate2-NES and eGFP-NLS under the control of P_{OMA}. pNH011 was digested with SbfI and MfeI, pOMA was amplified from pUMa2675 using oligos oNH621 and oNH622.</p>	this work
pNH044	<p>P_{SV40}-eGFP-pA_{SV40}</p> <p>Vector coding for eGFP under the control of P_{SV40}. pLH002 was amplified by PCR with oNH631 and oNH632, to exchange NheI by EcoRI. The PCR product was assembled by AQUA cloning</p>	
pNH045	<p>nosT-UVR8(12-381)-PIP-P_{hCMVmin}-CMVenhancer(5'→3')-P_{hCMVmin}-COP1(WD40)-VP16ff-nosT</p> <p>Bicistronic vector encoding UVR8(12-381)-PIP and COP1(WD40)-VP16ff under the control of a bidirectional P_{CMV}. pNH037 was digested with MfeI. UVR8 was amplified from pLHNNH027 using oNH670 and oNH671. PIP was amplified from pLHNNH028 using oNH106 and oNH107. UR8 and PIP were fused via PCR using oNH672 and oNH673. Parts were assembled via AQUA cloning. The resulting plasmid pNH045a was digested with Ascl. COP1(WD40) was amplified from pLHNNH022 using oNH674 and oNH675. VP16ff was amplified from pUMa2055 using oNH676 and oNH113. COP1(WD40) and VP16ff were fused via PCR using oNH677 and oNH121.</p>	this work

pNH047	<p>nosT-AsLOV2pep-PIP-P_{hCMVmin}-CMVenhancer(5'→3')-P_{hCMVmin}-ePDZb-VP16ff-nosT</p> <p>Bicistronic vector encoding AsLOV2pep-PIP and ePDZb-VP16ff under the control of a bidirectional P_{CMV}. pNH037 was digested with MfeI. LOV2pep was amplified from pLHNNH028 using oNH679 and oNH680. PIP was amplified from pLHNNH028 using oNH106 and oNH107. LOV2pep and PIP were fused via PCR using oNH672 and oNH681. Parts were assembled via AQUA cloning. The resulting plasmid oNH047a was digested with AscI. ePDZb was amplified from pLHNNH024 using oNH682 and oNH683. VP16ff was amplified from pUMa2055 using oNH684 and oNH113. ePDZb and VP16ff were fused via PCR using oNH685 and oNH121.</p>	this work
pNH054	<p>P_{CRG}-FLuc-nosT-P_{O2tef}-RLuc-nosT</p> <p>Bicistronic vector encoding FLuc under the control of the inducible P_{CRG} and RLuc under the control of P_{O2tef}. pLHNNH030 was digested with SbfI. FLuc was amplified from pLHNNH017 using oLH014 and oLH018, nosT was amplified from pUMa3132 using oNH715 and oNH144. FLuc and nosT were fused via PCR using oNH717 and oNH144. P_{CRG} was amplified from pUMa4175 using oNH718 and oNH719. FLuc-nosT and P_{CRG} were fused via PCR using oNH720 and oNH716.</p>	this work
pNH056	<p>PIR₃-FLuc-nosT</p> <p>Vector encoding FLuc under the control of the PIR₃ operating sequence. pNH023 was digested with PaeI and SbfI. PIR₃ was amplified from pKM006 using oNH735 and oNH736.</p>	this work
pLH002	<p>P_{SV40}-eGFP-pA</p> <p>Vector encoding eGFP under the control of P_{SV40}, with a NheI restriction site upstream of P_{SV40}.</p>	Provided by L. Hüsemann in our lab

COP1/SPA1/DELLA interaction

Plasmid	Description	Reference
pMZ333	P_{SV40}-PhyB(1-908)-L-mCherry-pA PhyB expression plasmid encoding the first 908 amino acids of PhyB, a short linker and mCherry under the control of P _{SV40} .	(Beyer et al. 2015)
pMZ1160	Plasmid encoding <i>Arabidopsis thaliana</i> SPA1 (AT2G46340)	this work
pCambia-COP1	pCambia_a1_p35S-DsRED-COP1-HA-T35S Vector encoding <i>Arabidopsis thaliana</i> COP1 (AT2G32950)	this work
pRSET	PT7-driven bacterial expression vector	Novagen
pSAM200	P_{SV40}-TetR-VP16-pA Constitutive TetR-VP16 expression vector.	(Fussenegger et al., 1997)
pSLS404	Plasmid encoding <i>Arabidopsis thaliana</i> GAI (AT1G14920)	this work
pSLS405	Plasmid encoding <i>Arabidopsis thaliana</i> RGA (AT2G01570)	this work
pTB206	Plasmid encoding the monomeric yellow fluorescent protein mVenus	this work

pTB208	Plasmid encoding the monomeric cyan fluorescent protein mCerulean	this work
pNH100	P_{SV40}-SPA1-pA Vector encoding SPA1 under the control of P _{SV40} . pMZ333 was digested with NotI and XbaI, SPA1 was amplified with oNH201 and oNH203 from pMZ1160.	this work
pNH117	P_{SV40}-COP1-pA Vector encoding COP1 under the control of P _{SV40} . pMZ333 was amplified with oNH222 and oNH223, COP1 was amplified from pCambia-Cop1 with oNH248 and oNH249.	this work
pNH120	P_{SV40}-mVenus-COP1-pA pMZ333 was PCR-amplified using the oligonucleotides oNH222 and oNH223, COP1 was amplified from pCambia_a1_p35S-DsRED-COP1-HA-T35S with oNH207 and oNH249. The pMZ333 fragment and COP1 were fused by PCR using oNH207 and oNH223. mVenus was amplified from pTB206 using oligonucleotides oNH250 and oNH251, fragments were assembled by AQUA cloning, resulting in a P _{SV40} -driven expression vector for COP1 fused to mVenus.	this Work
pNH122	P_{SV40}::mCerulean-SPA1-NLS:pA pMZ333 was PCR-amplified using oligonucleotides oNH222 and oNH223. SPA1 was amplified from pMZ1160 with oNH200 and oNH255 adding a simian virus 40 derived nuclear localization sequence (NLS, PKKKRKV) to the SPA1 c-terminus. SPA1 and the pMZ333 fragments were fused by PCR, using oNH200 and oNH223. mCerulean was amplified from pTB208 with oNH250 and oNH254. Fragments were assembled via AQUA cloning, resulting in a P _{SV40} -driven expression vector for SPA1 fused to mCerulean and the NLS	this Work
pNH130	P_{SV40}-GAI-VP16-IRES-TetR-COP1-pA Bicistronic vector encoding GAI-VP16 and TetR-COP1 under the control of P _{SV40} . pJATB001 was digested with NotI and Ascl. COP1 was amplified from pNH102 using oligos oNH261 and oNH209, TetR was amplified from pJATB001 using oligos oNH269 and oNH268, TetR and COP1 were fused via PCR using oligos oNH267 and oNH262. parts were assembled via AQUA cloning	this work
pNH131	P_{SV40}-RGA-VP16-IRES-TetR-COP1-pA Bicistronic vector encoding RGA-VP16 and TetR-COP1 under the control of P _{SV40} . pJATB002 was digested with NotI and Ascl. COP1 was amplified from pNH102 using oligos oNH261 and oNH209, TetR was amplified from pJATB001 using oligos oNH269 and oNH268, TetR and COP1 were fused via PCR using oligos oNH267 and oNH262. parts were assembled via AQUA cloning	this work

pNH132	<p>P_{SV40}-GAI-VP16-IRES-TetR-SPA1-pA</p> <p>Bicistronic vector encoding GAI-VP16 and TetR-SPA1 under the control of P_{SV40}. pJATB001 was digested with NotI and Ascl, SPA1 was amplified from pNH101 using oligos oNH263 and oNH259, TetR was amplified from pJATB001 using oligos oNH269 and oNH268, SPA1 and TetR were fused via PCR using oligos oNH267 and oNH264, parts were assembled via AQUA cloning</p>	this work
pNH133	<p>P_{SV40}-RGA-VP16-IRES-TetR-SPA1-pA</p> <p>Bicistronic vector encoding GAI-VP16 and TetR-COP1 under the control of P_{SV40}. pJATB002 was digested with NotI and Ascl. SPA1 was amplified from pNH101 using oligos oNH263 and oNH202, TetR was amplified from pJATB001 using oligos oNH269 and oNH268, TetR and SPA1 were fused via PCR using oligos oNH267 and oNH264. parts were assembled via AQUA cloning</p>	this work
pNH134	<p>P_{SV40}-VP16-SPA1-IRES-TetR-COP1-pA</p> <p>Bicistronic vector encoding VP16-SPA1 and TetR-COP1 under the control of P_{SV40}. pNH130 was digested with PstI and SpeI. VP16 was amplified from pNH130 using oNH272 and oNH273. SPA1 was amplified from pNH100 using oNH274 and oNH202. VP16 and SPA1 were fused via PCR using oNH275 and oNH276.</p>	this work
pNH135	<p>P_{SV40}-GAI-VP16-IRES-TetR-COP1-pA</p> <p>Bicistronic vector encoding GAI-VP16 and TetR-COP1 under the control of P_{SV40}. pNH133 was digested with XhoI and PstI. VP16 was amplified from pNH130 using oNH272 and oNH273. COP1 was amplified from pNH117 using oNH277 and oNH209. VP16 and COP1 were fused via PCR with oNH278 and oNH279.</p>	this work
pTB200	<p>P_{SV40}::GAI-mCherry:pA</p> <p>pMZ333 was digested with NotI and XbaI. GAI was PCR-amplified from pSLS404 using the oligonucleotides oTB064 and oTB065. mCherry was amplified from pMZ333 using oTB066 and oTB067. Fragments were assembled via AQUA cloning, resulting in a P_{SV40}-driven expression vector for GAI fused to mCherry.</p>	provided by T. Blomeier in our lab
pTB201	<p>P_{SV40}::RGA-mCherry:pA</p> <p>pMZ333 was digested with NotI and XbaI. RGA was PCR-amplified from pSLS405 using the oligonucleotides oTB068 and oTB069. mCherry was amplified from pMZ333 using oTB070 and oTB067. Fragments were assembled via AQUA cloning (ref 1), resulting in a P_{SV40}-driven expression vector for RGA fused to mCherry.</p>	provided by T. Blomeier in our lab
pPF034	<p>tetO13-PhCMVmin-SEAP-pA-PSV40-GLuc-pA</p> <p>Bicistronic vector encoding SEAP under the control of a TetR-inducible P_{hCMVmin} and GLuc under the control of the constitutive SV40 promoter.</p>	Provided by P. Fischbach in our lab

pJATB001	P_{SV40}-GAI-VP16-IRES-TetR-PIF6(1-100)-pA Bicistronic vector encoding GAI-VP16 and TetR-PIF6(1–100) under control of P _{SV40} .	provided by J. Andres and T. Blomeier in our lab
pJATB002	P_{SV40}-RGA-VP16-IRES-TetR-PIF6(1-100)-pA Bicistronic vector encoding RGA-VP16 and TetR-PIF6(1–100) under control of P _{SV40} .	provided by J. Andres and T. Blomeier in our lab

ABA sensor and pifold

Plasmid	Description	Reference
pNH1001	pMDC83_P_{35S}::cPYL8-GFP-6HIS	Received from P. Rodriguez Egea (Polytechnic University of Valencia)
pNH1003	pAlligator_2P_{35S}::3HA-RFA4fl	P. Rodriguez Egea
CtrlQuant	P_{35S}-RLuc-2A-GAGAGAGAGAGAGA-FLuc-myc-nosT Vector for the expression of a ratiometric luminescent biosensor used as a control, where the SM is replaced with a repeated GA sequence.	(Samodelov et al. 2016)
pGEN016	P_{35S}-mEGFP-nosT Vector encoding mEGFP under the control of P _{35S} .	Received from M. Rodriguez-Franco (University of Freiburg)
pHB1114	P_{35S}-RLuc-2A-BES1-FLuc-myc-nosT Bicistronic expression vector encoding RLuc and BES1-Fluc under control of P _{35S} .	Provided by H. Beyer in our lab
pNH303	P_{35S}-RLuc-2A-cPYL8-RLuc-myc-nosT Bicistronic expression vector encoding RLuc and PYL8-FLuc under control of P _{35S} . pHB1114 was digested with NheI and EcoRI, cPYL8 was amplified from pNH1001 with oNH405 and oNH423, the product was again amplified with oNH430 and oNH416 adding overhangs and an n-terminal 2A-petide.	this work
pNH308	P_{35S}-RFA4fl-nosT Expression vector encoding RFAfl under control of P _{35S} . pGEN016 was digested with AgeI and EcoRI. RFA4fl was amplified from pNH1003 using oligos oNH427 and oNH428.	this work
pLHNH100 (pifold)	P_{35S}-RLuc-2A-GAGAGAGAGAGAGA-PEST-FLuc-myc-nosT Bicistronic expression plasmid encoding RLuc and GA ₇ -PEST-FLuc under control of P _{35S} . pSW209 was digested with NheI. The three oligo pairs pLHNH001 + oLHNH008, oLHNH002 + oLHNH009 and oLHNH003 + oLHNH010 were pre-annealed in annealing buffer. Parts were assembled in an AQUA cloning reaction.	this work

5.5 Oligonucleotides

Table 3: Oligonucleotides used in this work

Oligo	Sequence (5'→3')	Description
oNH008	CGGGATCCCCCGGGCTGCAGGAATTCGATCCCCAATTGATGGTGTCC GAGCTCAT	Fw mKate2
oNH011	ATTTACCATTATTCTCTTCATTTACTGAG	Fw cco1 UF probe
oNH012	CGGGATCCCCCGGGCTGCAGGAATTCGATCCCCAATTGATGGAGGAC GCCAAGAA	Fw FLuc
oNH013	CCGGGCAAATGCCTATC	Rev cco1 UF probe
oNH015	GCGAGATGGAAGTGCC	Fw cco1 DF probe
oNH016	CGGGATCCCCCGGGCTGCAGGAATTCGATCCCCAATTGATGGGCGTC AAGGTG	Fw GLuc
oNH017	ATTTCTTGCTAGGACTGAAAGC	Rev cco1 DF probe
oNH018	CCTGCATTTAAATGTGTCAGGG	Fw upp3 UF probe
oNH020	CGGGATCCCCCGGGCTGCAGGAATTCGATCCCCAATTGATGACCAGC AAGGTCTAC	Fw RLuc
oNH021	CTGCTATGGTGAGACGC	Rev upp3 UF probe
oNH043	GGCCTAGGCTCGCT	Fw upp3 DF probe
oNH044	ATTTAAATGCTGATCCGCACATT	Rev upp3 DF probe
oNH048	CGGGATCCCCCGGGCTGCAGGAATTCGATCCCCAATTGATGGTGCTC GGTCCTT	Fw SEAP
oNH057	CTTGTACAGCTCGTCCATG	Rev eGFP
oNH058	ATGGTGTCGGAGCTCATC	Fw mKate2
oNH070	GCCGGGCGGCCGGCGCGCCGGCCGCTAGATCTTTAGTCGATGTCCA TGTTCCG	Rev SEAPn-term
oNH081	TCACCATAGCAGGCCTAGATGGCCCTGCAGGTGCAGGTCGGAGTAC TG	Fw (UAS _G) ₅
oNH082	CTAAACGAGCTCTGCTTATATAGGTTAATTAACCCTCTAGAGTCTCCGC	Rev (UAS _G) ₅ phCMVmin
oNH083	GAGGAAAGGCCTTGCTAATACTAGTTAATTAACCCTCTAGAGTCTCCG C	Rev (UAS _G) ₅ pmfa1min
oNH084	CCTATATAAGCAGAGCTCGTTTAG	Fw P _{hCMVmin}
oNH085	AGCAGCATGCAAGGACCGAGCACCATCAATTGAGGCTGGATCGGTCC	Rev P _{hCMVmin}
oNH086	CTAGTATTAGCAAGGCCTTTCC	Fw P _{mfa1min}
oNH087	AGCAGCATGCAAGGACCGAGCACCATCAATTGGTGATAGAAGTAAGG TAGTTGATTTG	Rev P _{mfa1min}
oNH090	TGCAGGTCGGAGTACTG	Fw (UAS _G) ₅
oNH091	AGGCTGGATCGGTCC	Rev P _{hCMVmin}
oNH092	GTGATAGAAGTAAGGTAGTTGATTTG	Rev P _{mfa1min}
oNH095	TCACCATAGCAGGCCTAGATGGCCCTGCAGGGATATCGAAATAGCG CTGTACAGC	Fw PIR ₃
oNH096	ACGGTTCACTAAACGAGCTCTGCTTATATAGGTTAATTAACCTGCAGC GTACGGTGTACGGGAAG	Rev PIR ₃
oNH097	CGGGATCTGAGGAAAGGCCTTGCTAATACTAGTTAATTAACCTGCAGC GTACGGTGTACGGGAAG	Rev PIR ₃
oNH098	GATATCGAAATAGCGCTGTACAGC	Fw PIR ₃
oNH104	ATGAAGCTGCTCTCGTC	Fw GAL4 _{BD}
oNH105	CGAGACGGTGAGCTG	Rev GAL4 _{BD}

oNH106	ATGTCGCGCGGC	Fw PIP
oNH107	CGCCTGCTCGACC	Rev PIP
oNH109	TTACTTGTCGTCGTCGTC	Rev p65
oNH110	CCAACAAGGGTCAGCGTCAGCTCACCGTCTCGGCCGGTTCGGGTGC CTCGTTAATTAACCAGTACCTGCCCGAC	Fw p65
oNH111	TCGCCGGTATCGACGCCATGGTCGAGCAGGCCGGCCGGTTCGGGTGC CTCGTTAATTAACCAGTACCTGCCCGAC	Fw p65
oNH113	TTACAGCATATCCAGGTCGAAG	Rev VP16ff
oNH114	CCAACAAGGGTCAGCGTCAGCTCACCGTCTCGGCCGGTTCGGGTGC CTCGTTAATTAACCTCCCCGCCGATG	Fw VP16ff
oNH115	TCGCCGGTATCGACGCCATGGTCGAGCAGGCCGGCCGGTTCGGGTGC CTCGTTAATTAACCTCCCCGCCGATG	Fw VP16ff
oNH116	GCCGGGCGGCCGGCGCGCCGGCCGCTAGATCTTTAGGCGTAGTCGG GCACGTCGTAAGGGTAGAGCGGACCCTGCTGCTCGTTCTTGAGCAC	Rev RLuc
oNH117	GCCGGGCGGCCGGCGCGCCGGCCGCTAGATCTTTAGGCGTAGTCGG GCACGTCGTAAGGGTAGAGCGGACCCTGGTCACCACCGGCAC	Rev GLuc
oNH119	GCCGGGCGGCCGGCGCGCCGGCCGCTAGATCTTTAGGCGTAGTCGG GCACGTCGTAAGGGTAGAGCGGACCCTGGACGGCGATCTTGCC	Rev FLuc
oNH120	TGTTTGAACGATCGCCGGGCGGCCGGCGCGCCTTAGACCTTTCTCTT CTTTTTTGAGGCGCTTTCTTGTCGTCGTCGTC	Rev p65
oNH121	TGTTTGAACGATCGCCGGGCGGCCGGCGCGCCTTAGACCTTTCTCTT CTTTTTTGAGGCGCTTTCAGCATATCCAGGTCGAAG	Rev VP16ff
oNH122	CATATGGCGGTGACCG	Rev mKate2
oNH123	ATGTTTGAACGATCGCCGGGCGGCCGGCGCGCCGGCCGCTTTAGAC CTTTCTCTTCTTTTTTGAGGCGCTTTCTTGACAGCTCGTCCATG	Rev eGFP
oNH124	ATCTGCCCTCGAAACTCGGTCACCGCCATATGATGACCAAGAAGTTTG GCACGCTCACCATCTAGGCCGGTTCGGGTGCCTCGTTAAAACAGCTC TGGGGTTG	Fw pIRES
oNH125	CCGGTGAACAGCTCCTCGCCCTTGCTCACCATACAATTCGCTTTATGA TAACAATCTGTGATTG	Rev pIRES
oNH126	ATCTGCCCTCGAAACTCGGTCACCGCCATATGATGACCAAGAAGTTTG GCACGCTCACCATCTAGGCCGGTTCGGGTGCCTCGGAGGGCCCGGA AAC	Fw eIRES
oNH127	CCGGTGAACAGCTCCTCGCCCTTGCTCACCATGATTATCATCGTGT TCAAAGGAAAAC	Rev eIRES
oNH128	ATCTGCCCTCGAAACTCGGTCACCGCCATATGATGACCAAGAAGTTTG GCACGCTCACCATCTAGGCCGGTTCGGGTGCCTCGAGCAGGTTTCCC CAATG	Fw fIRES
oNH129	CCGGTGAACAGCTCCTCGCCCTTGCTCACCATGGAAAGGAAAGGTGC CGAC	Rev fIRES
oNH130	CCACCCAGCTCATCTCGAACATGGACATCGACGTCATCCTCGGTGGT G	Fw SEAP
oNH131	CGCCGGGCGGCCGGCGCGCCGGCCGCTAGATCTCTATCCAGGGTGG GCG	Rev SEAP
oNH132	GCCGGGCGGCCGGCGCGCCGGCCGCTAGATCTTTAGGCGTAGTCGG GCACGTCGTAAGGGTAGAGCGGACCCTGCTATCCAGGGTGGGCG	Rev SEAP
oNH135	AGGCTGGATCGGTCCCCTGCTTCTATGGAGGTCAAACAGCGTGG ATGGCGTCTCCAGGCGATCTGACGGTTCACTAAACG	Rev P _{hCMVmin}
oNH136	CTCCATAGAAGACACCGGGACCGATCCAGCCTGGCGGCCATGGTGA GCAAGGGCG	Fw GFP
oNH137	TATTAATAGTAATCAATTACGGGGTCATTAGTTC	Fw P _{CMV}
oNH139	CACGCTGTTTTGACCTCCATAGAAGACACCGGGACCGATCCAGCCTC AATTGATGGTGTGCGAGCTCATC	Fw mKate2
oNH140	AATGGGCGGTAGGCGGTACGGTGGGAGGTCTATATAAGCAGAGCTC GTTTAGTGAACCGTCAGATCGCCTGGAGACGCCATCCACGCTGTTTTG ACCTCC	Fw P _{hCMV}

oNH141	CCAAATGTTTGAACGATCGCCGGGCGGCCAATTGCTAGATGGTGAG CGTGCCAAACTTCTTGGTCATCATATGGCGGTGACCG	Rev mKate2
oNH142	GGCCGCCCGG	
oNH143	TCACCATAGCAGGCCTAGATGGCCCTGCAGGCTCATGTTTGACAGC TTATCATCG	Fw nosT
oNH144	CTCATGTTTGACAGCTTATCATCG	Rev nosT
oNH145	GTCTGGATCGAAGCTTGGGCTGCAGGTCGACTTCTAGATCACACCTTC CGCTTTTTCTTGGGCTTGTACAGCTCGTCCATG	Rev eGFP
oNH146	AGCCTTGTACAGCTCGTC	Rev mCherry
oNH147	AAACTCATCAATGTATCTTATCATGTCTGACCGGTTTAGATGGTCAGG GTGCCGAAGCTTCTTGGTCATAGCCTTGTACAGCTCGTC	Rev mCherry
oNH148	CAGACATGATAAGATAATTGATGAGTTTG	Fw SV40pA
oNH149	CAATTCTCATGTTTGACAGCTTATCATCGATAAGAATTCCTAAAAACC TCCACACCTC	Rev SV40pA
oNH150	CACGCTGTTTTGACCTCCATAGAAGACACCGGGACCGATCCAGCCTA CCGGTCCACCATGGTGAGCAAGGGCGAGGAG	Fw mCherry
oNH151	CACGCTGTTTTGACCTCCATAGAAGACACCGGGACCGATCCAGCCTG GATCCCCACCATGGTGAGCAAGGGC	Fw eGFP
oNH152	TTGAACATCAAATCAACTACCTTACTCTATCACAATTGATGGTGAGCAA GGGCG	Fw eGFP
oNH153	TTGAACATCAAATCAACTACCTTACTCTATCACAATTGATGGTGCGGA GCTCATC	Fw mKate2
oNH157	AGTGTGGCACTCGAATCCCCCTGCTCGAGAAGAATCCGACAGCCAAA CCTC	Fw P _{mfa1min}
oNH158	GCCCGGCGATCGTTC	Fw nosT
oNH166	CGGGATCCCCGGGCTGCAGGAATTCGATCCCCAATTGCATATGAAG CTGCTCTCGTC	Fw GAL4 _{BD}
oNH167	CGGGATCCCCGGGCTGCAGGAATTCGATCCCCAATTGCATATGTCC CGCGGC	Fw PIP
oNH169	ACTAGTCAATAATCAATGTCAACATGGCGGTCCAATGGGCGGTAGGC G	Fw P _{hCMVmin}
oNH174	TTGCCAAATGTTTGAACGATCGCCGGGCGGCCGGCGCGCCGGCCGC TTTAGACGGCGATCTTGC	Rev FLuc
oNH175	ACAATCACAGATTGTTATCATAAAGCGAATTGGCGATCGCATGGAGGA CGCCAAGAA	Fw FLuc
oNH177	ACGTGGTTTTCTTTGAAAAACACGATGATAAGCGATCGCATGGAGGA CGCCAAGAA	Fw FLuc
oNH178	TCAAGAAGACAGGGCCAGGTTTCCGGGCCCTCGCGATCGCTTACTGC TCGTTCTTGAGC	Rev RLuc
oNH179	AATAGGTGACCGGAGGTGCGCACCTTTCTTTGCGATCGCATGGAGG ACGCCAAGAA	Fw FLuc
oNH180	TTGCACGTTTTGTGTCATTGGGAAACCTGCTGCGATCGCTTACTGCT CGTTCTTGAGC	Rev RLuc
oNH181	CTGGGGTGGGTACAACCCAGAGCTGTTTTAAGCGATCGCTTACTGC TCGTTCTTGAGC	Rev RLuc
oNH182	CTCCATAGAAGACACCGGGACCGATCCAGCCTCAATTGATGGGCGTC AAGGTG	Fw GLuc
oNH183	TTTGAACGATCGCCGGGCGGCCGGCGCGCCGGCCGCTTTAGTCACC ACCGGCA	Rev GLuc
oNH184	CTCCATAGAAGACACCGGGACCGATCCAGCCTCAATTGATGGAGGAC GCCAAGAA	Fw FLuc
oNH185	GAACATCAAATCAACTACCTTACTTCTATCACCAATTGATGGGCGTCAA GGTG	Fw GLuc
oNH186	GAACATCAAATCAACTACCTTACTTCTATCACCAATTGATGGAGGACG CCAAGAA	Fw FLuc
oNH196	CACGCTGTTTTGACCTCCATAGAAGACACCGGGACCGATCCAGCCTC AATTGATGACCAGCAAGGTCTAC	Fw RLuc

oNH197	TTGCCAAATGTTTGAACGATCGCCGGGCGGCCCAATTGTTACTGCTCG TTCTTGAGC	Rev RLuc
oNH198	CTCCATAGAAGACACCGGGACCGATCCAGCCTGGCGCGCCATGGAG GACGCCAAGAA	Fw FLuc
oNH200	ATGCCTGTTATGGAAGAGTAGC	Fw SPA1
oNH201	TGTCTTTTATTTTCAGGTCCCGGATCGAATTGCGGCCGCATGCCTGTTA TGGAAGAGTAGC	Fw SPA1
oNH202	TCAAACAAGTTTTAGTAGCTTCATGTTTC	Rev SPA1
oNH203	GTCTGGATCGAAGCTTGGGCTGCAGGTGCGACTCTAGATCAAACAAGTT TTAGTAGCTTCATGTTTC	Rev SPA1
oNH205	ATGGTGAGCAAGGGCG	Fw mCerulean, mVenus, mCherry, eGFP
oNH207	ATGGAAGAGATTTTCGACGGATC	Fw COP1
oNH209	CGCAGCGAGTACCAGA	Rev COP1
oNH222	TCTAGAGTCGACCTGCAG	Rev P _{SV40}
oNH223	GCGGCCGCAATTC	Fw SV40pA
oNH248	TTATTTTCAGGTCCCGGATCGAATTGCGGCCGCCACCACCATGGAAGAGA TTTCGACGGATC	Fw COP1
oNH249	ATCGAAGCTTGGGCTGCAGGTGCGACTCTAGATCACGCAGCGAGTACC AGA	Rev COP1
oNH250	TGTCTTTTATTTTCAGGTCCCGGATCGAATTGCGGCCGCCACCACCATGGT GAGCAAGGGCG	Fw mVenus/ mCerulean
oNH251	GGAACAACCGGATCCGTGCAATCTCTTCCATGCTGCCCTTGTACAGC TCGTCCATG	Rev mVenus/ mCerulean
oNH254	GTTTCTTCAGCTACTCTTCCATAACAGGCATGCTGCCCTTGTACAGCT CGTCCATG	Rev mVenus/ mCerulean
oNH255	GGATCGAAGCTTGGGCTGCAGGTGCGACTCTAGATCACACCTTCCGCT TTTTCTTGGGAACAAGTTTTAGTAGCTTCATGTTTCC	Rev SPA
oNH259	AACAAGTTTTAGTAGCTTCATGTTTCC	Rev SPA1
oNH261	GAGGCGGTGGAAGTGGTGGCGGAGGTAGCGATTGTACAATGGAAGA GATTTTCGACGGATC	Fw COP1
oNH262	TGTATCTTATCATGTCTGGATCGAAGCTTTTAGGCGCGCCTTAAGCGT AATCTGGAACATCGTATGGGTACGCAGCGAGTACCAGA	Rev COP1
oNH263	GAGGCGGTGGAAGTGGTGGCGGAGGTAGCGATTGTACAATGCCTGTTA GGAAAGAGTAGC	Fw SPA1
oNH264	TGTATCTTATCATGTCTGGATCGAAGCTTTTAGGCGCGCCTTAAGCGT AATCTGGAACATCGTATGGGTAAACAAGTTTTAGTAGCTTCATGTTTC	Rev SPA1
oNH267	TCACAGATTGTTATCATAAAGCGAATTGGATTGCGGCCGCGAATTCAT ATGTC	Fw TetR
oNH268	ATCGCTACCTCCGCC	Rev TetR
oNH269	GGCCGCGAATTCATATGTC	Fw TetR
oNH401	CACGTCGCCGCGCCAGTTTTGAGGAGATCGAAGTTGAGCAGCTGTTTCA CGGGGAATTCAGCCTTGTACAGCTCGTC	Rev mCherry
oNH403	TCATTTGGAGAGAACACGGGGACTCTAGCGCTACCGGTGCCACCAT GGTGAGCAAGGGCG	Fw mCherry/eGFP
oNH405	TTCGATCTCCTCAAACCTGGCCGGCGACGTGGAATCAAATCCTGGACC CGCGCGCATGGAAGCTAACGGGATTGAG	Fw PYL8
oNH413	AGCCTTGTACAGCTCGTC	Rev mCherry
oNH416	GGGCCTTTCTTTATGTTTTGGCGTCTTCCATGCTAGCGACTCTCGATT CTGTCTGTG	Rev PYL8
oNH418	AGGAGATCGAAGTTGAGCAGCTGTTTCACGGGGAATTCCTTGTACAG CTCGTCCATG	Rev eGFP
oNH419	ACGATCGGGAAATTCGCCTCGAGATCAGTTATCTAGATTAAGCCTTG TACAGCTCGTC	Rev mCherry
oNH420	GGATCACTCTCGGCATGGACGAGCTGTACAAGGAATCCCCGTGAAA CAGCTGCTCAAACCTCGATCTCCTCAAACCTGGC	Fw 2A
oNH421	GCCCGGGGAATTCGGCCGCTGCCGCAGCGGCAGCGGCCGCGAGCTC CGGAGCCTTGTACAGCTCGTC	Rev mCherry

oNH422	TTCGATCTCCTCAAACCTGGCCGGCGACGTGGAATCAAATCCTGGACC CGCGCGCGGTGCAGGCGCTGGAGCCGGTGCCGGGGCAGGCGCTGG CGCTAGCATGGTGAGCAAGGGCC	Fw mCherry/eGFP
oNH423	GACTCTCGATTCTGTCTGTG	Rev PYL8
oNH424	CCCTCGAGGCGCGCCAAGCTATCACCACTTTGTACAAGAAAGCTGGG TCGAATTCGCCCTTGACTCTCGATTCTGTCTGTG	Rev PYL8
oNH426	CCCAGCTTTCTTGTACAAAGTGGTGATAGCTTGGCGCGCCTCGAGGG GGGGCCCGGTACCGGTAGAAAAAATGGTGAGCAAGGGC	Fw eGFP
oNH427	TCATTTGGAGAGAACACGGGGACTCTAGCGCTACCGGTATGGCATA CCATACGACG	Fw RFA4
oNH428	GATCCGGTGGATCCAAGCTTCTCGAGCCCGGGGAATTCTCAGTTGCT CTCATCTTTCTG	Rev RFA4
oNH429	GATCCGGTGGATCCAAGCTTCTCGAGCCCGGGGAATTCTCAGCATCC TCGTTGGTTC	Rev RFAdeltaC
oNH430	CGTTTCGTTGAGCGAGTTCTCAAAAATGAACAAGAATCCCCGTGAAAC AGCTGCTCAACTTCGATCTCCTCAAACCTGGC	Fw 2A
oNH434	TCCAGGATTTGATTCCACGTCGCCGGCCAGTTTGAGGAGATCGAAGTT GAGCAGCTGTTTCACGGGGGAATTCAGCCTTGACAGCTCGTC	Rev mCherry
oNH435	AACTGGCCGGCGACGTGGAATCAAATCCTGGACCCGCGCGCCAGGT GGTGGCTGGCCGCCGGTGCAGCTATCGAAAAATGGTGAGCAAG GGCG	Fw eGFP/mCherry
oNH437	CCAGGATTTGATTCCACGTCGCCGGCCAGTTTGAGGAGATCGAAGTT GAGCAGCTGTTTCACGGGGGAATTCCTTGACAGCTCGTCCATG	Rev eGFP
oNH443	ACGATCGGGGAAATTCGCCTCGAGATCAGTTATCTAGATTAGGCCGCT GCCGCAGCGGCAGCGGCCCGCCTTGACAGCTCGTCCATG	Rev eGFP
oNH448	TCCACCGGCGGCATGGACGAGCTGTACAAGGCTGAATCCCCGTGAA ACAGCTGCTCAACTTCGATCTCCTCAAACCTGGC	Fw 2A
oNH601	CTAAAAAACCTCCCACACCTC	Rev SV40pA
oNH612	TTAAAAACAGCTCTGGGGTTG	Fw pIRES
oNH613	CAATTCGCTTTATGATAACAATCTGTGATTG	Rev pIRES
oNH614	GAGGGCCCGGAAAC	Fw eIRES
oNH615	TTATCATCGTGTGTTTTCAAAGGAAAAC	Rev eIRES
oNH616	AGCAGGTTTCCCCAATG	Fw fIRES
oNH617	AAAGGAAAGGTGCCGAC	Rev fIRES
oNH621	CACGCGTCTACCATAGCAGGCCTAGATGGCCCCTGCAGGCTTCTCG AGCAGGGGG	Fw P _{OMA}
oNH622	TGCATGTTCTCCTTGATGAGCTCCGACACCATCAATTGTGATAGAGTA AGGTAGTTGATTTGATGTTG	Rev P _{OMA}
oNH623	CGGGATCCCCCGG	Fw IRES-fusion
oNH624	TGCCAAATGTTTGAACGATCG	Rev IRES-fusion
oNH625	CGGGATCCCCCGGGCTGCAGGAATTCGATCCCCAATTGGACCGCCAT GTTGACATTGATTATTGACTAGTTATTAATAGTAATCAATTACGGGGTC ATTAGTTC	Fw P _{CMV}
oNH626	CGGGATCCCCCGGGCTGCAGGAATTCGATCCCCAATTGCTTCTCGAG CAGGGGG	Fw P _{OMA}
oNH627	TCACTTCTCGCCCGTTCTTTTTGAACATCAAATCAACTACCTTACTCTAT CACAATTGATGACCAGCAAGGTCTAC	Fw RLuc
oNH628	AATCCGACAGCCAAACCTCATCCACTCTCACTTTCACACTCTAACTTAT ACGATCACTTCTCGCCCGTTC	Fw P _{mfa1min}
oNH631	CTTCTGTGGAATGTGTGTGTCAGTTA	Fw P _{SV40}
oNH632	CCCTAACTGACACACATTCCACAGAAGAATTCTTATCGATGATAAGCT GTCAAACATGAG	Rev pMZ333
oNH645	TTGCCAAATGTTTGAACGATCGCCGGGCGGCCGGCGCGCCGGCCCG TTTACTGCTCGTTCTTGAGC	Rev RLuc
oNH646	CTCCATAGAAGACACCGGGACCGATCCAGCCTGGCGCGCCATGACCA GCAAGGTCTAC	Fw RLuc
oNH647	TTGCCAAATGTTTGAACGATCGCCGGGCGGCCCAATTGTTAGACGGC GATCTTGC	Rev FLuc
oNH652	CTTTTATTTTCAGGTCCCGGATCGGAATTGCGCGGCCGCGACCGCCAT	Fw CMVenhancer,

	GTTGACATTGATTATTGACTAGTTATTAATAGTAATCAATTACGGGGTC ATTAGTTC	
oNH653	ACTAGTCAATAATCAATGTCAACATGGCGGTCCAAATGGGCGGTAGGC	Fw P _{mfa1min}
oNH654	GTCTGGATCGAAGCTTGGGCTGCAGGTCGACTTCTAGATTAGATGGT CAGGGTGCCGAACCTTCTGGTCATAGCCTTGTACAGCTCGTC	Rev mCherry
oNH655	CTCCATAGAAGACACCGGGACCGATCCAGCCTACCGGTCCACCATGG TGAGCAAGGGCG	Fw eGFP
oNH656	TCCAAACTCATCAATGTATCTTATCATGTCTGACCGTTACACCTTCC GCTTTTTCTTG	Rev eGFP
oNH657	CTCCATAGAAGACACCGGGACCGATCCAGCCTGGCGGCCATGGTGT CGGAGCTCATC	Fw mKate2
oNH658	TGTTTGAACGATCGCCGGGCGGCCGGCGCCCTAGATGGTGAGCG TGCCAAACTTCTTGGTCATCATATGGCGGTGACCG	Rev mKate2
oNH659	CTCCATAGAAGACACCGGGACCGATCCAGCCTCAATTGATGGTGAGC AAGGGC	Fw eGFP
oNH660	TTGCCAAATGTTTGAACGATCGCCGGGCGGCCCAATTGGGCGGCTTT AGACCTTTCTCTTCTTTTTTGGAGGCGCTTTCTTGTACAGCTCGTCCAT G	Rev eGFP
oNH669	CTCGATAGGCATTTGCCCGGGCCTAGATGGCCCCTG	Fw upp3 UFcterm
oNH670	TCGCCGGTATCGACGCCATGGTCGAGCAGGCGGCCGGTTCGGGTGC CTCGGCTCCTCCGCGC	Fw UVR8
oNH671	TCAGCCGTGACCGAGA	Rev UVR8
oNH672	CTCCATAGAAGACACCGGGACCGATCCAGCCTCAATTGATGTGCGCG GGC	Fw PIP
oNH673	TTGCCAAATGTTTGAACGATCGCCGGGCGGCCCAATTGTCAGCCGTC GACCGAGA	Rev UVR8
oNH674	ATGTAICTCGAACGGTCTCG	Fw COP1(WD40)
oNH675	GGCGGCGAGGAC	Rev COP1(WD40)
oNH676	AGGGCACCATCAAGGTGCTCGTCTCGCCGCCGGTTCGGGTGC CTCGTCCCCCGCCGATG	Fw VP16ff
oNH677	CTCCATAGAAGACACCGGGACCGATCCAGCCTGGCGGCCATGTACT CGAACGGTCTCG	Fw COP1(WD40)
oNH679	TCGCCGGTATCGACGCCATGGTCGAGCAGGCGGCCGGTTCGGGTGC CTCGCTCGCCGCCGCT	Fw AsLOV2pep
oNH680	TCAGACCCAGGTGTCGAC	Rev AsLOV2pep
oNH681	TTGCCAAATGTTTGAACGATCGCCGGGCGGCCCAATTGTCAGACCCA GGTGTGAC	Rev AsLOV2pep
oNH682	ATGCCCCGAGCTCGG	Fw ePDZb
oNH683	GGTGCGGTAGTTGATCGAG	Rev ePDZb
oNH684	ACTCGTCCCATCTCGATCAACTACCGCACCGCCGGTTCGGGTGCC TCGTCCCCCGCCGATG	Fw VP16ff
oNH685	CTCCATAGAAGACACCGGGACCGATCCAGCCTGGCGGCCATGCC GAGCTCGG	Fw ePDZb
oNH695	AAGATCAAGGGTGCCGGTGGTGACTAATTAATTAATAACTTCTCGCCCC TTCTTTTGAACATCAAATCAACTACTTACTCTATCAGGCGGCCATGG AGGACGCCAAGAA	Fw FLuc
oNH696	TGATTTGATGTTCAAAGAACGGGCGAGAAGTGATCGTATAAGTTAGA GTGTGAAAGTGAGAGTGGATGAGGTTTGGCTGTCGGATTCTCCCTTAT ATCCTTGACGGTAC	Rev P _{OMA}
oNH698	GCCTAGATGGCCCCTGCAGGCTCATGTTTGACAGCTTATCATCG	Fw nosT
oNH715	AGGCCAAGAAGGGTGGCAAGATCGCCGTCTAAGCGATCGCGGCCGC CCGG	Fw nosT
oNH716	CGAGCTCGGTACGGGGGATCCACTAGTTCTAGCTCATGTTTGACAGC TTATCATCG	Rev nosT
oNH717	GAGGCCAAAAAAGATACCATAATAGGCCTGAGTTAATTAATGGAGGA CGCCAAGAA	Fw FLuc
oNH718	CATAGTACATCAGGCTACTAAGTGTG	Fw P _{CRG}
oNH719	CTCAGGCCTATTATGGTATCTTTTTTTG	Rev P _{CRG}
oNH720	CACGCGTCTCACCATAGCAGGCCTAGATGGCCCCTGCAGGCATAGTA	Fw P _{CRG}

	CATCAGGCTACTAACTGTC	
oNH721	TTGAACATCAAATCAACTACCTTACTCTATCAGGCGGCCATGGTGAG CAAGGGCG	Fw eGFP
oNH722	TTGAACATCAAATCAACTACCTTACTCTATCAGGCGGCCATGGTGTC GGAGCTCATC	Fw mKate2
oNH731	CTTCGACGATGCTGTTTCGTCGC	Fw cco1 genotyping
oNH733	CACGAGGTGATGCAGCGTCATTG	Fw upp3 genotyping
oNH735	TCTCACCATAGCAGGCCTAGATGGCCCCTGCAGGCCTATATAAGCAG AGCTCGTTTAGTG	Fw P _{hCMVmin}
oNH736	CTTCTTGATGTTCTTGGCGTCCTCCATCAATTGAGGCTGGATCGGTCC	Rev P _{hCMVmin}
oLH014	ATGGAGGACGCCAAGAA	Fw FLuc
oLH015	ATGACCAGCAAGGTCTAC	Fw RLuc
oLH017	ATGGTGCTCGGTCTT	Fw SEAP
oLH018	TTAGACGGCGATCTTGC	Rev FLuc
oLH019	TACTGCTCGTTCTTGAGC	Rev RLuc
oLH021	TTAGTCGATGTCCATGTTCCG	Rev SEAP
oLHNH001	TGCCGGGGCAGGCGCTGGCGCTAGCAAGCTCTCTCATGGATTCCCG CCAGCTGTAGCCGCTCAGGACGATGGA	Fw PESTpart1
oLHNH002	TAGCCGCTCAGGACGATGGAACCTACCCATGAGCTGCGCGCAAGAA TCTGGCATGGATCGACATCCTGCAGC	Fw PESTpart2
oLHNH003	ATGGATCGACATCCTGCAGCCTGCGCTTCCGCAAGGATTAACGTGGG CGCGCCATGGAAGACGCCAAAAACAT	Fw PESTpart3
oLHNH008	TCCATCGTCCTGAGCGGCTACAGCTGGCGGGAATCCATGAGAGAGCT TGCTAGCGCCAGCGCCTGCCCCGGCA	Rev PESTpart1
oLHNH009	GCTGCAGGATGTCGATCCATGCCAGATTCTTGCGCGCAGCTCATGGG TAGGGTTCCATCGTCCTGAGCGGCTA	Rev PESTpart2
oLHNH010	ATGTTTTTGGCGTCTTCCATGGCGCGCCACGTTAATCCTTGCGGAAG CGCAGGCTGCAGGATGTCGATCCAT	Rev PESTpart3
oTB064	TCTTTTATTTCAAGTCCCGGATCGAATTGCGCGGCCGCCACCATGAA GAGAGATCAT	Fw GAI
oTB065	ATCCTCCTCGCCCTTGCTCACCATTGCTGAATTGGTGGAGAGTTTCCA A	Rev GAI
oTB066	GCCACCTCGGCTTGAAACTCTCCACCAATTCAGCAATGGTGAGCAA GGG	Fw mCherry
oTB067	CTGGATCGAAGCTTGGGCTGCAGGTCGACTTCTAGACTACTTGTACAG CTCGTCCATGC	Rev mCherry
oTB068	GTCTTTTATTTCAAGTCCCGGATCGAATTGGCGGCCGCCACCATGAA GAGAGATCATCACCA	Fw RGA
oTB069	ATCCTCCTCGCCCTTGCTCACCATTGCTGAGTACGCCGCCGTCGA	Rev RGA
oTB070	TCCGCTTGAAACTCTCGACGGCGGCGTACTCAGCAATGGTGAGCAA GGG	Fw mCherry

5.6 *Ustilago maydis* strains

Table 4: *Ustilago maydis* strains used in this work.

Strain	Description	Origin
sNH001	AB33_upp3D::P _{O2ef} ::RLuc-pIRES-FLuc-nosT-NatR	this work
sNH003	AB33_upp3D::P _{O2ef} ::RLuc-eIRES-FLuc-nosT-NatR	this work
sNH004	AB33_upp3D::P _{O2ef} ::RLuc-fIRES-FLuc-nosT-NatR	this work
sNH005	AB33_upp3D::nosT-NES-mKate2::P _{hCMVmin} -CMVenhancer(5'→3')-P _{hCMVmin} ::eGFP-NLS-nosT-NatR	this work
sNH006	AB33_upp3D::nosT-NES-mKate2::P _{hCMVmin} -CMVenhancer(5'←3')-P _{hCMVmin} ::eGFP-NLS-nosT-NatR	this work
sNH007	AB33_upp3D::nosT-NES-mKate2::P _{mfa1min} -(prf1) ₄ (5'→3')-P _{mfa1min} ::GFP-NLS-nosT-NatR	this work
sNH008	AB33_upp3D::nosT-NES-mKate2::P _{mfa1min} -(prf1) ₄ (5'←3')-P _{mfa1min} ::GFP-NLS-nosT-NatR	this work
sNH011	AB33_upp3D::nosT-RLuc::P _{hCMVmin} -CMVenhancer(5'→3')-P _{hCMVmin} ::FLuc-nosT-NatR	this work
sNH012	AB33_upp3D::nosT-RLuc::P _{hCMVmin} -CMVenhancer(5'←3')-P _{hCMVmin} ::FLuc-nosT-NatR	this work
sNH013	AB33_upp3D::nosT-RLuc::P _{mfa1min} -(prf1) ₄ (5'→3')-P _{mfa1min} ::FLuc-nosT-NatR	this work
sNH025	AB33_upp3D::Gal4UAS ₅ -P _{hCMVmin} ::GLuc-nosT-NatR	this work
sNH026	AB33_upp3D::Gal4UAS ₅ -P _{hCMVmin} ::FLuc-nosT-NatR	this work
sNH027	AB33_upp3D::Gal4UAS ₅ -P _{hCMVmin} ::GLuc-nosT-NatR	this work
sNH028	AB33_upp3D::Gal4UAS ₅ -P _{hCMVmin} ::FLuc-nosT-NatR	this work
sNH029	AB33_upp3D::PIR ₃ -P _{hCMVmin} ::GLuc-nosT-NatR	this work
sNH030	AB33_upp3D::PIR ₃ -P _{hCMVmin} ::FLuc-nosT-NatR	this work
sNH031	AB33_upp3D::PIR ₃ -P _{mfa1min} ::GLuc-nosT-NatR	this work
sNH032	AB33_upp3D::PIR ₃ -P _{mfa1min} ::FLuc-nosT-NatR	this work
sNH034	AB33_upp3D::PIR ₃ -P _{hCMVmin} ::FLuc-nosT-NatR _{cco1D} ::nosT-UVR8(12-381)-PIP::dP _{CMV-A} ::COP1(WD40)-VP16ff-NLS-nosT-HygR	this work
sNH039	AB33_upp3D::P _{CRG} ::FLuc-nosT-P _{O2ef} ::GLuc-nosT-NatR	this work
sNH041	AB33_upp3D::P _{hCMVmin} ::FLuc-nosT-NatR	this work
sNH054	AB33_cco1D::P _{O2ef} ::PIP-VP16ff-NLS-nosT-HygR	this work
sNH055	AB33_cco1D::P _{O2ef} ::PIP-VP16ff-NLS-nosT-HygR _{upp3D} ::PIR ₃ -P _{hCMVmin} ::GLuc-nosT-NatR	this work
sNH056	AB33_cco1D::P _{O2ef} ::PIP-VP16ff-NLS-nosT-HygR _{upp3D} ::PIR ₃ -P _{hCMVmin} ::FLuc-nosT-NatR	this work

sNH057	AB33_cco1D::P _{O2tef} ::PIP-VP16ff-NLS-nosT-HygR_upp3D::PIR ₃ -P _{mfa1min} ::GLuc-nosT-NatR	this work
sNH058	AB33_cco1D::P _{O2tef} ::PIP-VP16ff-NLS-nosT-HygR_upp3D::PIR ₃ -P _{mfa1min} ::FLuc-nosT-NatR	this work
sLHNH004	AB33_upp3D::P _{O2tef} ::SEAP-nosT-NatR	this work
sLHNH005	AB33_upp3D::P _{O2tef} ::RLuc-HA-nosT-NatR	this work
sLHNH006	AB33_upp3D::P _{O2tef} ::GLuc-HA-nosT-NatR	this work
sLHNH007	AB33_upp3D::P _{O2tef} ::SEAP-HA-nosT-NatR	this work
sLHNH008	AB33_upp3D::P _{O2tef} ::FLuc-HA-nosT-NatR	this work
sLHNH009	AB33_upp3D::P _{O2tef} ::mKate2-NES-pIRES-eGFP-NLS-nosT-NatR	this work
sLHNH010	AB33_upp3D::P _{O2tef} ::mKate2-NES-eIRES-eGFP-NLS-nosT-NatR	this work
sLHNH011	AB33_upp3D::P _{O2tef} ::mKate2-NES-fIRES-eGFP-NLS-nosT-NatR	this work
AB33	<i>Pnar bW1, pnar bE1/2</i>	A. Brachmann
UMa486	Strain expressing eGFP under control of the constitutive P _{O2tef}	
UMa890	Strain expressing an HA-tag under control of the constitutive P _{O2tef}	
UMa1986	Strain expressing mKate under control of the constitutive P _{O2tef}	
UMa2686	Strain expressing an HA-tag under control of the constitutive P _{O2tef}	
UMa3212	Strain expressing FLuc under the control of the inducible P _{CRG1}	

Plasmids with pLHNH Number were planned and generated together with L. Hüseemann.

The strains sLHNH005-sLHNH011 were produced together with L. Hüseemann.

The strains AB33, UMa486, UMa890, UMa1986, UMa2686 and UMa3212 were kindly provided by K. Müntjes from the institute for microbiology of the HHU Düsseldorf.

6. References

- Alabadí D, Gallego-Bartolomé J, Orlando L, García-Cárcel L, Rubio V, Martínez C, Frigerio M, Iglesias-Pedraz JM, Espinosa A, Deng XW, et al (2007)** Gibberellins modulate light signaling pathways to prevent Arabidopsis seedling de-etiolation in darkness. *Plant J* **53**: 324–335
- Andersen CR, Nielsen LS, Baer A, Tolstrup AB, Weilguny D (2011)** Efficient expression from one CMV enhancer controlling two core promoters. *Mol Biotechnol* **48**: 128–137
- Arana M V., Marin-de la Rosa N, Maloof JN, Blazquez MA, Alabadi D (2011)** Circadian oscillation of gibberellin signaling in Arabidopsis. *Proc Natl Acad Sci* **108**: 9292–9297
- Banks GR, Shelton PA, Kanuga N, Holden DW, Spanos A (1993)** The *Ustilago maydis* nar 1 gene encoding nitrate reductase activity: sequence and transcriptional regulation. *Gene* **131**: 69–78
- Baron U, Freundlieb S, Gossen M, Bujard H (1995)** Co-regulation of two gene activities by tetracycline via a bidirectional promoter. *Nucleic Acids Res* **23**: 3605–3606
- Becker J, Hosseinpour Tehrani H, Gauert M, Mampel J, Blank LM, Wierckx N (2020)** An *Ustilago maydis* chassis for itaconic acid production without by-products. *Microb Biotechnol* **13**: 350–362
- Belda-Palazon B, Gonzalez-Garcia MP, Lozano-Juste J, Coego A, Antoni R, Julian J, Peirats-Llobet M, Rodriguez L, Berbel A, Dietrich D, et al (2018)** PYL8 mediates ABA perception in the root through non-cell-autonomous and ligand-stabilization–based mechanisms. *Proc Natl Acad Sci U S A* **115**: E11857–E11863
- Belsham GJ, Brangwyn JK (1990)** A region of the 5' noncoding region of foot-and-mouth disease virus RNA directs efficient internal initiation of protein synthesis within cells: involvement with the role of L protease in translational control. *J Virol* **64**: 5389–5395
- Berger J, Hauber J, Hauber R, Geiger R, Cullen BR (1988)** Secreted placental alkaline phosphatase: a powerful new quantitative indicator of gene expression

- in eukaryotic cells. *Gene* **66**: 1–10
- Berger J, Howard AD, Gerber L, Cullen BR, Udenfriend S** (1987) Expression of active, membrane-bound human placental alkaline phosphatase by transfected simian cells. *Proc Natl Acad Sci U S A* **84**: 4885–4889
- Bernier G, Périlleux C** (2005) A physiological overview of the genetics of flowering time control. *Plant Biotechnol J* **3**: 3–16
- Beyer HM, Gonschorek P, Samodelov SL, Meier M, Weber W, Zurbriggen MD** (2015) AQUA cloning: A versatile and simple enzyme-free cloning approach. *PLoS One* **10**: 1–20
- Blanco-Touriñán N, Legris M, Minguet EG, Costigliolo-Rojas C, Nohales MA, Iniesto E, García-León M, Pacín M, Heucken N, Blomeier T, et al** (2020) COP1 destabilizes DELLA proteins in Arabidopsis. *Proc Natl Acad Sci U S A*. doi: 10.1101/2020.01.09.897157
- Bösch K, Frantzeskakis L, Vraneš M, Kämper J, Schipper K, Göhre V** (2016) Genetic manipulation of the plant pathogen *Ustilago maydis* to study fungal biology and plant microbe interactions. *J Vis Exp* **2016**: 1–9
- Bottin A, Kämper J, Kahmann R** (1996) Isolation of a carbon source-regulated gene from *Ustilago maydis*. *Mol Gen Genet MGG* **253**: 342–352
- Brachmann A, König J, Julius C, Feldbrügge M** (2004) A reverse genetic approach for generating gene replacement mutants in *Ustilago maydis*. *Mol Genet Genomics* **272**: 216–226
- Brachmann A, Weinzierl G, Kämper J, Kahmann R** (2001) Identification of genes in the bW/bE regulatory cascade in *Ustilago maydis*. *Mol Microbiol* **42**: 1047–1063
- Briciu-Burghina C, Heery B, Regan F** (2015) Continuous fluorometric method for measuring β -glucuronidase activity: comparative analysis of three fluorogenic substrates. *Analyst* **140**: 5953–5964
- Brown TL, Rogers MT** (1957) The Preparation and Properties of Crystalline Lithium Alkyls. *J Am Chem Soc* **79**: 1859–1861
- Bryan BJ, Szent-Gyorgyi C** (2001) Luciferases, fluorescent proteins, nucleic acids

encoding the luciferases and fluorescent proteins and the use thereof in diagnostics, high throughput screening and novelty items.

Chatelle C, Ochoa-Fernandez R, Engesser R, Schneider N, Beyer HM, Jones AR, Timmer J, Zurbriggen MD, Weber W (2018) A Green-Light-Responsive System for the Control of Transgene Expression in Mammalian and Plant Cells. *ACS Synth Biol* **7**: 1349–1358

Chng J, Wang T, Nian R, Lau A, Hoi KM, Ho SCL, Gagnon P, Bi X, Yang Y (2015) Cleavage efficient 2A peptides for high level monoclonal antibody expression in CHO cells. *MAbs* **7**: 403–412

Christie JM, Arvai AS, Baxter KJ, Heilmann M, Pratt AJ, O'Hara A, Kelly SM, Hothorn M, Smith BO, Hitomi K, et al (2012) Plant UVR8 Photoreceptor Senses UV-B by Tryptophan-Mediated Disruption of Cross-Dimer Salt Bridges. *Science* (80-) **335**: 1492–1496

Couturier M, Navarro D, Olivé C, Chevret D, Haon M, Favel A, Lesage-Meessen L, Henrissat B, Coutinho PM, Berrin JG (2012) Post-genomic analyses of fungal lignocellulosic biomass degradation reveal the unexpected potential of the plant pathogen *Ustilago maydis*. *BMC Genomics* **13**: 57

Darwin C, Darwin F (1880) The power of Movement in Plants. doi: 10.1017/CBO9780511693670

Daviere J-M, Achard P (2013) Gibberellin signaling in plants. *Development* **140**: 1147–1151

DeLuca M, McElroy WD (1984) Two kinetically distinguishable ATP sites in firefly luciferase. *Biochem Biophys Res Commun* **123**: 764–770

DeLuca M, McElroy WD (1978) Purification and properties of firefly luciferase. *Methods Enzymol* **57**: 3–15

Depuydt S, Hardtke CS (2011) Hormone signalling crosstalk in plant growth regulation. *Curr Biol* **21**: R365–R373

Dill A, Thomas SG, Hu J, Steber CM, Sun T (2004) The Arabidopsis F-Box Protein SLEEPY1 Targets Gibberellin Signaling Repressors for Gibberellin-Induced Degradation. *Plant Cell* **16**: 1392–1405

- Djakovic-Petrovic T, Wit M de, Voesenek LACJ, Pierik R** (2007) DELLA protein function in growth responses to canopy signals. *Plant J* **51**: 117–126
- Dorokhov YL, Skulachev M V., Ivanov PA, Zvereva SD, Tjulkina LG, Merits A, Gleba YY, Hohn T, Atabekov JG** (2002) Polypurine (A)-rich sequences promote cross-kingdom conservation of internal ribosome entry. *Proc Natl Acad Sci U S A* **99**: 5301–5306
- Dubois R** (1885) Fonction Photogénique des Pyrophores. *Comptes rendus des séances la société Biol* **8**: 661–664
- Dupeux F, Santiago J, Betz K, Twycross J, Park S-Y, Rodriguez L, Gonzalez-Guzman M, Jensen MR, Krasnogor N, Blackledge M, et al** (2011) A thermodynamic switch modulates abscisic acid receptor sensitivity. *EMBO J* **30**: 4171–4184
- Eichenberg K, Bäurle I, Paulo N, Sharrock RA, Rüdiger W, Schäfer E** (2000) Arabidopsis phytochromes C and E have different spectral characteristics from those of phytochromes A and B. *FEBS Lett* **470**: 107–112
- Fan F, Wood K V.** (2007) Bioluminescent assays for high-throughput screening. *Assay Drug Dev Technol* **5**: 127–136
- Favory JJ, Stec A, Gruber H, Rizzini L, Oravecz A, Funk M, Albert A, Cloix C, Jenkins GI, Oakeley EJ, et al** (2009) Interaction of COP1 and UVR8 regulates UV-B-induced photomorphogenesis and stress acclimation in Arabidopsis. *EMBO J* **28**: 591–601
- Feldbrügge M, Kellner R, Schipper K** (2013) The biotechnological use and potential of plant pathogenic smut fungi. *Appl Microbiol Biotechnol* **97**: 3253–3265
- De Felipe P, Hughes LE, Ryan MD, Brown JD** (2003) Co-translational, intraribosomal cleavage of polypeptides by the foot-and-mouth disease virus 2A peptide. *J Biol Chem* **278**: 11441–11448
- Fernandez MA, Belda-Palazon B, Julian J, Coego A, Lozano-Juste J, Inigo S, Rodriguez L, Bueso E, Goossens A, Rodriguez PL** (2019) RBR-type E3 ligases and the Ub-conjugating enzyme UBC26 regulate ABA receptor levels

and signaling. *Plant Physiol* pp.00898.2019

- Fields S, Song OK** (1989) A novel genetic system to detect protein-protein interactions. *Nature* **340**: 245–246
- Fussenegger M, Morris RP, Fux C, Rimann M, Stockar B Von, Thompson CJ, Bailey JE** (2000) Streptogramin-based gene regulation systems for mammalian cells. *Nat Biotechnol* **18**: 1203–1208
- Fussenegger M, Moser S, Mazur X, Bailey JE** (1997) Autoregulated multicistronic expression vectors provide one-step cloning of regulated product gene expression in mammalian cells. *Biotechnol Prog* **13**: 733–740
- Gazzarrini S, Tsai AY-L** (2015) Hormone cross-talk during seed germination. *Essays Biochem* **58**: 151–164
- Geiser E, Wierckx N, Zimmermann M, Blank LM** (2013) Identification of an endo-1,4-beta-xylanase of *Ustilago maydis*. *BMC Biotechnol* **13**: 1
- Gibson DG, Young L, Chuang RY, Venter JC, Hutchison CA, Smith HO** (2009) Enzymatic assembly of DNA molecules up to several hundred kilobases. *Nat Methods* **6**: 343–345
- Gonzalez-Guzman M, Pizzio GA, Antoni R, Vera-Sirera F, Merilo E, Bassel GW, Fernández MA, Holdsworth MJ, Perez-Amador MA, Kollist H, et al** (2012) Arabidopsis PYR/PYL/RCAR receptors play a major role in quantitative regulation of stomatal aperture and transcriptional response to abscisic acid. *Plant Cell* **24**: 2483–2496
- Gopinath K, Wellink J, Porta C, Taylor KM, Lomonossoff GP, Van Kammen A** (2000) Engineering cowpea mosaic virus RNA-2 into a vector to express heterologous proteins in plants. *Virology* **267**: 159–173
- Guevarra ED, Tabuchi T** (1990) Accumulation of itaconic, 2-hydroxyparaconic, itatartaric, and malic acids by strains of the genus *ustilago*. *Agric Biol Chem* **54**: 2353–2358
- Hao Q, Yin P, Li W, Wang L, Yan C, Lin Z, Wu JZ, Wang J, Yan SF, Yan N** (2011) The Molecular Basis of ABA-Independent Inhibition of PP2Cs by a Subclass of PYL Proteins. *Mol Cell* **42**: 662–672

- Heijde M, Ulm R** (2013) Reversion of the Arabidopsis UV-B photoreceptor UVR8 to the homodimeric ground state. *Proc Natl Acad Sci U S A* **110**: 1113–1118
- Hewald S, Linne U, Scherer M, Marahiel MA, Kämper J, Bölker M** (2006) Identification of a gene cluster for biosynthesis of mannosylerythritol lipids in the basidiomycetous fungus *Ustilago maydis*. *Appl Environ Microbiol* **72**: 5469–5477
- Hoecker U** (2017) The activities of the E3 ubiquitin ligase COP1/SPA, a key repressor in light signaling. *Curr Opin Plant Biol* **37**: 63–69
- Hosseinpour Tehrani H, Becker J, Bator I, Saur K, Meyer S, Rodrigues Lóia AC, Blank LM, Wierckx N** (2019) Integrated strain- And process design enable production of 220 g L⁻¹ itaconic acid with *Ustilago maydis*. *Biotechnol Biofuels* **12**: 1–11
- Hubbard KE, Nishimura N, Hitomi K, Getzoff ED, Schroeder JI** (2010) Early abscisic acid signal transduction mechanisms: Newly discovered components and newly emerging questions. *Genes Dev* **24**: 1695–1708
- Jang SK, Kräusslich HG, Nicklin MJ, Duke GM, Palmenberg AC, Wimmer E** (1988) A segment of the 5' nontranslated region of encephalomyocarditis virus RNA directs internal entry of ribosomes during in vitro translation. *J Virol* **62**: 2636–2643
- Jefferson RA, Kavanagh TA, Bevan MW** (1987) GUS fusions: beta-glucuronidase as a sensitive and versatile gene fusion marker in higher plants. *EMBO J* **6**: 3901–3907
- Kang J, Hwang J-U, Lee M, Kim Y-Y, Assmann SM, Martinoia E, Lee Y** (2010) PDR-type ABC transporter mediates cellular uptake of the phytohormone abscisic acid. *Proc Natl Acad Sci* **107**: 2355–2360
- Khanna R, Huq E, Kikis EA, Al-Sady B, Lanzatella C, Quail PH** (2004) A novel molecular recognition motif necessary for targeting photoactivated phytochrome signaling to specific basic helix-loop-helix transcription factors. *Plant Cell* **16**: 3033–3044
- Koornneef A, Pieterse CMJ** (2008) Cross talk in defense signaling. *Plant Physiol* **146**: 839–844

- Kuromori T, Miyaji T, Yabuuchi H, Shimizu H, Sugimoto E, Kamiya A, Moriyama Y, Shinozaki K** (2010) ABC transporter AtABCG25 is involved in abscisic acid transport and responses. *Proc Natl Acad Sci* **107**: 2361–2366
- Lavery P, Brown MJB, Pope A** (2001) 2001 Lavery simple absorbance based assays for ultr-high throughput screening.pdf. *Joural Biomol Screen* **6**: 3–9
- León-Ramírez CG, Sánchez-Arreguín JA, Ruiz-Herrera J** (2014) *Ustilago maydis*, a Delicacy of the Aztec Cuisine and a Model for Research. *Nat Resour* **5**: 256–267
- Liu B, Paton JF, Kasparov S** (2008) Viral vectors based on bidirectional cell-specific mammalian promoters and transcriptional amplification strategy for use in vitro and in vivo. *BMC Biotechnol* **8**: 1–8
- Lorenz WW** (1996) Expression of the *Renilla reniformis* luciferase gene in mammalian cells. *J Biolumin Chemilumin* **11**: 31–37
- Lorenz WW, McCann RO, Longiaru M, Cormier MJ** (1991) Isolation and expression of a cDNA encoding *Renilla reniformis* luciferase. *Proc Natl Acad Sci U S A* **88**: 4438–4442
- Lu X-D, Zhou C-M, Xu P-B, Luo Q, Lian H-L, Yang H-Q** (2015) Red-Light-Dependent Interaction of phyB with SPA1 Promotes COP1–SPA1 Dissociation and Photomorphogenic Development in Arabidopsis. *Mol Plant* **8**: 467–478
- Luke GA, de Felipe P, Lukashev A, Kallioinen SE, Bruno EA, Ryan MD** (2008) Occurrence, function and evolutionary origins of “2A-like” sequences in virus genomes. *J Gen Virol* **89**: 1036–1042
- Matthews JC, Hori K, Cormier MJ** (1977) Purification and properties of *Renilla reniformis* luciferase. *Biochemistry* **16**: 85–91
- Mayerhofer R, Langridge WHR, Cormier MJ, Szalay AA** (1995) Expression of recombinant *Renilla* luciferase in transgenic plants results in high levels of light emission. *Plant J* **7**: 1031–1038
- McComb RB, Bowers GN** (1972) Study of optimum buffer conditions for measuring alkaline phosphatase activity in human serum. *Clin Chem* **18**: 97–104
- Müller J, Pohlmann T, Feldbrügge M** (2019) Core components of endosomal

- mRNA transport are evolutionarily conserved in fungi. *Fungal Genet Biol* **126**: 12–16
- Müller K, Engesser R, Metzger S, Schulz S, Kämpf MM, Busacker M, Steinberg T, Tomakidi P, Ehrbar M, Nagy F, et al (2013a)** A red/far-red light-responsive bi-stable toggle switch to control gene expression in mammalian cells. *Nucleic Acids Res.* doi: 10.1093/nar/gkt002
- Müller K, Engesser R, Schulz S, Steinberg T, Tomakidi P, Weber CC, Ulm R, Timmer J, Zurbriggen MD, Weber W (2013b)** Multi-chromatic control of mammalian gene expression and signaling. *Nucleic Acids Res.* doi: 10.1093/nar/gkt340
- Müller K, Engesser R, Timmer J, Nagy F, Zurbriggen MD, Weber W (2013c)** Synthesis of phycocyanobilin in mammalian cells. *Chem Commun* **49**: 8970–8972
- Müller K, Siegel D, Rodriguez Jahnke F, Gerrer K, Wend S, Decker EL, Reski R, Weber W, Zurbriggen MD (2014)** A red light-controlled synthetic gene expression switch for plant systems. *Mol Biosyst* **10**: 1679–1688
- Park S-Y, Fung P, Nishimura N, Jensen DR, Fujii H, Zhao Y, Lumba S, Santiago J, Rodrigues A, Chow T -f. F, et al (2009)** Abscisic Acid Inhibits Type 2C Protein Phosphatases via the PYR/PYL Family of START Proteins. *Science* (80-). doi: 10.1126/science.1173041
- Parsons SJW, Rhodes SA, Connor HE, Rees S, Brown J, Giles H (2000)** Use of a dual firefly and Renilla luciferase reporter gene assay to simultaneously determine drug selectivity at human corticotrophin releasing hormone 1 and 2 receptors. *Anal Biochem* **281**: 187–192
- Pelletier J, Sonenberg N (1988)** Internal initiation of translation of eukaryotic mRNA directed by a sequence derived from poliovirus RNA. *Nature* **334**: 320–325
- Raghavendra AS, Gonugunta VK, Christmann A, Grill E (2010)** ABA perception and signalling. *Trends Plant Sci* **15**: 395–401
- Reyes-Dominguez Y, Narendja F, Berger H, Gallmetzer A, Fernandez-Martin R, Garcia I, Scazzocchio C, Strauss J (2008)** Nucleosome positioning and histone

- H3 acetylation are independent processes in the *Aspergillus nidulans* prnD-prnB bidirectional promoter. *Eukaryot Cell* **7**: 656–663
- Roberts AG, Santa Cruz S, Roberts IM, Prior DAM, Turgeon R, Oparka KJ** (1997) Phloem unloading in sink leaves of *Nicotiana benthamiana*: Comparison of a fluorescent solute with a fluorescent virus. *Plant Cell* **9**: 1381–1396
- Robinson RA, Biggs AI** (1955) The thermodynamic ionization constant of p-nitrophenol from spectrophotometric measurements. *Trans Faraday Soc* **51**: 901–903
- Ryan MD, Drew J** (1994) Foot-and-mouth disease virus 2A oligopeptide mediated cleavage of an artificial polyprotein. *EMBO J* **13**: 928–933
- Sadowski I, Ma J, Triezenberg S, Ptashne M** (1988) GAL4-VP16 is an unusually potent transcriptional activator. *Nature* **335**: 563–564
- Salah-Bey K, Thompson CJ** (1995) Unusual regulatory mechanism for a *Streptomyces* multidrug resistance gene, ptr, involving three homologous protein-binding sites overlapping the promoter region. *Mol Microbiol* **17**: 1109–1119
- Samodelov SL, Beyer HM, Guo X, Augustin M, Jia KP, Baz L, Ebenhöf O, Beyer P, Weber W, Al-Babili S, et al** (2016) Strigoquant: A genetically encoded biosensor for quantifying Strigolactone activity and specificity. *Sci Adv*. doi: 10.1126/sciadv.1601266
- Santner A, Calderon-Villalobos LIA, Estelle M** (2009) Plant hormones are versatile chemical regulators of plant growth. *Nat Chem Biol* **5**: 301–307
- Schuster M, Schweizer G, Reissmann S, Kahmann R** (2016) Genome editing in *Ustilago maydis* using the CRISPR-Cas system. *Fungal Genet Biol* **89**: 3–9
- Sheen J** (2010) Discover and Connect Cellular Signaling. *Plant Physiol* **154**: 562–566
- Sheerin DJ, Menon C, zur Oven-Krockhaus S, Enderle B, Zhu L, Johnen P, Schleifenbaum F, Stierhof Y-D, Huq E, Hiltbrunner A** (2015) Light-Activated Phytochrome A and B Interact with Members of the SPA Family to Promote Photomorphogenesis in *Arabidopsis* by Reorganizing the COP1/SPA Complex.

Plant Cell **27**: 189–201

Shimomura O, Johnson FH, Saiga Y (1962) Extraction, purification and properties of aequorin, a bioluminescent. J Cell Comp Physiol **59**: 223–239

Spellig T, Bottin A, Kahmann R (1996) Green fluorescent protein (GFP) as a new vital marker in the phytopathogenic fungus *Ustilago maydis*. Mol Gen Genet **252**: 503–509

Stock J, Sarkari P, Kreibich S, Brefort T, Feldbrügge M, Schipper K (2012) Applying unconventional secretion of the endochitinase Cts1 to export heterologous proteins in *Ustilago maydis*. J Biotechnol **161**: 80–91

Suzuki N, Geletka LM, Nuss DL (2000) Essential and Dispensable Virus-Encoded Replication Elements Revealed by Efforts To Develop Hypoviruses as Gene Expression Vectors. J Virol **74**: 7568–7577

Teichmann B, Linne U, Hewald S, Marahiel MA, Bölker M (2007) A biosynthetic gene cluster for a secreted cellobiose lipid with antifungal activity from *Ustilago maydis*. Mol Microbiol **66**: 525–533

Terfrüchte M, Joehnk B, Fajardo-Somera R, Braus GH, Riquelme M, Schipper K, Feldbrügge M (2014) Establishing a versatile Golden Gate cloning system for genetic engineering in fungi. Fungal Genet Biol **62**: 1–10

Thomas CL, Maule AJ (2000) Limitations on the use of fused green fluorescent protein to investigate structure-function relationships for the cauliflower mosaic virus movement protein. J Gen Virol **81**: 1851–1855

Thompson SR, Gulyas KD, Sarnow P (2001) Internal initiation in *Saccharomyces cerevisiae* mediated by an initiator tRNA/eIF2-independent internal ribosome entry site element. Proc Natl Acad Sci U S A **98**: 12972–12977

Thorne N, Inglese J, Auld DS (2010) Illuminating Insights into Firefly Luciferase and Other Bioluminescent Reporters Used in Chemical Biology. Chem Biol **17**: 646–657

Triezenberg SJ, Kingsbury RC, McKnight SL (1988) Functional dissection of VP16, the trans-activator of herpes simplex virus immediate early gene expression. Genes Dev **2**: 718–729

- Varnavski AN, Young PR, Khromykh AA** (2000) Stable High-Level Expression of Heterologous Genes In Vitro and In Vivo by Noncytopathic DNA-Based Kunjin Virus Replicon Vectors. *J Virol* **74**: 4394–4403
- Verhaegen M, Christopoulos TK** (2002) Recombinant Gaussia luciferase: Overexpression, purification, and analytical application of a bioluminescent reporter for DNA hybridization. *Anal Chem* **74**: 4378–4385
- Verma V, Ravindran P, Kumar PP** (2016) Plant hormone-mediated regulation of stress responses. *BMC Plant Biol* **16**: 1–10
- Vlad F, Rubio S, Rodrigues A, Sirichandra C, Belin C, Robert N, Leung J, Rodriguez PL, Laurière C, Merlot S** (2009) Protein Phosphatases 2C Regulate the Activation of the Snf1-Related Kinase OST1 by Abscisic Acid in Arabidopsis. *Plant Cell* **21**: 3170–3184
- Wagner D, Fairchild CD, Kuhn RM, Quail PH** (1996) Chromophore-bearing NH₂-terminal domains of phytochromes A and B determine their photosensory specificity and differential light lability. *Proc Natl Acad Sci U S A* **93**: 4011–4015
- Wend S, Dal Bosco C, Kämpf MM, Ren F, Palme K, Weber W, Dovzhenko A, Zurbriggen MD** (2013) A quantitative ratiometric sensor for time-resolved analysis of auxin dynamics. *Sci Rep* **3**: 1–7
- de Wet JR, Wood K V, DeLuca M, Helinski DR, Subramani S** (1987) Firefly luciferase gene: structure and expression in mammalian cells. *Mol Cell Biol* **7**: 725–737
- Di Wu, Hu Q, Yan Z, Chen W, Yan C, Huang X, Zhang J, Yang P, Deng H, Wang J, et al** (2012) Structural basis of ultraviolet-B perception by UVR8. *Nature* **484**: 214–219
- Wu W, Liu Y, Wang Y, Li H, Liu J, Tan J, He J, Bai J, Ma H** (2017) Evolution Analysis of the Aux/IAA Gene Family in Plants Shows Dual Origins and Variable Nuclear Localization Signals. *Int J Mol Sci* **18**: 2107
- Yamaguchi S** (2008) Gibberellin Metabolism and its Regulation. *Annu Rev Plant Biol* **59**: 225–251
- Zarnack K, Maurer S, Kaffarnik F, Ladendorf O, Brachmann A, Kämper J,**

Feldbrügge M (2006) Tetracycline-regulated gene expression in the pathogen *Ustilago maydis*. *Fungal Genet Biol* **43**: 727–738

Ziegler T, Möglich A (2015) Photoreceptor engineering. *Front Mol Biosci* **2**: 1–25

7. Appendix: original publications and manuscripts

Nicole Heucken,* Lisa C. Hüsemann* and Matias D. Zurbriggen. AQUA 2.0: an upgrade to AQUA cloning. Manuscript in preparation. *equal contribution

Contribution: Design, performance and analysis of the experiment. Preparation of the figures and writing of the manuscript.

Noel Blanco-Touriñán^{a,1}, Martina Legris^{b,1}, Eugenio G. Minguet^{a,1}, Cecilia Costigliolo-Rojas^{b,1}, María A. Nohales^c, Elisa Iniesto^d, Marta García-León^d, Manuel Pacín^e, Nicole Heucken^f, Tim Blomeier^f, Antonella Locascio^a, Martin Černý^g, David Esteve-Bruna^a, Mónica Díez-Díaz^h, Břetislav Brzobohatý^g, Henning Frerigmannⁱ, Matías D. Zurbriggen^f, Steve A. Kay^c, Vicente Rubio^d, Miguel A. Blázquez^a, Jorge J. Casal^{b,e,*}, David Alabadí^{a,*} COP1 destabilizes DELLA proteins in *Arabidopsis*. Manuscript accepted in PNAS.

Contribution: Design, performance and analysis of cell culture experiments. Confocal fluorescence microscopy. Processing of microscopy pictures and preparation of figures related to the cell culture experiments.

7.1 AQUA 2.0: an upgrade to AQUA cloning

AQUA 2.0: an upgrade to AQUA cloning

Nicole Heucken, Lisa C. Hüsemann and Matias D. Zurbriggen

Key words assembly cloning, plant synthetic biology, *Arabidopsis thaliana*

Abstract

Assembly cloning methods like Gibson and AQUA (advanced quick assembly), are increasingly replacing conventional restriction enzyme and DNA ligase-dependent cloning methods for reasons of efficiency and performance. AQUA Cloning harnesses intrinsic in vivo processing of linear DNA fragments with short regions of homology of 16 to 32 bp mediated by *Escherichia coli*. Here, we describe an update to AQUA and demonstrate the possibility of integrating short DNA sequences encoding e.g. for signal peptides into existing vectors. This is achieved by assembly of several pre-annealed oligonucleotide pairs with the digested vector backbone. In this protocol the integration of a PEST sequence into an already existing vector, its transformation into *Arabidopsis thaliana* protoplasts and a subsequent Luciferase assay enables the determination of the potential induction-fold for sensor modules used in the reconstruction of plant hormone signaling pathways.

Introduction

The implementation of synthetic biology approaches requires complex combinations of a wide variety of proteins and genetic tools, including synthetic protein modules, reporter genes, promoters, and many others. The assembly of such complex constructs makes it necessary to simplify the cloning process and make it more efficient by inventing new methods that are flexible, fast and cheap. One of such methods is AQUA [1]. It has already proven to be a versatile, robust and, compared to other commonly used cloning methods, cheap and fast cloning approach. It fully relies on homologous overhang pairing and is therefore completely independent of the addition of enzymes. Beyer et al. already exemplified the applicability of AQUA cloning for various application. What we want to present here is an update of this list of proven applications. Therefore, we demonstrate how AQUA cloning can be used to add short sequences, too long to be included in a primer overhang, and too short to be effectively amplified via PCR, to your plasmid.

Here we cloned a PEST sequence of 126 bp into a plasmid containing Firefly and Renilla luciferases separated by a 2A peptide (see fig. 2). In this experimental setup, the PEST sequence is the product of three forward and their complementary reverse primers. These oligonucleotides are assembled to double stranded DNA fragments via primer annealing (see fig. 1). The idea is to tag this sequence to Firefly luciferase leading to a degradation of the protein. The successful inclusion of the sequence and its functionality are verified by Firefly/Renilla assays (see fig. 3).

Materials

All solutions should be prepared using double distilled water and p.a. purity grade chemicals. For all plant growth and protoplast isolation media we recommend to use plant cell culture tested reagents. The reagents must be prepared and stored at 4 °C unless indicated otherwise.

2.1 Plant Growth

1. SCA (Seedling Culture Arabidopsis) (modified from [2]): 0,32 % (w/v) Gamborg B5 basal salt powder with vitamins (bioWORLD), 4 mM $\text{MgSO}_4 \cdot 7\text{H}_2\text{O}$, 43.8 mM sucrose, and 0,8 % (w/v) phytoagar. Mix and adjust to pH 5.8 and autoclave. Add 0,1 % (v/v) Gamborg B5 Vitamin Mix (bioWORLD) and 1:2000 ampicillin and pour 50 ml of the medium into 12-cm² plates (Greiner Bio-One).
2. Seed sterilization solution for *A. thaliana* (modified from [3]): 5 % (w/v) calcium hypochloride, 0,02 % (v/v) Triton X-100 in 80 % (v/v) EtOH. Combine all chemicals and mix for a few hours at room temperature. Let the formed precipitate settle and store the solution at 4 °C. Do not agitate the bottle before use.
3. Parafilm
4. Syringe and 22 µm filter
5. Ampicillin stock (100 mg/ml)

2.2 Protoplast Isolation and PEG Mediated Protoplast Transformation

1. MMC (MES, Mannitol, Calcium) [2]: 10 mM MES, 40 mM $\text{CaCl}_2 \cdot \text{H}_2\text{O}$, add mannitol until obtaining an osmolarity of 550 mOsm (ca. 85 g/l). Adjust to pH 5.8 and filter sterilize.
2. Enzyme solution stock 5 % (10x concentrated): cellulase Onozuka R10 and macroenzyme R10 (SERVA Electrophoresis GmbH, Germany) in MMC. Add 10 g of cellulase and 10 g of macroenzyme and dissolve in preheated (37 °C)

MMC to a total volume of 200 ml H₂O. Sterile filter the solution with a bottle-top filter and make aliquots of 2 ml. Store aliquots at -20 °C and avoid any thaw-freeze cycles.

3. MSC (MES, Sucrose, Calcium) [2]: 10 mM MES, 0.4 M sucrose, 20 mM MgCl₂·6H₂O, add mannitol until you obtain an osmolarity of 550 mOsm (ca. 85 g/l). Adjust to a pH of 5.8 and filter sterilize.

4. W5 solution (modified from [4]): 2 mM MES, 154 mM glucose. Adjust to pH 5.8 and filter sterilize.

5. MMM (MES, Mannitol, Magnesium) [2]: 15 mM MgCl₂, 5 mM MES, mannitol up to 600 mOsm (ca. 85 g/l). Adjust to a pH of 5.8 and filter sterilize.

6. PEG solution: freshly made for each experiment. Mix 2.5 ml of 0.8 M mannitol, 1 ml of 1 M CaCl₂, 4 g PEG₄₀₀₀ and 3 ml H₂O. Do not filter. Use directly after placing the tube at 37 °C for dissolution of PEG.

7. PCA (Protoplast Culture Arabidopsis) (modified from [2]): 0.32 % (w/v) Gamborg B5 basal salt powder with vitamins (bioWORLD), 2 mM MgSO₄·7H₂O, 3.4 mM CaCl₂·2H₂O, 5 mM MES, 0.342 mM l-glutamine, 58.4 mM sucrose, glucose 550 mOsm (ca. 80 g/l), 8.4 µM Ca-panthotenate, 2 % (v/v) biotin from a biotin solution 0.02 % (w/v) in H₂O (biotin solution should be warmed up to dissolve). Adjust the pH to 5.8 and filter sterilize. Add 0.1 % (v/v) Gamborg B5 Vitamin Mix and 1:2000 ampicillin to the PCA before use.

8. Scalpel

9. Disposable 70 µm pore size sieve (Greiner bio-one international, Germany)

10. Petri dish 94 x 16 mm

11. Parafilm

12. 200 µl and 1 ml large orifice pipette tips

13. Round-bottom 15 ml Falcon tubes

14. Rosenthal cell counting chamber

15. Nontreated 6-well plates

2.3 Luminescence Reporter Assay

1. Costar® 96-well flat-bottom white plate
2. Firefly luciferase substrate: 20 mM tricine, 2.67 mM MgSO₄·7H₂O, 0.1 mM EDTA·2H₂O, 33.3 mM DTT, 0.52 mM ATP, 0.27 mM acetyl-CoA, 0.47 mM d-luciferin (Biosynth AG), 5 mM NaOH, 264 µM MgCO₃·5H₂O, in H₂O. Prepare a beaker with a magnetic stirrer and add the components in the order as above. Then add the luciferin and H₂O and mix the solution. Finally add the NaOH and the MgCO₃·5H₂O. Adjust the solution to a pH of 8. Make aliquots in precooled black Falcon tubes and store them at -80 °C.
3. Renilla luciferase substrate (Coelenterazine): 472 mM coelenterazine stock solution in methanol, diluted with PBS directly before use.

2.4 Plasmid generation and purification

1. Plasmid digestion: 2 – 5 µg of plasmid, 5 µl of 10 x CutSmart® buffer (NEB), 17 u of restriction enzyme, fill up to 50 µl with ddH₂O. Before loading on gel add 10 u of CIP and incubate for 1 h at 37 °C.
2. TAE buffer (50 x): 242 g Tris base in water, add 57.1 ml glacial acetic acid, and 100 ml of 500 mM EDTA (pH 8.0) solution. Bring the solution to a final volume of 1 l.
3. Plasmid purification: 0.8 % agarose gel (0.8 g/100 ml TAE 1x) with 1 µg/ml ethidium bromide.
4. Plasmid gel extraction: QIAquick Gel Extraction Kit (QIAGEN); DNA is eluted in 20 µl ddH₂O.
5. Gel electrophoresis chambers
6. Heating block with shaking function

2.5 AQUA cloning

1. ddH₂O

2. Oligonucleotides (Sigma; stock 100 μ M)
3. Annealing buffer (1x): 10 mM Tris (pH 7.5 -8), 50 mM NaCl, 1 mM EDTA

2.6 *E. coli* transformation

1. TOP10 (Invitrogen) *E. coli* strain prepared for chemical competency
2. LB liquid medium

Methods

3.1 AQUA cloning

1. digest the vector plasmid (pSW209) with NheI for 2 h at 37°C. Afterwards add CIP and incubate for another 30 min.
2. Load the digest on a 0.8 % agarose gel and let it run for 20 min.
3. Extract the DNA from the gel using the QIAquick Gel Extraction Kit (QIAGEN) and following the protocol of the manufacturer.
4. dilute oligonucleotides 1:10 in annealing buffer; mix 5 μ l of each forward primer with 5 μ l of the complementary reverse primer in 1.5 ml reaction tubes (reaction 1 - 3); put the 3 reactions to 95 °C for 5 min; let cool down to room temperature; mix 3 μ l of each reaction and 1 μ l of vector plasmid in a 1.5 ml reaction tube; incubate for 1 h at room temperature.
5. Transform 10 μ l into chemically competent *E. coli* TOP10 cells and incubate on ice for 30 min.
6. Heat shock at 42 °C for 45 sec.
7. Add 250 μ l LB medium and incubate on a shaker at 37 °C and 700 rpm for 1 h.
8. Plate the whole reaction on LB-ampicillin plates and incubate at 37 °C over night.

9. Single out colonies on new LB-ampicillin plates and incubate at 37 °C over night.
10. Perform a miniprep and test digest the plasmids. Positive clones should be sequenced.
11. Inoculate 100 ml of LB medium with antibiotics in shaking flasks with plasmid containing *E. coli* cells and incubate shaking over night at 37 °C.
11. Perform a midiprep. Make a 1:10 dilution and load the following mixture on an 1 % agarose gel to determine the quality of the plasmid preparation: 3 µl plasmid dilution, 7 µl H₂O and 2 µl loading dye.

3.2 Seed Sterilization and Plant Material

1. The sterilization of *A. thaliana* (Wild type, Columbia-0) seed should be done in a sterile working hood in 1.5 ml tubes. The maximum filling volume of a single tube should not exceed 250 µl, otherwise the sterilization efficiency may vary.
2. Rinse seed multiple times with 80 % (v/v) ethanol until all large dirt and other particles are removed.
3. sterilize the seeds of *A. thaliana* sterilization solution for 10 min under agitation.
4. Remove the solution and add 1 ml of 80 % (v/v) ethanol and incubate for 5 min under agitation.
5. Repeat step 4 with an incubation time of 2 min.
6. Replace the solution with 1 ml absolute Ethanol and incubate for 1 min under agitation.
7. Remove the ethanol and let seeds dry completely.
8. Add autoclaved water and plate the seeds in a line on autoclaved filter paper strips (200 – 300 seeds/strip) placed on 12 cm square plates containing SCA medium. Seal the plates with parafilm.
9. Place the prepared plates in a growth chamber with a 16 h light regime at 22 °C. The seedlings should be 2 – 3 weeks to be used for protoplast isolation.

3.3 Protoplast isolation and Polyethylene Glycol-Mediated Transformation

A. thaliana protoplast isolation and transformation were performed as described in [2] and [5] with a few alterations. For any pipetting, only wide open orifice tips were used to avoid damaging the protoplasts. Use medium acceleration and lowest deceleration settings for the centrifugation steps (140 s acceleration, and 300 s deceleration according to DIN58970).

1. Slice the plant leaves of *A. thaliana* with a scalpel in 2 ml of MMC.
2. Transfer cut leaf material into a new petri dish containing 7 ml of MMC.
3. Add 1 ml of 10 x enzyme stock solution to start the enzymatic digestion (final concentration of each enzyme: 0.5 %)
4. Seal the dish with parafilm and cover it with aluminum foil. Incubate the dish over night (12 – 16 h) in the dark at 22 °C.
5. Homogenize (carefully) the leaf material to release the protoplasts by pipetting the mixture up and down.
6. Pass the mixture through a disposable 70 µm pore size sieve.
7. Transfer the filtered protoplast solution to 15 ml round bottom Falcon tubes. Use one tube for each plate of digested leaf material, and complete all remaining steps in these tubes.
8. Centrifuge the filtered protoplasts solution at 100 x g for 10 – 20 min for sedimentation of the protoplasts. Remove the supernatant and resuspend the protoplasts in 10 ml MSC.
9. Carefully overlay the protoplast solution with 2 ml of MMM.
10. Centrifuge for 10 min at 80 x g for accumulation of the protoplasts at the interface of MSC and MMM.
11. Collect the protoplasts from the interphase and transfer them into a new Falcon tube containing 7 ml of W5 solution. Prepare two W5-filled collection Falcon tubes for each floatation tube. Multiple rounds of protoplast collection can be done.

12. Centrifuge the protoplasts for 10 min at 100 x g to pellet and resuspend in 10 – 15 ml of W5 for counting.
13. Determine the density using a Rosenthal cell counting chamber.
14. Centrifuge for 5 min at 80 x g to sediment the protoplasts. Remove the supernatant and adjust the density to 5×10^6 cells/ml with MMM solution.
15. For the transformation of *A. thaliana* protoplasts, prepare 15 – 30 µg of DNA in H₂O (mentioned DNA amounts are total amounts of DNA. When more than one plasmid is used, the amounts of DNA must be adjusted proportionally. Before transformation the plasmid DNA must be purified using a midiprep kit, and the quality of the plasmid DNA must be checked by agarose gel electrophoresis) adjusted to a maximum volume of 20 µl with MMM solution. Transfer the 20 µl DNA solution to the rim of a well of a 6-well culture plate. Dispense 100 µl of protoplast solution to each well with DNA and mix gently by pipetting. Incubate the mixture for 5 min.
16. Gently shake the 6-well plate to distribute the protoplasts and DNA along the rim before directly adding 120 µl of PEG₄₀₀₀ dropwise (tip-in-tip). Do not mix after addition of PEG. Incubate for 8 min and quickly add 120 µl of MMM and, directly afterwards, 1.2 ml of PCA. Gently mix by tilting the plate.
17. If only one condition is to be tested, leave the protoplast suspension in the 6-well plate.

3.4 Reporter Assay

1. To determine reporter expression, gently mix the protoplast suspension and transfer 80 µl (25,000 protoplasts) into one Costar® 96-well flat bottom white plate for Firefly assay, and into one for Renilla assay, including 4 – 6 replicates for each.
2. Add 20 µl of firefly luciferase (final concentration of 131 µg/ml) and 20 µl of coelenterazine (472 mM coelenterazine stock solution in methanol, diluted directly before use, 1:15 in cooled phosphate-buffered saline) and monitor the luminescence in a plate reader. The following program is advisable: 10 s of

shaking plate for homogeneous substrate availability and direct luminescence measurement for 20 min with an interval of 2 min.

References

1. Beyer H, Gonschorek P, Samodelov SL, Meier M, Weber W, Zurbriggen MD (2015) AQUA Cloning: A versatile and simple enzyme-free cloning approach. PLoS ONE 10(9): e0137652
2. Dovzhenko A, Bergen U, Koop HU (1998) Thin-alginate-layer technique for protoplast culture of tobacco leaf protoplasts: shoot formation in less than two weeks. Protoplasma 204(1-2):114–118
3. Luo Y, Koop H-U (1997) Somatic embryogenesis in cultured immature zygotic embryos and leaf protoplasts of *Arabidopsis thaliana* ecotypes. Planta 202(3):387–396
4. Menczel L, Galiba G, Nagy F, Maliga P (1982) Effect of radiation dosage on efficiency of chloroplast transfer by protoplast fusion in *Nicotiana glauca*. Genetics 100(3):487–495
5. Koop H-U, Steinmüller K, Wagner H, Rößler C, Eibl C, Sacher L (1996) Integration of foreign sequences into the tobacco plastome via polyethylene glycol-mediated protoplast transformation. Planta 199(2):193–201
6. Wend S, Bosco CD, Kämpf MM, Ren F, Palme K, Weber W, Dovzhenko A, Zurbriggen MD (2013) A quantitative ratiometric sensor for time-resolved analysis of auxin dynamics. Sci Rep 3:2052

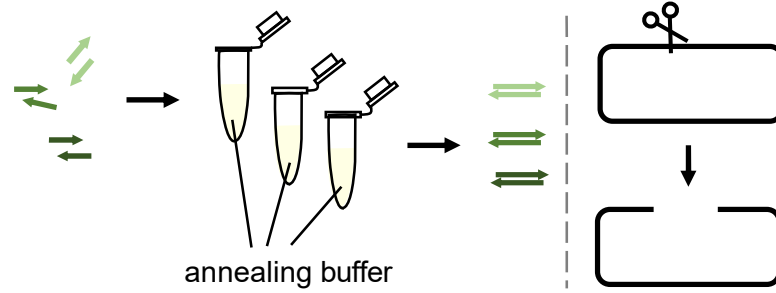
Figure legends

Fig. 1 AQUA 2.0 Cloning work-flow. (1) DNA parts are generated by Oligo pre-annealing and PCR amplification or restriction digest. (2) Vector backbone is purified by gel-electrophoresis. (3) pre-annealed oligos and digested plasmid are mixed and incubated in water prior to transformation into chemically competent *E. coli* Top10 cells for in vivo assembly. (4) Finally, obtained colonies are confirmed for correct assembly by standard methods such as analytical PCR, restriction digest, or comprehensive sequencing.

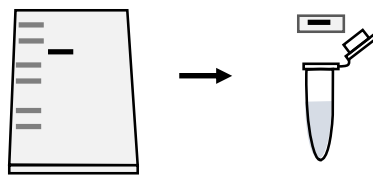
Fig. 2 Design of the pifold (potential-induction-fold-determination) gene expression system in plants. (a) Configuration of the vectors. (b) Mode of function. Pifold construct expressing a renilla luciferase (RLuc; blue) connected via a 2A peptide to the degradation module (PEST) fused to a firefly luciferase (FLuc; green), under the control of a constitutive 35S promoter. The 2A peptide in the synthetic construct leads to stoichiometric coexpression of RLuc (normalization element) and PEST-FLuc. PEST-FLuc becomes degraded, whereas RLuc expression remains constant, leading to a decrease in the FLuc/RLuc ratio.

Fig. 3 Potential-induction-fold-determination for biosensors in *Arabidopsis thaliana* mesophyll protoplasts. Protoplasts were isolated from WT seedlings and transformed with the respective plasmid. Twenty-four hours after transformation, luciferase activity was determined. Results are averaged FF/REN ratios, normalized to the sample without PEST sequence. The data shown correspond to one representative experiment. Error bars represent SEM from the individual experimental data shown. n = 12.

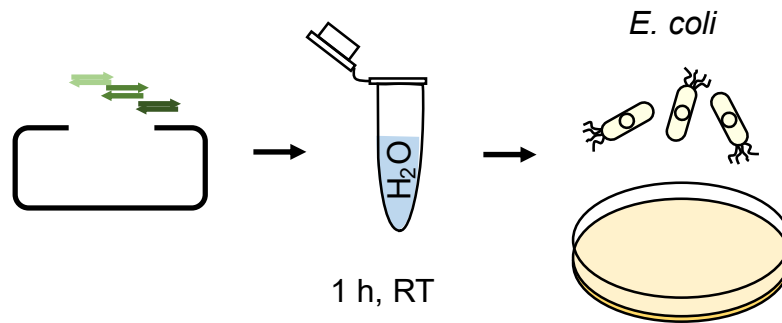
(1) Oligo pre-annealing and vector digest



(2) Gel-electrophoresis and extraction



(3) Mixing and transformation



(4) Preparation and analysis

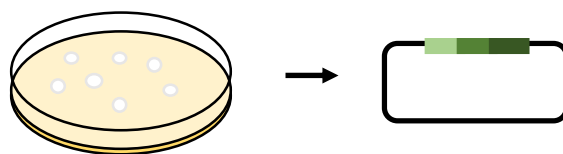


Fig. 1

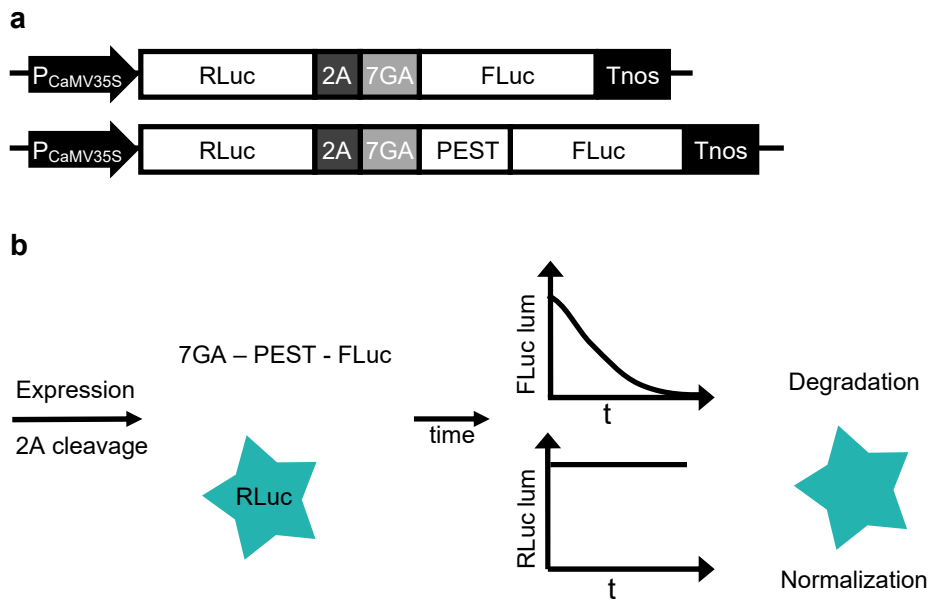


Fig.2

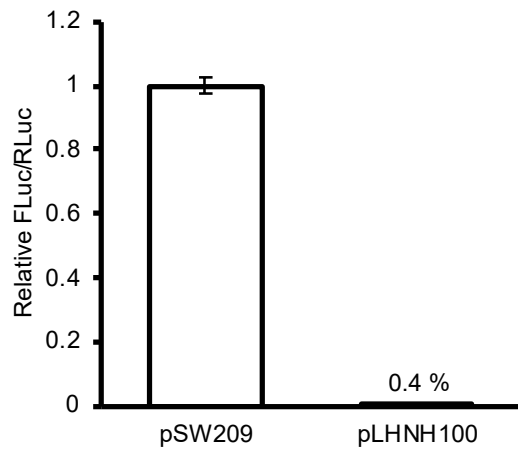


Fig. 3

Table 1**Description of the plasmids CtrlQuant and Pifold for plant use**

Vector	Description	Reference
SW209	<p>$P_{CaMV35S}$-AtRLuc-2A-(GA)₇-AtFLuc-Tnos</p> <p>Vector encoding firefly luciferase (FLuc), a 2A-peptide, a small repeated GA sequence and renilla luciferase (RLuc) under the control of the Cauliflower mosaic virus (CaMV) 35S promoter. (1)</p>	[6]
pLHNH100	<p>$P_{CaMV35S}$-AtRLuc-2A-(GA)₇-PEST-AtFLuc-Tnos</p> <p>Vector encoding firefly luciferase (FLuc), a 2A-peptide, a small repeated GA sequence, a PEST sequence and renilla luciferase (RLuc) under the control of the Cauliflower mosaic virus (CaMV) 35S promoter. The PEST sequence was introduced by assembly of 3 pre-annealed Oligonucleotide pairs (oLHNH001 + oLHNH008, oLHNH002 + oLHNH009 and oLHNH003 + oLHNH010) of 73 bp in length each and NheI + CIP digested pSW209 as the backbone.</p>	This work

Table 2**Oligonucleotides used in this work**

Oligo	Sequence (5'→ 3')
oLHNH001	TGCCGGGGCAGGCGCTGGCGCTAGCAAGCTCTCTCATGGATTCC CGCCAGCTGTAGCCGCTCAGGACGATGGA
oLHNH002	TAGCCGCTCAGGACGATGGAACCCTACCCATGAGCTGCGCGCAAG AATCTGGCATGGATCGACATCCTGCAGC
oLHNH003	ATGGATCGACATCCTGCAGCCTGCGCTTCCGCAAGGATTAACGTG GGCGCGCCATGGAAGACGCCAAAAACAT
oLHNH008	TCCATCGTCCTGAGCGGCTACAGCTGGCGGGAATCCATGAGAGAG CTTGCTAGCGCCAGCGCCTGCCCCGGCA
oLHNH009	GCTGCAGGATGTTCGATCCATGCCAGATTCTTGCGCGCAGCTCATG GGTAGGGTTCCATCGTCCTGAGCGGCTA
oLHNH010	ATGTTTTTGGCGTCTTCCATGGCGCGCCCACGTTAATCCTTGCGGA AGCGCAGGCTGCAGGATGTTCGATCCAT

7.2 COP1 destabilizes DELLA proteins in *Arabidopsis*

Q: 1, 2, 3, 4, 5, 6

COP1 destabilizes DELLA proteins in *Arabidopsis*

Noel Blanco-Touriñán^{a,1}, Martina Legris^{b,1}, Eugenio G. Minguet^{a,1}, Cecilia Costigliolo-Rojas^{b,1},
 Maria A. Nohales^c, Elisa Iniesto^d, Marta García-León^d, Manuel Pacín^e, Nicole Heucken^f, Tim Blomeier^f,
 Antonella Locascio^g, Martin Černý^g, David Esteve-Bruna^h, Mónica Díez-Díaz^h, Břetislav Brzobohatý^g,
 Henning Frerigmannⁱ, Matias D. Zurbriggenⁱ, Steve A. Kay^c, Vicente Rubio^d, Miguel A. Blázquez^g,
 Jorge J. Casal^{b,e,2}, and David Alabadí^{a,2}

^aInstituto de Biología Molecular y Celular de Plantas, Consejo Superior de Investigaciones Científicas, Universidad Politécnica de Valencia, 46022 Valencia, Spain; ^bFundación Instituto Leloir, Consejo Nacional de Investigaciones Científicas y Técnicas, Instituto de Investigaciones Bioquímicas de Buenos Aires, 1405 Buenos Aires, Argentina; ^cDepartment of Neurology, Keck School of Medicine, University of Southern California, Los Angeles, CA 90098; ^dDepartamento de Genética Molecular de Plantas, Consejo Superior de Investigaciones Científicas, Centro Nacional de Biotecnología, 28049 Madrid, Spain; ^eIFEVA, Facultad de Agronomía, Consejo Nacional de Investigaciones Científicas y Técnicas, Universidad de Buenos Aires, 1417 Buenos Aires, Argentina; ^fInstitute of Synthetic Biology and Cluster of Excellence in Plant Sciences, University of Düsseldorf, 40225 Düsseldorf, Germany; ^gDepartment of Molecular Biology and Radiobiology, CEITEC, Faculty of AgriSciences, Mendel University in Brno, CZ-61300 Brno, Czech Republic; ^hUniversidad Católica de Valencia, 46001 Valencia, Spain; and ⁱDepartment of Plant Microbe Interactions and Cluster of Excellence in Plant Sciences, Max Planck Institute for Plant Breeding Research, 50829 Cologne, Germany

Edited by Tai-ping Sun, Duke University, Durham, NC, and accepted by Editorial Board Member Joseph R. Ecker April 21, 2020 (received for review May 11, 2019)

DELLA transcriptional regulators are central components in the control of plant growth responses to the environment. This control is considered to be mediated by changes in the metabolism of the hormones gibberellins (GAs), which promote the degradation of DELLAs. However, here we show that warm temperature or shade reduced the stability of a GA-insensitive DELLA allele in *Arabidopsis thaliana*. Furthermore, the degradation of DELLA induced by the warmth preceded changes in GA levels and depended on the E3 ubiquitin ligase CONSTITUTIVELY PHOTOMORPHOGENIC1 (COP1). COP1 enhanced the degradation of normal and GA-insensitive DELLA alleles when coexpressed in *Nicotiana benthamiana*. DELLA proteins physically interacted with COP1 in yeast, mammalian, and plant cells. This interaction was enhanced by the COP1 complex partner SUPPRESSOR OF *phyA-105* 1 (SPA1). The level of ubiquitination of DELLA was enhanced by COP1 and COP1 ubiquitinated DELLA proteins in vitro. We propose that DELLAs are destabilized not only by the canonical GA-dependent pathway but also by COP1 and that this control is relevant for growth responses to shade and warm temperature.

shade avoidance | thermomorphogenesis | environment | gibberellin | growth

A plant can adopt markedly different morphologies depending on the environment it has to cope with. This plastic behavior relies on highly interconnected signaling pathways, which offer multiple points of control (1). Light and temperature are among the most influential variables of the environment in plant life. For instance, light cues from neighboring vegetation as well as elevated ambient temperature (e.g., 28 °C) enhance the growth of the hypocotyl (among other responses), respectively, to avoid shade (2) and enhance cooling (3).

Several features place DELLA proteins as central elements in environmental responses (4). First, DELLAs are nuclear-localized proteins that interact with multiple transcription factors and modulate their activity (5). Second, they are negative elements in the gibberellin (GA) signaling pathway and their stability is severely diminished upon recognition of their N-terminal domain by the GA-activated GIBBERELLIN INSENSITIVE1 (GID1) receptor, which recruits the SCF^{SLY1/GID2} complex to promote their ubiquitination-dependent degradation by the proteasome (6). Third, GA metabolism is regulated by the environment; for instance, shade and warm temperature induce GA accumulation (3, 7).

DELLA levels increase during seedling deetiolation or cold exposure and promote transcriptional changes associated with photomorphogenesis or with the adaptation to low temperatures, respectively (8–10). On the contrary, they decrease during the

night and in response to shade inflicted by neighbor plants or to warm ambient temperature, allowing the promotion of hypocotyl and/or petiole elongation by transcription factors such as PHYTOCHROME INTERACTING FACTOR4 (11–14). Interestingly, the role of DELLAs in all these processes is the opposite to that of CONSTITUTIVELY PHOTOMORPHOGENIC1 (COP1), another central regulator of light and temperature responses. COP1 is an E3 ubiquitin ligase that promotes proteasome-dependent degradation of a number of transcription factors involved in light and temperature signaling. COP1 becomes inactivated by light perceived by phytochromes and cryptochromes and by low-to-moderate temperature (4 °C to 23 °C) (15–20) and requires the activity of the SUPPRESSOR OF *phyA-105* proteins (SPA1 to 4 in *Arabidopsis*) to be active in vivo (21). Here we show the direct physical interaction between DELLAs and COP1/SPA1 complex and propose a mechanism of regulation of DELLA stability different from the canonical GA signaling pathway.

Significance

DELLA proteins are plant-specific transcriptional regulators that act as signaling hubs at the interface between the environment and the transcriptional networks that control growth. The growth-promoting hormone gibberellin destabilizes DELLAs. Here we describe an alternative pathway to destabilize these proteins. We show that DELLAs are substrate of COP1, an E3 ubiquitin ligase that increases its activity to promote growth in response to shade or warmth. Our results show that COP1, and not changes in gibberellin levels, mediates the rapid destabilization of DELLAs in response to environmental cues.

Author contributions: N.B.-T., M.L., E.G.M., C.C.-R., M.D.Z., V.R., M.A.B., J.J.C., and D.A. designed research; N.B.-T., M.L., E.G.M., C.C.-R., M.A.N., E.J., M.G.-L., M.P., N.H., T.B., M.D.Z., V.R., and D.A. performed research; N.B.-T., E.G.M., A.L., D.E.-B., M.D.-D., H.F., and D.A. contributed new reagents/analytic tools; N.B.-T., M.L., E.G.M., C.C.-R., M.A.N., E.J., M.G.-L., M.P., N.H., T.B., M.C., B.B., H.F., M.D.Z., S.A.K., V.R., M.A.B., J.J.C., and D.A. analyzed data; and J.J.C. and D.A. wrote the paper.

The authors declare no competing interest.

This article is a PNAS Direct Submission. T.S. is a guest editor invited by the Editorial Board.

Published under the PNAS license.

¹N.B.-T., M.L., E.G.M., and C.C.-R. contributed equally to this work.

²To whom correspondence may be addressed. Email: casal@ifeva.edu.ar or dalabadi@ibmcp.upv.es.

This article contains supporting information online at <https://www.pnas.org/lookup/suppl/doi:10.1073/pnas.1907969117/-DCSupplemental>.

125
126
127
128
129
130
131
132
133
134
135
136
137
138
139
140
141
142
143
144
145
146
147
148
149
150
151
152
153
154
155
156
157
158
159
160
161
162
163
164
165
166
167
168
169
170
171
172
173
174
175
176
177
178
179
180
181
182
183
184
185
186

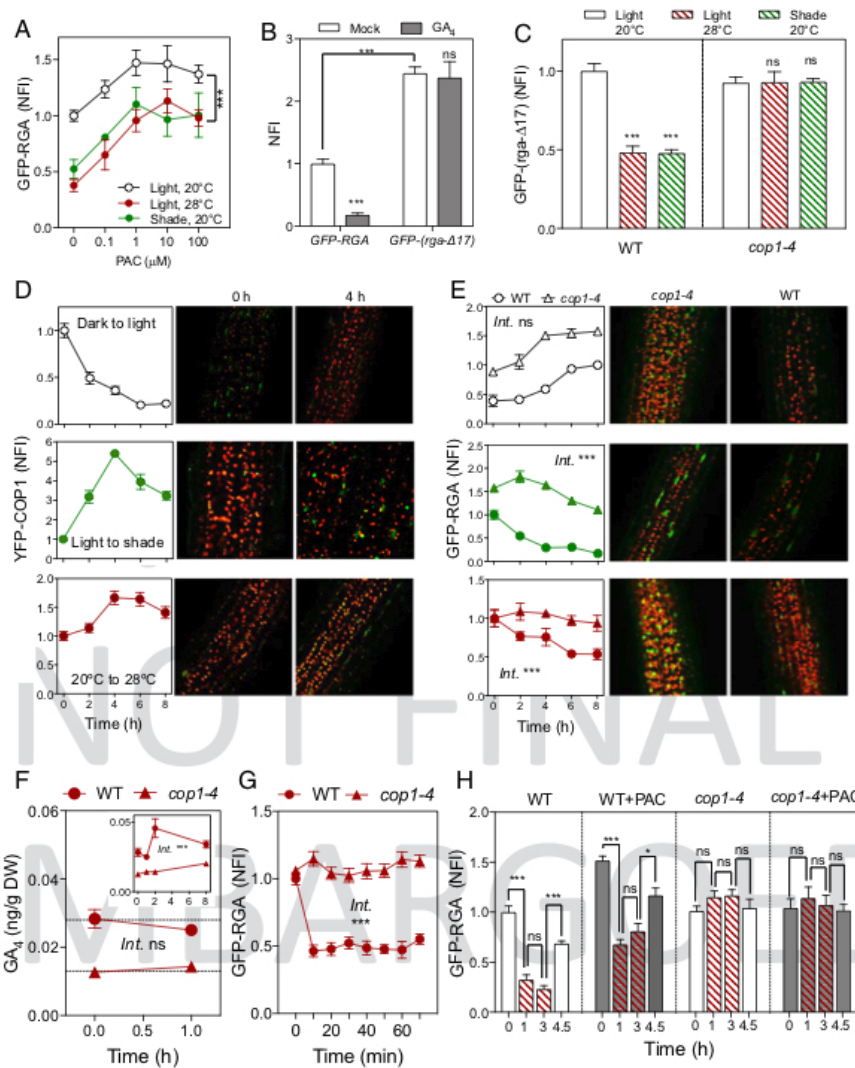


Fig. 1. COP1 regulates RGA levels in *Arabidopsis* hypocotyls in response to shade and warmth. (A) GFP-RGA levels respond to shade and warmth in the absence of GA synthesis. We incubated the seedlings with the indicated doses of PAC for 8 h, before exposure to shade or 28 °C for 4 h. (B) GFP-(*rga-Δ17*) is insensitive to GA-induced degradation. Seedlings of *pRGA::GFP-RGA* and *pRGA::GFP-(rga-Δ17)* lines were mock treated or treated with 3 μM GA₄ for 4 h. (C) Shade or warmth reduces GFP-(*rga-Δ17*) levels in a COP1-dependent-manner. Seedlings were exposed to the treatment for 3 d. (D and E) Dynamics of nuclear accumulation of YFP-COP1 (D) in the wild type and of GFP-RGA (E) in the wild type (circles) and *cop1-4* mutants (triangles) after the transfer from darkness to light (white symbols), light to shade (green symbols), and 20 °C to 28 °C (red symbols). (F) Time course of GA₄ levels in wild-type and *cop1-4* seedlings before (time = 0 h) and after transfer to 28 °C (Inset shows an extended time course). (G) Time course of nuclear levels of GFP-RGA in wild-type and *cop1-4* seedlings before (time = 0 h) and after transfer to 28 °C. (H) The reduction of GFP-RGA levels in response to 28 °C is reversible, unaffected by a saturating dose of PAC and dependent on COP1. Seedlings of *pRGA::GFP-RGA* in the wild-type and *cop1-4* backgrounds were returned to 20 °C after 3 h-treatment of 28 °C. We incubated the seedlings with PAC for 8 h before exposure to 28 °C. Confocal data (A, E, G, and H) show the normalized fluorescence intensity (NFI) in nuclei (NFI = 1 in the wild-type seedling control, and in B in the wild-type RGA control). For representative images, see D and E (8-h time point) and SI Appendix, Fig. S2 A and B. Confocal microscopy data are means and SE of 5 to 10 (A), 6 to 9 (B), 6 to 14 (C), 18 (D and E), 6 to 13 (G), and 18 (H) seedlings (a minimum of 10 and up to 50 nuclei were averaged per seedling replicate). GA₄ data are means and SE of three independent biological replicates. In A, C, and G we indicate the significance of the differences with the control condition (B also shows the difference between genotypes) in Student's *t* test or ANOVA followed by Bonferroni tests. In E-G we indicate the significance of the term accounting for the interaction (Int.) between condition (light, temperature) and genotype (wild type, *cop1*) in multiple regression analysis. In H, we indicate the significance of the comparison with the preceding bar in ANOVA followed by Bonferroni tests. **P* < 0.05, ***P* < 0.01, ****P* < 0.005; ns, nonsignificant.

187
188
189
190
191
192
193
194
195
196
197
198
199
200
201
202
203
204
205
206
207
208
209
210
211
212
213
214
215
216
217
218
219
220
221
222
223
224
225
226
227
228
229
230
231
232
233
234
235
236
237
238
239
240
241
242
243
244
245
246
247
248

249
250
251
252
253
254
255
256
257
258
259
260
261
262
263
264
265
266
267
268
269
270
271
272
273
274
275
276
277
278
279
280
281
282
283
284
285
286
287
288
289
290
291
292
293
294
295
296
297
298
299
300
301
302
303
304
305
306
307
308
309
310

Results

Warm Temperature or Shade Decreases the Abundance of a GA-Insensitive DELLA Protein. Warm temperatures (28 °C hereafter) or shade decrease the abundance of the DELLA protein REPRESSOR OF *gal-3* (RGA) (Fig. 1A and *SI Appendix, Fig. S1A*) (11, 14). Two observations indicate that changes in GA cannot fully account for these reductions. First, increasing doses of the GA-inhibitor paclobutrazol (PAC) elevated RGA nuclear abundance observed by confocal microscopy in a *pRGA:GFP-RGA* line (22), but the reductions caused by shade or warmth

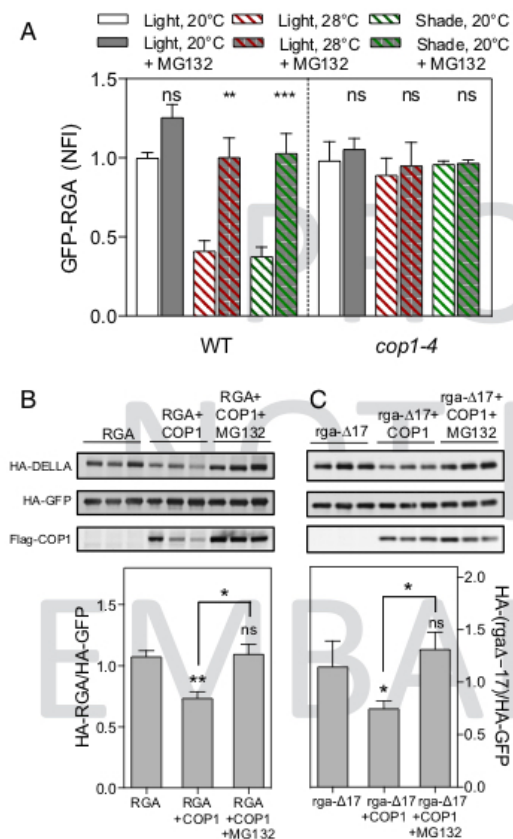


Fig. 2. COP1 destabilizes DELLAs. (A) The reduction of GFP-RGA levels by warm temperature or shade requires the 26S proteasome and COP1. Confocal data show the NFI in nuclei (NFI = 1 in the wild-type seedling control). NFI data are means and SE of 6 to 9 seedlings (10 to 30 nuclei were averaged per seedling replicate). Asterisks indicate that the difference is statistically significant (Student's *t* test, ***P* < 0.05 and ****P* < 0.001; ns, nonsignificant). (B and C) COP1 destabilizes RGA (B) and the GA-insensitive *rga-Δ17* (C) in *N. benthamiana* leaves. HA-RGA and HA-(*rga-Δ17*) were transiently expressed alone or with FLAG-COP1 in leaves of *N. benthamiana*. For MG132 treatments, leaves were infiltrated with a solution of 25 μM of the inhibitor 8 h before sampling. HA-GFP was used as control to demonstrate the specificity of COP1 action. Blots show data from three individual infiltrated leaves per mixture. Plots show HA-RGA and HA-(*rga-Δ17*) normalized against HA-GFP. Data are means and SE of three leaves from one experiment, repeated twice with similar results. Asterisks indicate that the difference is statistically significant (Student's *t* test, **P* < 0.05 and ***P* < 0.01; ns, nonsignificant).

Blanco-Touriñán et al.

persisted even under saturating levels of the inhibitor (Fig. 1A and *SI Appendix, Fig. S2A*). Second, warm temperature or shade reduced the levels of *rga-Δ17*, a mutant version of RGA that is fully insensitive to GA, in the *pRGA:GFP-(rga-Δ17)* line (Fig. 1B and C and *SI Appendix, Figs. S1A and S2B*) (23). Changes in RGA transcript levels do not mediate the altered RGA abundance in response to shade (14) or warm temperature (*SI Appendix, Fig. S1B*). Importantly, treatment with the inhibitor of the 26S proteasome MG132 fully impaired changes in RGA abundance (Fig. 2A). Altogether, these results suggest the existence of a noncanonical pathway of DELLA degradation.

COP1 Affects RGA Levels in Response to Shade and Warmth. RGA levels are elevated in *cop1-4* seedlings (24). Compared to light at moderate temperature, darkness, or 2 to 8 h of shade or warm temperature increased the nuclear abundance of COP1 (15, 25, 26) in a *35S:YFP-COP1 cop1-4* line (27), while reducing RGA levels (9, 11, 14) (Fig. 1D and E). The light-induced increase in RGA showed wild-type kinetics in the *cop1-4* seedlings (note parallel curves), suggesting that this change is driven by a COP1-independent light-induced down-regulation of GA biosynthesis (8, 9, 28, 29). Conversely, *cop1-4* seedlings grown in the light at moderate temperature (20 °C) and transferred either to shade at the same temperature or to light at 28 °C, showed a weaker decrease in GFP-RGA (Fig. 1E).

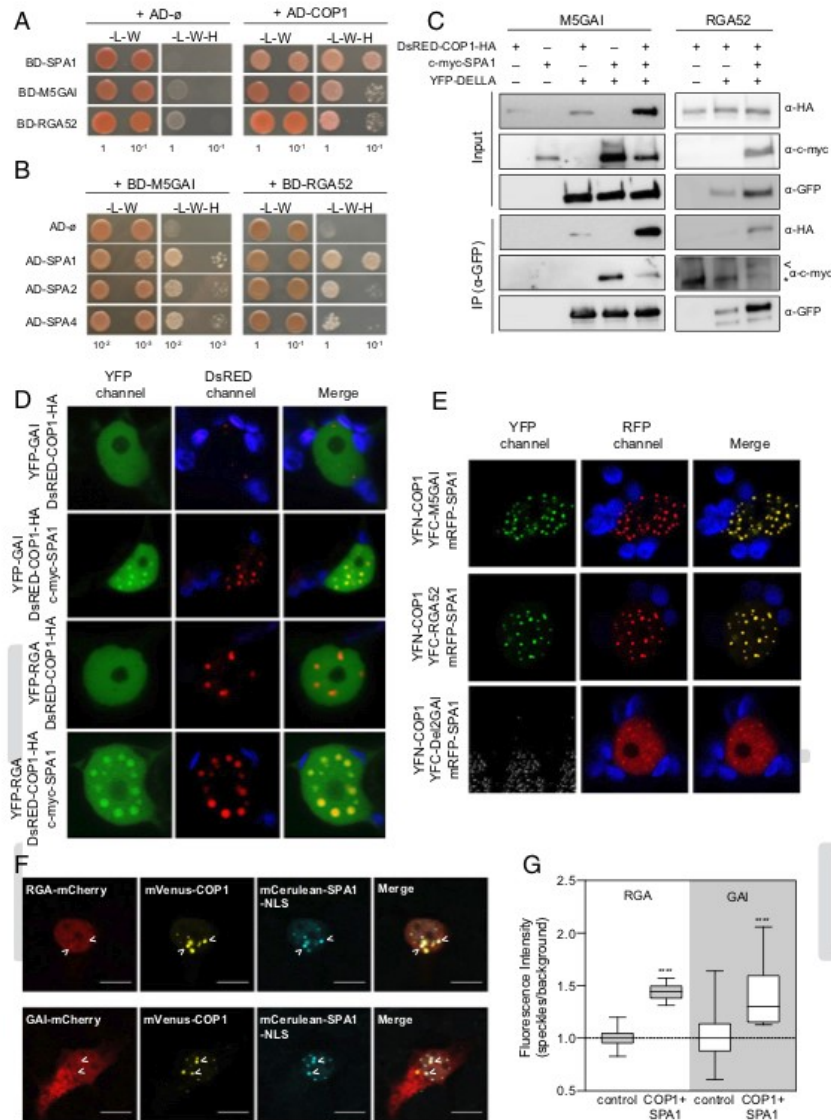
Changes in RGA Abundance Precede Changes in GA. GA₄ levels were unaffected by transferring the seedlings from 20 °C to 28 °C for 1 h (Fig. 1F), while 10 min of warm temperature were enough to induce significant nuclear accumulation of COP1 (*SI Appendix, Fig. S2C*) and decrease GFP-RGA levels in a COP1-dependent manner (Fig. 1G). These results indicate that rapid warmth-induced degradation of RGA requires COP1 and precedes changes in GA.

Relative Contribution of Each Pathway. GA levels did increase after 2 h of warm temperature (Fig. 1F, *Inset*). However, two observations indicate a negligible contribution of these changes in GA levels to the reduced GFP-RGA abundance in response to warmth. First, we observed no significant decreases in GFP-RGA between 1 and 3 h at 28 °C (i.e., concomitantly with the increase in GA) (Fig. 1H), despite the fact that GFP-RGA responds to exogenously applied GA in less than 15 min (22). Second, application of a saturating dose of PAC to block GA synthesis significantly increased GFP-RGA levels, but resulted in a parallel kinetics in response to warm temperature (Fig. 1H). GFP-RGA levels increased rapidly after returning the seedlings from 28 °C to 20 °C, a response also observed in the presence of PAC (Fig. 1H). *cop1-4* showed reduced levels of GA₄ but retained some GA₄ response to temperature (*P* < 0.05, Fig. 1F, *Inset*), which may have contributed to residual GFP-RGA degradation observed in this mutant beyond 4 h of shade or warmth (*P* < 0.05, Fig. 1E). Similarly, the *cop1* mutation lowers GA levels in the pea without eliminating its response to light (30). Taken together, these observations indicate that changes in GA have no major direct contribution to the rapid changes in RGA abundance, because when GA levels are elevated, COP1 has already induced RGA decay. However, the canonical GA pathway would make an indirect contribution to the rapid changes, setting basal RGA levels within a range where the system becomes sensitive to COP1. In fact, although shade and warmth did reduce GFP-(*rga-Δ17*) levels (Fig. 1C and *SI Appendix, Fig. S2B*), these effects were not rapid (*SI Appendix, Fig. S2D and E*). Similarly, warm temperature does not provoke rapid changes in RGA levels in the GA-deficient mutant *gal1* (11).

COP1 Promotes Degradation of a GA-Insensitive DELLA Protein. The fact that warm temperature or shade failed to reduce the nuclear

311
312
313
314
315
316
317
318
319
320
321
322
323
324
325
326
327
328
329
330
331
332
333
334
335
336
337
338
339
340
341
342
343
344
345
346
347
348
349
350
351
352
353
354
355
356
357
358
359
360
361
362
363
364
365
366
367
368
369
370
371
372

373
374
375
376
377
378
379
380
381
382
383
384
385
386
387
388
389
390
391
392
393
394
395
396
397
398
399
400
401
402
403
404
405
406
407
408
409
410
411
412
413
414
415
416
417
418
419
420
421
422
423
424
425
426
427
428
429
430
431
432
433
434



435
436
437
438
439
440
441
442
443
444
445
446
447
448
449
450
451
452
453
454
455
456
457
458
459
460
461
462
463
464
465
466
467
468
469
470
471
472
473
474
475
476
477
478
479
480
481
482
483
484
485
486
487
488
489
490
491
492
493
494
495
496

Fig. 3. COP1 physically interacts with DELLA proteins. (A and B) Y2H assays showing the interaction between N-terminal deleted versions of GAI and RGA with COP1 (A) and SPAs (B). L, leucine; W, tryptophan; H, histidine. Numbers indicate the dilutions used in the drop assay. (C) Coimmunoprecipitation assays showing interactions in plants. YFP-M5GAI and YFP-RGA52 were transiently expressed in leaves of *N. benthamiana* together with DsRED-COP1-HA, c-myc-SPA1, or both. Proteins were immunoprecipitated with anti-GFP antibody-coated paramagnetic beads. Leaves expressing DsRED-COP1-HA or c-myc-SPA1 alone were used as negative controls. The arrowhead and asterisk mark the coimmunoprecipitated c-myc-SPA1 and a nonspecific band, respectively. (D) YFP-GAI and YFP-RGA colocalize with DsRED-COP1-HA in nuclear bodies in the presence of c-myc-SPA1. Fusion proteins were transiently expressed in leaves of *N. benthamiana* and observed by confocal microscopy. One representative nucleus is shown. (E) BiFC assay showing that COP1 and SPA1 form a complex with M5GAI or RGA52 in nuclear bodies. The indicated proteins were transiently expressed in leaves of *N. benthamiana* and observed by confocal microscopy. One representative nucleus is shown. (F) Representative HEK-293T cells cotransfected with mVenus-COP1, NLS-mCerulean-SPA1, and either GAI-mCherry or RGA-mCherry. (Scale bar, 10 μm). The arrowheads point to two representative speckles co-occupied by DELLAs, SPA1, and COP1. (G) Fluorescence from GAI-mCherry or RGA-mCherry accumulates in the regions corresponding to speckles formed by COP1 and SPA1 in cells coexpressing mVenus-COP1 and mCerulean-SPA1-NLS. Data are mean from 10 to 13 transfected cells. The boxes extend from the first to the third quartile around the median, while whiskers go down to the smallest value and up to the largest. Asterisks indicate that the difference is statistically significant with the control condition (Student's t test, *****P* < 0.0001).

497 abundance of RGA or *rga-Δ17* in *cop1-4* mutants (Figs. 1 C, E, 498 G, and H, and 2A) and that these changes are dependent on the 499 26S proteasome (Fig. 2A), suggests that COP1 promotes DELLA 500 degradation. We first tested this possibility in transient 501 expression assays in *Nicotiana benthamiana* leaves. Coexpression 502 of COP1 caused 26S proteasome-dependent decrease of HA- 503 RGA and HA-*(rga-Δ17)* in leaves of long-day-grown *N. bent-* 504 *hamiana* plants, while it had no impact on levels of the unrelated 505 protein HA-GFP (Fig. 2B and C). Warm temperature decreased 506 HA-*(rga-Δ17)* in a COP1-mediated manner (SI Appendix, Fig. 507 S3). This suggests that COP1 mediates the destabilization of 508 RGA by noncanonical mechanisms.

509 **COP1 Interacts Physically with GAI and RGA in Yeast.** To explore if 510 COP1 mediates RGA degradation by noncanonical mechanisms, 511 we first investigated whether COP1 physically interacts with 512 DELLA proteins. We performed yeast two-hybrid (Y2H) assays 513 between COP1 and the two DELLAs with a major role in light- 514 and temperature-dependent growth, RGA and GIBBERELLIC 515 ACID INSENSITIVE (GAI) (11, 12, 31). To avoid the reported 516 strong autoactivation of full-length DELLAs in yeast, we used 517 previously established variants with deletions of the N terminus 518 named M5GAI and RGA52 (13, 32). COP1 was able to interact 519 with both (Fig. 3A). SUPPRESSOR OF *phyA-105* 1 (SPA1) and 520 other SPA proteins involved in a functional complex with COP1 521 (21, 33) were also able to interact with GAI and RGA in Y2H 522 assays (Fig. 3B).

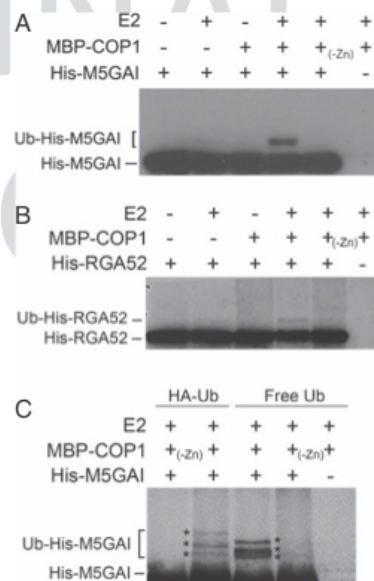
523 **COP1 Interacts with GAI and RGA In Planta.** To investigate whether 524 the interaction between DELLAs and COP1 also occurs in plant 525 cells, we first performed coimmunoprecipitation assays in leaves 526 of *N. benthamiana* coexpressing DsRED-COP1-HA and YFP- 527 M5GAI or YFP-RGA52. While DsRED-COP1-HA was pulled 528 down by anti-GFP antibodies from leaf extracts coexpressing 529 YFP-M5GAI, and the interaction appeared to be enhanced in 530 the presence of c-myc-SPA1, the DsRED-COP1-HA and YFP- 531 RGA52 interaction was only observed when the three proteins 532 were coexpressed (Fig. 3C). c-myc-SPA1 was also specifically 533 coimmunoprecipitated with YFP-M5GAI (Fig. 3C). These re- 534 sults suggest that SPA1 enhances the interaction between COP1 535 and DELLA proteins. Consistent with this idea, we observed 536 relocalization of YFP-GAI, YFP-RGA, and RGA52-YFP to 537 nuclear bodies co-occupied by DsRED-COP1-HA in the pres- 538 ence of c-myc-SPA1 (Fig. 3D and SI Appendix, Fig. S4A).

539 **COP1-SPA1 Forms a Ternary Complex with DELLA.** The formation of 540 a ternary complex was evidenced by bimolecular fluorescence 541 complementation (BiFC) assays in leaves of *N. benthamiana*, in 542 which the colocalization of signals from mRFP-SPA1 and the 543 reconstituted YFP, due to the interaction between YFP- 544 DELLAs and YFN-COP1, was evident in nuclear bodies 545 (Fig. 3E and SI Appendix, Fig. S4B). Similarly, YFP signal in 546 nuclear bodies was observed by coexpressing c-myc-SPA1 (SI 547 Appendix, Fig. S4C). However, no YFP fluorescence was de- 548 tected in the absence of SPA1 or when YFC was fused to 549 Del2GAI, a truncated version of GAI that does not interact with 550 SPA1 (Fig. 3E and SI Appendix, Fig. S4B-E). As expected, 551 mRFP-SPA1 was recruited to nuclear bodies when coexpressed 552 with YFN-COP1 (Fig. 3E and SI Appendix, Fig. S4B) (34).

553 To quantify the interaction between GAI or RGA and the 554 COP1-SPA1 complex we expressed these proteins tagged to 555 fluorescent reporters in mammalian cells. This orthogonal sys- 556 tem allows the performance of such studies with the components 557 of interest, in the absence of other plant proteins that might 558 interfere with the evaluation. The fluorescence from DELLA- 559 mCherry fusions in the cytosol and nucleus was relatively ho- 560 mogeneous when either GAI or RGA was expressed alone (Fig. 561 3F; note the ratio of fluorescence between different nuclear

559 regions close to 1 in Fig. 3G). However, the ratio between 560 DELLA fluorescence inside/outside the speckle-like structures 561 formed in the nucleus by the COP1-SPA1 complex was above 1 562 (Fig. 3F and G and SI Appendix, Fig. S5), suggesting that the 563 COP1-SPA1 complex drags RGA and GAI to the speckles by 564 physical interaction. Taken together, these observations demon- 565 strate that the COP1-SPA1 complex interacts with 566 DELLA proteins.

567 **COP1 Ubiquitinates GAI and RGA In Vitro.** In vivo levels of ubiq- 568 uitinated GFP-RGA were enhanced by overexpression of COP1 569 (SI Appendix, Fig. S6). To test whether this is the result of the 570 direct interaction between COP1 and DELLAs, we performed 571 an in vitro ubiquitination assay using recombinant MBP-COP1 572 and 6xHis-M5GAI or 6xHis-RGA52. A slow-migrating band 573 corresponding to the size of Ub-6xHis-M5GAI or Ub-6xHis- 574 RGA52 was observed only when MBP-COP1 and the E2 enzyme 575 were included in the assays (Fig. 4A and B). The delayed band 576 did not appear, however, when Zn^{2+} ions, which are required for 577 the proper arrangement of the RING domain of E3 ubiquitin 578 ligases like COP1 (35), were excluded from the reaction mixtures 579 (Fig. 4A and B). To confirm that the slow migration of 6xHis- 580 M5GAI and 6xHis-RGA52 is due to ubiquitination, we repeated 581 the assay for 6xHis-M5GAI in the presence of HA-tagged 582 ubiquitin. We detected low-migrating bands in the immunoblot 583 with anti-GAI antibody when free ubiquitin was included in the 584 assay, which were further upshifted when we used the HA-tagged 585 version of ubiquitin instead (Fig. 4C). This result indicates that 586 M5GAI and RGA52 are targets of the E3 ubiquitin ligase ac- 587 tivity of COP1 in vitro.



588 **Fig. 4.** COP1 ubiquitinates GAI and RGA. (A and B) The 6xHis-M5GAI (A) and 6xHis-RGA52 (B) ubiquitination assay using recombinant MBP-COP1, rice E2, and unmodified ubiquitin. (C) The 6xHis-M5GAI ubiquitination assay using unmodified and HA-tagged ubiquitin. Modified and unmodified 6xHis-M5GAI and 6xHis-RGA52 were detected with anti-GAI and anti-6xHis antibodies, respectively.

621
622
623
624
625
626
627
628
629
630
631
632
633
634
635
636
637
638
639
640
641
642
643
644
645
646
647
648
649
650
651
652
653
654
655
656
657
658
659
660
661
662
663
664
665
666
667
668
669
670
671
672
673
674
675
676
677
678
679
680
681
682

COP1 Controls Hypocotyl Elongation in a DELLA-Dependent Manner. The growth phenotypes caused by GA deficiency or *cop1* mutations in the dark (31, 36), in response to light cues from neighbors (14, 26) or to warm temperature (11, 15, 37), are very similar. To determine the physiological relevance of the regulation of DELLA levels by COP1, we studied how mutations at *COP1* and *DELLA* genes and GA treatments impact on the hypocotyl growth rate of dark-grown seedlings transferred to light at 20 °C (deetiolation) as well as light-grown seedlings transferred to shaded or warm environments. Noteworthy, the patterns differed between the first case, where DELLA levels build up, and the other two cases, where DELLA levels decrease (Fig. 1E). In fact, during deetiolation, growth in the presence of 5 μM GA₄ promoted the rate of hypocotyl elongation in seedlings transferred to the light but not in seedlings that remained in the dark, suggesting that endogenous GA levels are not limiting in darkness (Fig. 5). As expected, the *cop1* mutants showed reduced growth in darkness; however, they retained a significant growth response to light. This response was only marginally enhanced by adding GA₄ or by the *gai-td1* and *rga-29* (24) mutations of *DELLA* genes. In other words, during deetiolation, the rapid inactivation of COP1 does not appear to be rate limiting for the RGA accumulation (Fig. 1E) or the growth inhibition (Fig. 5) responses. Addition of 5 μM GA₄ promoted growth in light-grown seedlings transferred to shade or to warm temperature (Fig. 5), suggesting that GA signaling is limiting under those conditions. The *cop1-4* and *cop1-6* mutants failed to respond to shade or warm temperatures but the responses were restored both by the application of GA₄ and by the presence of mutations

of both *DELLA* genes. This indicates that the responses were limited by the elevated levels of DELLAs in *cop1* and reducing the DELLA pool either genetically or by the GA treatment was enough to rescue the *cop1* phenotype.

Discussion

The results presented here establish a functional link between DELLA proteins and COP1, two of the major hubs in the control of plant architecture. The growth of the hypocotyl of *Arabidopsis* shifted from light at moderate temperatures to either warm or shade conditions requires COP1 only if DELLA proteins are present (Fig. 5). These environmental cues reduce phyB activity (2, 38, 39) and enhance COP1 nuclear abundance (Fig. 1D), while reducing the levels of RGA in a COP1-dependent manner (Fig. 1E). COP1 does not simply reduce DELLA protein abundance by increasing GA levels. First, COP1 migrates to the nucleus and mediates RGA degradation in response to warm temperature well before increasing GA levels (Fig. 1 F-H and *SI Appendix, Fig. S2C*). Similarly, simulated shade takes more than 4 h to modify GA levels (40) while already causing large COP1-mediated effects on RGA at 2 h (Fig. 1E). Second, warm temperature or shade reduces the abundance of RGA in the presence of saturating levels of a GA synthesis inhibitor (Fig. 1A). Third, warm temperature or shade reduces the abundance of the mutant protein *rga-Δ17*, which cannot be recognized by *GID1* (41) and is fully insensitive to GA (Fig. 1 B and C and *SI Appendix, Fig. S2*). The latter effects require COP1, providing evidence for a branch of COP1 action on DELLA that does not involve activating the canonical GA/GID1 pathway.

683
684
685
686
687
688
689
690
691
692
693
694
695
696
697
698
699
700
701
702
703
704
705
706
707
708
709
710
711
712
713
714
715
716
717
718
719
720
721
722
723
724
725
726
727
728
729
730
731
732
733
734
735
736
737
738
739
740
741
742
743
744

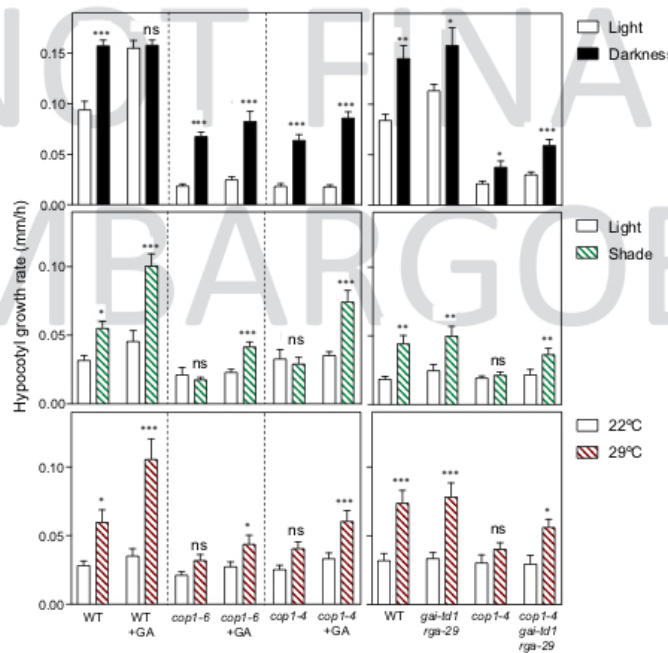


Fig. 5. COP1 regulates the rate of hypocotyl elongation in response to shade and warm temperature in a DELLA-dependent manner. Bars indicate the hypocotyl growth rate of seedlings of the indicated genotypes during deetiolation or after transfer to shade or 28 °C measured over a period of 9 h. Where indicated, seedlings were germinated and grown in the presence of 5 μM GA₄. Values correspond to the mean and SE of 8 (light treatments) or 24 (temperature treatments) replicate boxes; 10 seedlings were averaged per replicate box. Asterisks indicate that the difference is statistically significant with the control condition (Student's t test, *P < 0.05, **P < 0.01, ***P < 0.005; ns, nonsignificant).

745 COP1 effects on RGA and *rga-Δ17* depend on the 26S pro-
746 teasome (Fig. 2). Taking into account the well-established role of
747 COP1 in E3-ligase complexes that ubiquitinate and target to
748 proteasomal degradation proteins involved in environmental
749 signaling (42), the simplest interpretation of the above observa-
750 tions is that COP1 directly regulates DELLA protein stability.
751 Different results lend support to this hypothesis. First, RGA and
752 GAI interact with COP1 and its complex partner SPA1 in yeast
753 (Fig. 3A and B) and in planta (Fig. 3C). Second, COP1, SPA1,
754 and GAI or RGA form a tertiary complex in mammalian and
755 plant cells, and this complex is present in nuclear bodies
756 (Fig. 3D–G and *SI Appendix*, Figs. S4A–C and S5). Third, COP1
757 ubiquitinates RGA and GAI in vitro (Fig. 4) and the levels of
758 ubiquitinated RGA in vivo are enhanced by COP1 (*SI Appendix*,
759 Fig. S6).

760 Tight regulation of abundance is a common feature of proteins
761 that act as signaling hubs in mammals (43) and in yeast (44).
762 Posttranslational modifications (45–47) and interaction with
763 other transcriptional regulators (48, 49) modulate DELLA ac-
764 tivity. However, the mechanism reported here is unique. In
765 contrast to previously reported modes of regulation of DELLA
766 abundance, which converge to control its stability via GA/GID1,
767 the rapid COP1-mediated regulation occurs by a mechanism that
768 acts in parallel to the canonical GA/GID1 pathway.

769 COP1 might represent an ancient regulatory mechanism of
770 control of DELLA levels, preceding the acquisition of the GA/
771 GID1 system because the GA/GID1 system appears in lycop-
772 hytes (50), while orthologs of COP1 and DELLA proteins are
773 already present in the genome of the liverwort *Marchantia pol-
774 ymorpia* (51). However, in *Arabidopsis*, these two pathways ap-
775 pear to operate in concert. Blocking GA synthesis with PAC
776 reveals that the canonical pathway makes a negligible direct
777 contribution to the rapid changes in RGA abundance in re-
778 sponse to warmth or shade (Fig. 1A and H), simply because by
779 the time GA levels increase, the COP1 pathway has already
780 acted (Fig. 1F and G and *SI Appendix*, Fig. S2C). However, the
781 GA pathway has a large effect in a developmental time scale, as
782 demonstrated by the massive accumulation of RGA in the GA-

783 deficient mutant *gal* (11, 22) or the GA-insensitive version *rga-
784 Δ17* (Fig. 1B) (23). Although *rga-Δ17* retains the COP1-
785 mediated response (Fig. 1C and *SI Appendix*, Fig. S2B), this ef-
786 fect is no longer rapid (*SI Appendix*, Fig. S2D and E), consis-
787 tently with the lack of rapid changes in RGA levels in response to
788 warmth in the *gal* mutant (11). This indicates that the GA
789 pathway sets the sensitivity to the COP1 pathway. Coexistence of
790 the COP1- and GA-dependent regulation would provide the
791 advantage of a faster and tunable adjustment to the suddenly
792 fluctuating cues of the natural environment.

793 Materials and Methods

794 Detailed description of the plant materials and growth conditions, and
795 methods used for protein-protein interaction assays, protein localization,
796 and in vitro ubiquitination can be found at *SI Appendix*, *Methods*.

797 **Data Availability.** All data discussed in the paper are available in the main text
798 and *SI Appendix*. Materials used in the paper are available upon request
799 from the corresponding authors.

800 **ACKNOWLEDGMENTS.** We thank Drs. Isabel Lopez-Diaz and Esther Carrera
801 for the gibberellin quantification carried out at the Plant Hormone
802 Quantification Service (IBMCP) and Luis López-Molina (University of Geneva)
803 and Karin Schumacher (University of Heidelberg) for the anti-GAI and anti-
804 DET3 antibodies, respectively. We also thank Prof. Salomé Prat and all mem-
805 bers of the SIGNAT consortium for helpful discussions about this work. This
806 work was supported by the Spanish Ministry of Economy, Industry and Com-
807 petitiveness and AEI/FEDER/EU (grants BIO2016-79133-P to D.A. and
808 BIO2013-46539-R and BIO2016-80551-R to V.R.); the European Union SIG-
809 NAT-Research and Innovation Staff Exchange (grant H2020-MSCA-RISE-
810 2014-644435 to M.A.B., D.A., and J.J.C.); the Argentinian Agencia Nacional
811 de Promoción Científica y Tecnológica (grant PICT-2016-1459 to J.J.C.); Uni-
812 versidad de Buenos Aires (grant 200201701005058A to J.J.C.); the National
813 Institute of General Medical Sciences of the National Institutes of Health
814 (award numbers R01GM067837 and R01GM056006 to S.A.K.); the German
815 Research Foundation (DFG) under Germany's Excellence Strategy/Initiative
816 (CEPLAS - EXC-2048/1, Project ID 390686111 to M.D.Z.); the International
817 Max Planck Research School of the Max Planck Society; the University of
818 Düsseldorf and the University of Cologne to T.B.; NRW-BioSC-FocusLabs
819 CombiCom to N.H. and M.D.Z.; and MEYS of the Czech Republic (project
820 LQ1601 CEITEC 2020 to B.B. and M.C.). N.B.-T., E.L., and M.G.-L. were sup-
821 ported by MINECO FPI Program fellowships.

822 1. J. J. Casal, C. Fankhauser, G. Coupland, M. A. Blázquez, Signalling for developmental
823 plasticity. *Trends Plant Sci.* **9**, 309–314 (2004).
824 2. J. J. Casal, Photoreceptor signaling networks in plant responses to shade. *Annu. Rev.*
825 *Plant Biol.* **64**, 403–427 (2013).
826 3. M. Quint et al., Molecular and genetic control of plant thermomorphogenesis. *Nat.*
827 *Plants* **2**, 15190 (2016).
828 4. H. Claeys, S. De Bodt, D. Inzé, Gibberellins and DELLAs: Central nodes in growth
829 regulatory networks. *Trends Plant Sci.* **19**, 231–239 (2014).
830 5. K. Van De Velde, P. Ruelens, K. Geuten, A. Rohde, D. Van Der Straeten, Exploiting
831 DELLA signaling in cereals. *Trends Plant Sci.* **22**, 880–893 (2017).
832 6. T. P. Sun, The molecular mechanism and evolution of the GA-GID1-DELLA signaling
833 module in plants. *Curr. Biol.* **21**, R338–R345 (2011).
834 7. D. Alabadi, M. A. Blázquez, Molecular interactions between light and hormone sig-
835 naling to control plant growth. *Plant Mol. Biol.* **69**, 409–417 (2009).
836 8. D. Alabadi et al., Gibberellins modulate light signaling pathways to prevent *Arabi-*
837 *dopsis* seedling de-etiolation in darkness. *Plant J.* **53**, 324–335 (2008).
838 9. P. Acharj et al., DELLAs contribute to plant photomorphogenesis. *Plant Physiol.* **143**,
839 1163–1172 (2007).
840 10. O. Lantzouni, A. Alkofer, P. Falter-Braun, C. Schwedheimer, GROWTH-REGULATING
841 FACTORS interact with DELLAs and regulate growth in cold stress. *Plant Cell* **32**,
842 1018–1034 (2020).
843 11. J. A. Stavang et al., Hormonal regulation of temperature-induced growth in *Arabi-*
844 *dopsis*. *Plant J.* **60**, 589–601 (2009).
845 12. M. V. Arana, N. Marin-de la Rosa, J. N. Maloof, M. A. Blázquez, D. Alabadi, Circadian
846 oscillation of gibberellin signaling in *Arabidopsis*. *Proc. Natl. Acad. Sci. U.S.A.* **108**,
847 9292–9297 (2011).
848 13. M. de Lucas et al., A molecular framework for light and gibberellin control of cell
849 elongation. *Nature* **451**, 480–484 (2008).
850 14. T. Djakovic-Petrovic, M. de Wit, L. A. Voosenek, R. Pierik, DELLA protein function in
851 growth responses to canopy signals. *Plant J.* **51**, 117–126 (2007).
852 15. Y. J. Park, H. J. Lee, J. H. Ha, J. Y. Kim, C. M. Park, COP1 conveys warm temperature
853 information to hypocotyl thermomorphogenesis. *New Phytol.* **215**, 269–280 (2017).
854 16. R. Catalá, J. Medina, J. Salinas, Integration of low temperature and light signaling
855 during cold acclimation response in *Arabidopsis*. *Proc. Natl. Acad. Sci. U.S.A.* **108**,
856 16475–16480 (2011).

857 17. D. J. Sheerin et al., Light-activated phytochrome A and B interact with members of
858 the SPA family to promote photomorphogenesis in *Arabidopsis* by reorganizing the
859 COP1/SPA complex. *Plant Cell* **27**, 189–201 (2015).
860 18. H. L. Lian et al., Blue-light-dependent interaction of cryptochrome 1 with SPA1 de-
861 fines a dynamic signaling mechanism. *Genes Dev.* **25**, 1023–1028 (2011).
862 19. B. Liu, Z. Zuo, H. Liu, X. Liu, C. Lin, *Arabidopsis* cryptochrome 1 interacts with SPA1 to
863 suppress COP1 activity in response to blue light. *Genes Dev.* **25**, 1029–1034 (2011).
864 20. X. D. Lu et al., Red-light-dependent interaction of phyB with SPA1 promotes COP1-
865 SPA1 dissociation and photomorphogenic development in *Arabidopsis*. *Mol. Plant* **8**,
866 467–478 (2015).
867 21. U. Hoeker, The activities of the E3 ubiquitin ligase COP1/SPA, a key repressor in light
868 signaling. *Curr. Opin. Plant Biol.* **37**, 63–69 (2017).
869 22. A. L. Silverstone et al., Repressing a repressor: Gibberellin-induced rapid reduction of
870 the RGA protein in *Arabidopsis*. *Plant Cell* **13**, 1555–1566 (2001).
871 23. A. Dill, H. S. Jung, T. P. Sun, The DELLA motif is essential for gibberellin-induced
872 degradation of RGA. *Proc. Natl. Acad. Sci. U.S.A.* **98**, 14162–14167 (2001).
873 24. J. I. Cagnola et al., Long-day photoperiod enhances jasmonic acid-related plant de-
874 fense. *Plant Physiol.* **178**, 163–173 (2018).
875 25. M. Pacin, M. Legris, J. J. Casal, Rapid decline in nuclear COP1 abundance anticipates
876 the stabilisation of its target HY5 in the light. *Plant Physiol.* **164**, 1134–1138 (2014).
877 26. M. Padin, M. Legris, J. J. Casal, COP1 re-accumulates in the nucleus under shade. *Plant*
878 *J.* **75**, 631–641 (2013).
879 27. A. Oravecz et al., CONSTITUTIVELY PHOTOMORPHOGENIC1 is required for the UV-B
880 response in *Arabidopsis*. *Plant Cell* **18**, 1975–1990 (2006).
881 28. J. Gil, J. L. Garcia-Martinez, Light regulation of gibberellin A1 content and expression
882 of genes coding for GA 20-oxidase and GA 3 β -hydroxylase in etiolated pea seedlings.
883 *Physiol. Plant.* **108**, 223–229 (2000).
884 29. X. Zhao et al., A study of gibberellin homeostasis and cryptochrome-mediated blue
885 light inhibition of hypocotyl elongation. *Plant Physiol.* **145**, 106–118 (2007).
886 30. J. L. Weller, V. Hecht, J. K. Vander Schoor, S. E. Davidson, J. J. Ross, Light regulation of
887 gibberellin biosynthesis in pea is mediated through the COP1/HY5 pathway. *Plant Cell*
888 **21**, 800–813 (2009).

869	32. J. Gallego-Bartolomé <i>et al.</i> , Molecular mechanism for the interaction between gibberellin and brassinosteroid signaling pathways in <i>Arabidopsis</i> . <i>Proc. Natl. Acad. Sci. U.S.A.</i> 109 , 13446–13451 (2012).	931
870		932
871	33. U. Hoecker, P. H. Quail, The phytochrome A-specific signaling intermediate SPA1 interacts directly with COP1, a constitutive repressor of light signaling in <i>Arabidopsis</i> . <i>J. Biol. Chem.</i> 276 , 38173–38178 (2001).	933
872		934
873	34. H. S. Seo <i>et al.</i> , LAF1 ubiquitination by COP1 controls photomorphogenesis and is stimulated by SPA1. <i>Nature</i> 423 , 995–999 (2003).	935
874		936
875	35. A. G. von Arnim, X. W. Deng, Ring finger motif of <i>Arabidopsis thaliana</i> COP1 defines a new class of zinc-binding domain. <i>J. Biol. Chem.</i> 268 , 19626–19631 (1993).	937
876		938
877	36. X. W. Deng, T. Caspar, P. H. Quail, <i>cop1</i> : A regulatory locus involved in light-controlled development and gene expression in <i>Arabidopsis</i> . <i>Genes Dev.</i> 5 , 1172–1182 (1991).	939
878		940
879	37. C. Delker <i>et al.</i> , The DET1-COP1-HY5 pathway constitutes a multipurpose signaling module regulating plant photomorphogenesis and thermomorphogenesis. <i>Cell Rep.</i> 9 , 1983–1989 (2014).	941
880		942
881	38. M. Legris <i>et al.</i> , Phytochrome B integrates light and temperature signals in <i>Arabidopsis</i> . <i>Science</i> 354 , 897–900 (2016).	943
882		944
883	39. J. H. Jung <i>et al.</i> , Phytochromes function as thermosensors in <i>Arabidopsis</i> . <i>Science</i> 354 , 886–889 (2016).	945
884		946
885	40. J. Bou-Torrent <i>et al.</i> , Plant proximity perception dynamically modulates hormone levels and sensitivity in <i>Arabidopsis</i> . <i>J. Exp. Bot.</i> 65 , 2937–2947 (2014).	947
886		948
887	41. B. C. Willige <i>et al.</i> , The DELLA domain of GA INSENSITIVE mediates the interaction with the GA INSENSITIVE DWARF1A gibberellin receptor of <i>Arabidopsis</i> . <i>Plant Cell</i> 19 , 1209–1220 (2007).	949
888		950
889		951
890		952
891		953
892		954
893		955
894		956
895		957
896		958
897		959
898		960
899		961
900		962
901		963
902		964
903		965
904		966
905		967
906		968
907		969
908		970
909		971
910		972
911		973
912		974
913		975
914		976
915		977
916		978
917		979
918		980
919		981
920		982
921		983
922		984
923		985
924		986
925		987
926		988
927		989
928		990
929		991
930		992